Probing Organometallic Reactions With ^{19}F NMR

Eric J. Hawrelak

Dissertation Submitted to the Faculty of

Virginia Polytechnic Institute and State University

in partial fulfillment of the requirements for the degree of

Doctor of Philosophy

In

Chemistry

Paul Deck, Chairman

Richard Gandour

Brian Hanson

James Tanko

Gordon Yee

November 18, 2002

Blacksburg, Virginia

Keywords: pentafluorophenyl, methylaluminoxane, ^{19}F NMR, metallocene

Probing Organometallic Reactions Using ^{19}F NMR

Eric J. Hawrelak

Abstract

This dissertation explores fundamental aspects of the reaction of group 4 metallocenes with methylaluminoxane (MAO) that lead to active Ziegler-Natta olefin polymerization catalysts. A novel experimental approach is described, in which a unique spectroscopic probe (a fluorinated substituent) is attached to the metallocene ancillary ligands and the metallocene/MAO mixtures are analyzed using ^{19}F NMR spectroscopy.

Group 4 metallocene dimethides bearing pentafluorophenyl (C_6F_5) substituents were synthesized and treated with MAO in benzene-d_6. ^{19}F NMR spectroscopic analysis demonstrated reversible methide transfer to form "cation-like" methylmetallocenium methylaluminates. A series of quantitative titration studies showed that fewer than 10% of the aluminum centers in MAO actually participate in the methide transfer process. A systematic study of metallocene substituent effects suggested that MAO contains active centers of extremely high but varying Lewis acidity. Activation of group 4 metallocene dichlorides using MAO was also analyzed using ^{19}F NMR. Initial Cl/CH_3 exchange was followed by Cl transfer to aluminum, whereas "normal" subsequent transfer of CH_3 from Al to the methylmetallocenium cation was apparently inhibited by the abstracted chloride. Additional studies showed that the ^{19}F NMR probe is sensitive to the *interactions* of Zr-Cl bonds with simple alkylaluminum species such as Me_3Al, Me_2AlCl, $MeAlCl_2$, and Et_3Al. However, the method was arguably less useful than ^{1}H NMR spectroscopy in following the *metathesis* of Zr-Cl and Al-R (R = Me, Et) bonds.

New methods of preparing methylhalometallocenes were investigated. The reactions of eleven metallocene dimethyls with triphenylmethyl chloride were highly selective (> 95%) with the five most electron-deficient metallocenes studied. Two other examples showed good selectivity on an NMR scale but could not be isolated from the 1,1,1-triphenylethane byproduct. Reactions of dimethylmetallocenes with benzyl bromide were also selective for formation of the corresponding methylbromo-metallocenes, however the reactions were too slow to be of practical value. The observation of long initation periods and the analysis of organic byproduct distributions suggested that these halogenation reactions may proceed by a radical chain mechanism rather than simple sigma bond metathesis.

To demonstrate "proof of concept" in the use of ^{19}F NMR to analyze the reactions of paramagnetic metallocenes, the coordination of CO and CN^- to C_6F_5-substituted chromocenes were analyzed. Whereas CO coordinates readily to chromocene, cyanide coordinates effectively to 1,1'-bis(pentafluorophenyl)chromocene. This observation is interpreted in terms of the electron-withdrawing effect of the C_6F_5 substituent, which should strengthen bonding to sigma-donor ligands (CN^-) and weaken bonding to pi-acceptors (CO)

Acknowledgments

I would like to thank my advisor, Dr. Paul Deck, who through his high quality scholarship and instruction provided a nurturing and exciting arena for the pursuit of chemistry. I would also like to thank the other members of my committee, Dr. Richard Gandour, Dr. Brian Hanson, Dr. James Tanko, and Dr. Gordon Yee for their help and support throughout my years at Virginia Tech.

To the members of the Deck research group, past and present, Matt Thornberry, Andrea Warren, Owen Lofthus, Frank Cavadas, and Ashley Milligan, I thank you for allowing me to work side by side with you. I have to give you all credit for putting up with me and my loud music in the lab.

To those involved in my life outside of chemistry (if there is life outside of chemistry) who kept me from going insane these past few years. I thank my mother, sister, and grandmother who have tirelessly supported me throughout my life. I thank my wife, for standing behind me through all my highs and lows while working toward my Ph.D. Your unconditional love and understanding is truly amazing. And finally to my two "boys" Bauer and Max, no matter how bad things got you were always there to cheer me up.

Experimental and theoretical investigations of the structure of methylaluminoxane (MAO) cocatalysts for olefin polymerizationYstenes, M.; Eilertsen, J. L.; Liu, J. K.; Ott, M.; Rytter, E.; Stovneng, J. A. Journal of Polymer Science Part a-Polymer Chemistry 2000. Reprinted by permission of John Wiley & Son, Inc.

Table of Contents

Table of Figures

Table of Tables

Chapter One: Overview of Olefin Polymerization Catalysts

Intent of Dissertation

The goal of this research is to understand important quantitative trends in the reactions of group 4 metallocenes with methylaluminoxane (MAO) and alkylaluminum halides. These reactions are fundamental to the process by which metallocenes are "activated" toward Ziegler-Natta olefin polymerization. A preliminary study of the coordination chemistry of perfluoroaryl-substituted chromocenes is also included. A common theme in these studies is the use of C_6F_5-substituted cyclopentadienyl ligands, which enable reactions of metallocenes to be followed by 19F NMR spectroscopy. This chapter reviews (1) the history of group 4 catalysts in olefin polymerization (2) the development of group 4 metallocenes as catalysts (3) the synthesis and characterization of MAO, an important cocatalyst for olefin polymerization, and (4) existing experimental studies of metallocenes and alkylaluminum compounds.

Ziegler-Natta Polymerization

In the early 1950s, Ziegler and Natta demonstrated that mixtures of titanium tetrachloride ($TiCl_4$) and triethylaluminum (Et_3Al) could catalyze the polymerization of both ethylene and propylene.[1] Ziegler produced high-molecular-weight, high density polyethylene at low pressures (up to 30 atm), and at temperatures as low as 20-50 °C, while Natta reported the production of crystalline, isotactic polypropylene. While Ziegler's research served as the basis for today's commercial polyolefin manufacturing processes, Natta's interest in the structure of the catalyst began nearly 50 years of research into catalyst design.

First Generation Ziegler-Natta Catalysts

Broadly defined, a Ziegler-Natta catalyst is any combination of an aluminum alkyl with a transition metal halide, alkoxide, or alkyl of groups 4 to 8.[2] Different "generations" are based upon variations in the catalyst composition, including supports and other modifiers. Natta, while investigating the polymerization of propylene, discovered that the active species in the $TiCl_4/Et_3Al$ system was $TiCl_3$, formed via the reduction of $TiCl_4$ by the aluminum alkyls (eq 1.1-1.2).[3]

$$TiCl_4 + 1/3\ AlEt_3 \rightarrow TiCl_3 \bullet 1/3\ AlCl_3 + 1/2\ C_2H_6 + 1/2\ C_2H_4 \qquad (1.1)$$

$$TiCl_4 + 1/2\ AlEt_2Cl \rightarrow TiCl_3 \bullet 1/2\ AlCl_3 + 1/2\ C_2H_6 + 1/2\ C_2H_4 \qquad (1.2)$$

Catalytic $TiCl_3$ may assume four different structural modifications, α, β, γ, and δ. The β form is brown, with a chainlike structure (Figure 1.1), while the α, γ, and δ forms are deep purple with layered structures (Figure 1.2).

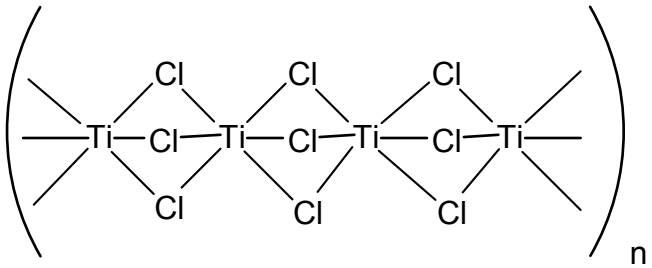

Figure 1.1. β-$TiCl_3$

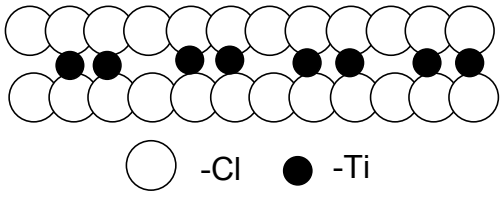

Figure 1.2. Individual $TiCl_3$ Layer

The different forms (α, γ, and δ) arise from variations in the packing of the layers. In each form, titanium atoms occupy two-thirds of the octahedral holes between two chloride layers. In the α-$TiCl_3$ form, the chloride layers are hexagonal closest packed, whereas they are cubic-closest-packed in the γ-$TiCl_3$ form. The δ-$TiCl_3$ form packs in a manner that is intermediate between the α- and γ-forms. Natta found that the β-$TiCl_3$ produced low isotacticity polypropylene while the α-, γ-, and δ-$TiCl_3$ yielded high isotacticity.

In the first generation, $TiCl_3 \bullet 1/3AlCl_3$ was precipitated from a hydrocarbon solution of $TiCl_4$, reduced at low temperature by Et_3Al.[3] However, the precipitate was β-$TiCl_3$. In order to convert into a more useful form (γ-$TiCl_3$), the slurry was annealed at 160-200 °C for several hours. Unfortunately, the conversion of β-$TiCl_3$ at high temperatures resulted in large particles of γ-$TiCl_3$, which decreased the activity of the catalyst system. While these catalysts polymerized ethylene and propylene, their selectivity and efficiency were modest. Two initial approaches toward improvement were (1) to ball-mill the $TiCl_3$ crystallites in order to generate smaller particles, creating more active centers and (2) to vary the cocatalyst, which is an important part of the Ziegler-Natta catalyst

The initial choice for the generation of the active $TiCl_3$ species was Et_3Al. With diethylaluminum chloride (Et_2AlCl), the degree of isotacticity increased from 70-85% to 90-95%. In contrast, the more Lewis acidic ethylaluminum dichloride ($EtAlCl_2$) was inert as a cocatalyst and actually poisoned otherwise active catalysts. Unfortunately, some $EtAlCl_2$ was formed in situ from Et_3Al during the reduction of the $TiCl_4$.[3]

Second Generation Ziegler-Natta Catalysts

The two major limitations of the first generation were poisoning by $EtAlCl_2$ and the large size of the $TiCl_3$ crystallites. While the second-generation catalysts were still a combination of $TiCl_4$ and an alkylaluminum, a simple modification in the preparation of the catalyst resulted in an increase in catalyst performance by a factor of four or more, without losing any stereoselectivity.

In the second generation, β-$TiCl_3 \bullet xAlCl_3$ was again precipitated from the reduction of $TiCl_4$ with an alkylaluminum at low temperature.[3] However, $AlCl_3$ was then extracted with ether before the conversion into γ-$TiCl_3$. The mixture was then annealed at 60 – 100 °C in the presence of excess $TiCl_4$. The use of $TiCl_4$ during the anneal removed the excess ether and catalyzed the transformation of β-$TiCl_3$ into γ-$TiCl_3$ at low temperatures (< 100 °C). Despite the fact that the second-generation catalysts were an improvement upon the first generation, problems still remained. The catalytic species needed to be deactivated (quenched) after polymerization, solvent removed in order to purify the polymer, and the amount of residual catalyst in the polymer minimized.

Third Generation Ziegler-Natta Catalysts

Third generation catalysts are supported second-generation catalysts and are strictly heterogeneous. Magnesium chloride ($MgCl_2$) is the optimal support for $TiCl_3$ because it has the same layer structure as the stereoselective γ-$TiCl_3$ catalysts which allows for epitaxial adsorption and small particle formation.[3] Supporting the catalyst provides several benefits. The polymerization can now be carried out in a solvent medium (slurry) or in the gas phase (fluidized bed).[4] Gas phase polymerization does not use solvents, so product recovery becomes easier and much cheaper. Immobilization also

disperses the catalyst and provides more exposed catalytic sites, increasing the activity per mole of titanium. Supporting the catalyst also minimizes bimetallic interactions between Ti atoms, which can decrease the catalytic activity (a problem in the first and second generations). Most of the demand for linear polyethylene today is still met by using $TiCl_3/MgCl_2/AlR_2Cl$ and related chromium-on-silica catalysts.

Metallocenes Catalysts

Metallocenes are traditionally defined as cyclopentadienyl (Cp) complexes of transition metals.[5] Cp ligands have a stable ring π-electron system that coordinates to a metal ion with the bonding distributed equally among the five carbon atoms of the ring.

The first metallocene, ferrocene $(C_5H_5)_2Fe$, was reported in 1951 by Kealy and Pauson.[6] The discovery of other bis(cyclopentadienyl)metal complexes broadened the definition of a metallocene to include (1) dicyclopentadienyl metals $(C_5H_5)_2M$ (M = transition metal), (2) dicyclopentadienyl metal halides $(C_5H_5)_2MX_{1-3}$ (X = halide), and (3) monocyclopentadienyl metal compounds $(C_5H_5)ML_{1-3}$ (L = CO, NO, halide, alkyl, etc).[5] Shortly after Wilkinson[7] developed synthetic approaches to group 4 and 5 metallocene dichlorides in the mid 1950s, the use of these complexes as polymerization catalysts was investigated.

Two of the earliest reports of metallocene dichlorides as polymerization catalysts used a Ti(IV) species, Cp_2TiCl_2. Natta[8] and Breslow[9] reported that a mixture of Cp_2TiCl_2 and an alkylaluminum compound (Et_3Al and Et_2AlCl, respectively), polymerized ethylene in hydrocarbon solvent with moderate activity, but propylene was not polymerized. Neither Cp_2TiCl_2 nor Et_3Al produced polymer independently under the same conditions. Et_3Al does oligomerize ethylene but only above 100 °C and at fairly

high pressure. The activity of these catalysts decreased continuously over time due to alkyl exchange, hydrogen transfer and reduction to inactive titanium(III) species and could not compete with heterogeneous catalysts.[10,11] Due to these limitations, the next two decades saw little advancement in the area of metallocene polymerization catalysts.

Although Ziegler-Natta catalysts are sensitive to hydrolysis, traces of water actually enhanced the polymerization activity of $Cp_2TiCl_2/AlEtCl_2$.[12] Similar results were obtained for different titanocene catalysts.[13-15] Breslow and Long proposed that the reaction of alkylaluminum halide and water resulted in a bridged compound, $ClR_2Al\text{-}O\text{-}AlR_2Cl$, which formed a stable, highly active complex with Cp_2TiCl_2.[13]

Motivated by these results, Sinn and Kaminsky reported that the addition of water to the aluminum component before mixing with the metallocene increases the activity of Cp_2TiCl_2.[4,16] Further work demonstrated that using methylaluminoxane (MAO) as the cocatalyst with Cp_2TiMe_2, Cp_2ZrMe_2, and Cp_2ZrCl_2 results in highly active catalysts for both ethylene and propylene.[17] This simple experiment prompted over 20 years of research in the field of metallocene/aluminoxane catalysts.[10,17-22]

Aluminoxanes

Aluminoxanes are a group of compounds that have a characteristic oxygen bridge binding two aluminum atoms, (Al-O-Al) and a general structure that can be represented by $[\text{-O-Al(R)-}]_n$ (R = alkyl). While several different aluminoxanes can by prepared (methylaluminoxane, MAO; ethylaluminoxane, EAO; t-butylaluminoxane, TBAO) by varying the alkyl group, MAO is the most active aluminoxane cocatalyst for metallocene catalysts as well as the most difficult to synthesize and characterize. An additional

problem with MAO is the high cost of trimethylaluminum, Me_3Al, the alkylaluminum precursor.

Synthesis of Methylaluminoxane

Organoaluminum compounds react violently when combined directly with water at room temperature producing only decomposition products (eq 1.3).[22] Therefore,

$$R_3Al + 3\ H_2O \rightarrow Al(OH)_3 + 3\ RH \qquad (1.3)$$

aluminoxanes are synthesized by the controlled partial hydrolysis of corresponding alkyl aluminum compounds. There are two general synthetic methods (1) reaction of organoaluminum compounds with water, (2) reaction with species containing reactive oxygen.

Hydrolytic Methods

Water has traditionally been introduced either directly or through a hydrate salt. Water can be directly introduced to a solution of the organoaluminum at low temperature,[23] or the organoaluminum can be added dropwise to wet benzene or toluene.[24] Direct addition of water can also be achieved with water vapor, water entrained in a nitrogen stream,[25] or by slow condensation into a cooled solution of organoaluminum.[26] While these direct methods produce the desired aluminoxanes, the reactions can be hard to control.

Razuvaev et al.[27] first demonstrated that the amount of water introduced into the reaction mixture could be better controlled by using copper sulfate hydrate (eq 1.4).

$$8\ AlR_3 + CuSO_4 \bullet 5H_2O \rightarrow 4\ RAl\text{-}O\text{-}AlR + CuSO_4 \bullet H_2O + 8\ RH \qquad (1.4)$$

Several different salts, such as $Al_2(SO_4)_3 \bullet 18H_2O$, $Al_2(SO_4)_3 \bullet 15H_2O$, $FeSO_4 \bullet 7H_2O$ can also be used. While control of the hydrolysis is achieved with these hydrate salts, the major drawback is that about 40% of the Al is lost as insoluble byproducts. To avoid this

problem, and to convert almost 90% of the organoaluminum into aluminoxane, lithium salt hydrates such as $LiCl \bullet H_2O$ or $LiOH \bullet H_2O$ can be used.[28]

Non-Hydrolytic Methods

Several methods have been reported for the synthesis of aluminoxanes without the use of any form of water. Some of the most common methods are described.

Zakharkin[29] produced tetraisobutylaluminoxane by reacting diisobutylaluminum hydride with an amide (eq 1.5) while Harney[30] allowed a carboxylic acid to react with trimethylaluminum to produce tetramethylaluminoxane (eq 1.6).

$$RCONR_2 + 2\ i\text{-}Bu_2AlH \rightarrow i\text{-}Bu_2AlOAl\text{-}i\text{-}Bu_2 + RCH_2NR_2 \qquad (1.5)$$

$$MeCO_2H + 2\ Me_3Al \rightarrow Me_2AlOAlMe_2 + Me_2CO \qquad (1.6)$$

Kosinska[31] reported that the reaction between methoxyaluminum ($Me_x(OMe)AlCl_{2-x}$, x = 0, 1, 2) with methylaluminum chloride (Me_yAlCl_{3-y}, y= 1, 2, 3) and Et_3Al produced aluminoxanes along with alkanes and methyl chloride. Boleslawski[32] showed that an aluminoxane could be synthesized by treating PbO with an organoaluminum (eq 1.7)

$$2\ R_3Al + PbO \rightarrow R_2AlOAlR_2 + PbR_2 \qquad (1.7)$$

Characterization and Structural Determination of Aluminoxanes

MAO is the most commonly used aluminoxane cocatalyst for the activation of metallocene precatalysts. However, understanding the mechanism of the reaction between MAO and a metallocene is still a major obstacle because the structure of MAO is not known. MAO is a complex "black box" mixture of compounds arising from oligomerization and disproportionation reactions. An X-ray structure of any component of commercial MAO has not been obtained. Determination of the structure must be

interpreted from ^{1}H, ^{13}C, and ^{27}Al NMR, comparison with well-characterized related compounds, or computational modeling.

MAO is soluble in toluene and benzene and the residues obtained from removal of solvent are white amorphous powders or glassy solids. X-ray powder diffraction confirms the amorphous nature. The degree of oligomerization is generally between 5 and 30, the C/Al ratio varies from 1.1 to 1.6, and the aluminum content is around 45%.[33] Cryoscopy has been used by several groups in an attempt to determine the molecular weight of MAO. However, in order to get dependable results, any residual solvent or Me_3Al must be removed and any solubility problems have to be addressed. Imhoff[34] reported molecular weights from cryoscopy in dioxane and corrected for Me_3Al content in the range 700-1000 g/mol, while Sinn[35] reported molecular weights in benzene or Me_3Al in the range 1000-1200 g/mol. Other values between 400 and 3000 g/mol have also been reported.[36,37]

Analysis of MAO by ^{1}H NMR spectroscopy revealed two main resonances: One very broad signal at –0.35 ppm and another sharper peak at –0.20 ppm. The former peak corresponds to the methyl groups of oligomeric $[\text{-O-Al(Me)-}]_n$. The observed broadening of the peak could be attributed to (1) the existence of several species having different structures (cyclic or linear) or (2) the tendency of MAO to aggregate,[33] leading to slow tumbling rates in solution. Independent analysis demonstrated that the sharp signal represented free Me_3Al in the sample. Commercially prepared MAO always contains residual Me_3Al and repeated extraction or vacuum evaporation can minimize but not completely remove the residual Me_3Al. Analysis by ^{13}C NMR spectroscopy showed an intense broad peak at –6.55 ppm.[33] Independent analysis revealed that the ^{13}C NMR

spectrum of Me_3Al consisted of a single sharp peat at –7.28 ppm.[38] The methyl resonances of other methyl alkoxy aluminum compounds are extremely broad, apparently due to quadrupolar coupling of the methyl carbon to the ^{27}Al nucleus (I = 5/2).[39] The downfield shift of the observed peak for MAO is in agreement with the inductive effect of the oxygen atoms. Additional structural information could not be obtained because of the quadrupolar relaxation by ^{27}Al NMR.

Sugano et al. used ^{27}Al NMR to investigate the structure of MAO. The chemical shift of the aluminum centers is 154 ppm for several different samples.[40] This is approximately the same as the chemical shift of tetracoordinate "bound" Me_3Al (153 ppm).

There is a useful relationship between the chemical shift and the coordination number of alkyl aluminum. A tetracoordinate Al atom shows a chemical shift between 140 and 180 ppm, tricoordinate between 250 and 300 ppm, and pentacoordinate between 100 and 125 ppm.[41] The line width of the peak is also useful. The line width, which is related to the mobility of the Al atom, was 1400 Hz for MAO, compared to 700 Hz for Me_3Al. Also the line width appeared to be related to the molecular weight of the MAO (Table 1.1).[40]

Table 1.1. Relationship Between ^{27}Al Line Width and Degree of Oligomerization of MAO[40]

Sample[a]	N[b]	Line Width (Hz)
MAO-1	14	1400
MAO-2	20	1650
MAO-3	21	1690

a: three MAO samples purchased from Tosch-Akzo Co.
b: N: $(RAlO)_N$; Benzene cryoscopic data

The effect of temperature on the ^{27}Al NMR was investigated for a sample of MAO which contained 1/10 mole triisobutylaluminum. At 90 °C, the line width decreased (2750 →

1690 Hz), suggesting that Al atoms undergo ligand exchange and reorganization more freely at higher temperature. The peak also shifted to lower magnetic field (152 → 164 ppm), which may indicate a smaller contribution from tetracoordinate structures. Based upon these results, a ladder structure for MAO was suggested (Figure 1.3).[40]

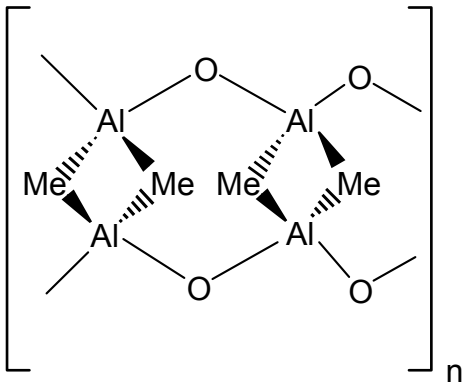

Figure 1.3. Proposed Dimethyl-bridged MAO Structure

Bryant used solid state ^{27}Al NMR along with ab initio molecular orbital calculations to investigate the structure of MAO.[42] Three model structures (Figure 1.4), $[(MeAl)(OMe)]_6$, **1** $[(MeAl)(OMe)]_{12}$, **2**, an edge-bridged dimer of **1**, and $[(MeAl)(OMe)]_{12}$ **3** a face-bridged dimer of **1** were proposed; calculations were performed to determine the C_q (quadrupole coupling constant) and η (asymmetry parameter) for each structure (Table 1.2)

Two samples of MAO were used for the solid state ^{27}Al NMR experiments, MAO_{solid}, prepared by removal of solvent from commercial MAO, and MAO_{gel}, prepared by allowing a solid sample of MAO to naturally gel at room temperature and prior to removal of excess solvent. A field-swept NMR experiment of MAO_{gel} was performed over four different fields, 254, 229, 215, and 152 MHz. Upon inspection of the spectra, it was concluded that **1** was not a good model for MAO_{gel}, while **2** proved to be the best model.

Table 1.2. Calculated ^{27}Al NMR Parameters for Aluminoxane Cage and Two Dimers[42]

Compound	Site	C_q/MHz	η
1, $[(MeAl)(OMe)]_6$ (cage, 4-coord, AlO_3C)	1	-21.43	0.646
	1	-24.06	0.751
	1	-18.91	0.618
	1	-23.71	0.742
2, $[(MeAl)(OMe)]_{12}$ edge-bridged dimer of **1**	1	-19.5	0.47
	5	-22.1	0.54
	9	-15.4	0.63
	11	-16.5	0.20
3, $[(MeAl)(OMe)]_{12}$ face-bridged dimer of **1**	1	-16.49	0.906
	5	-18.04	0.614
	9	-22.57	0.407

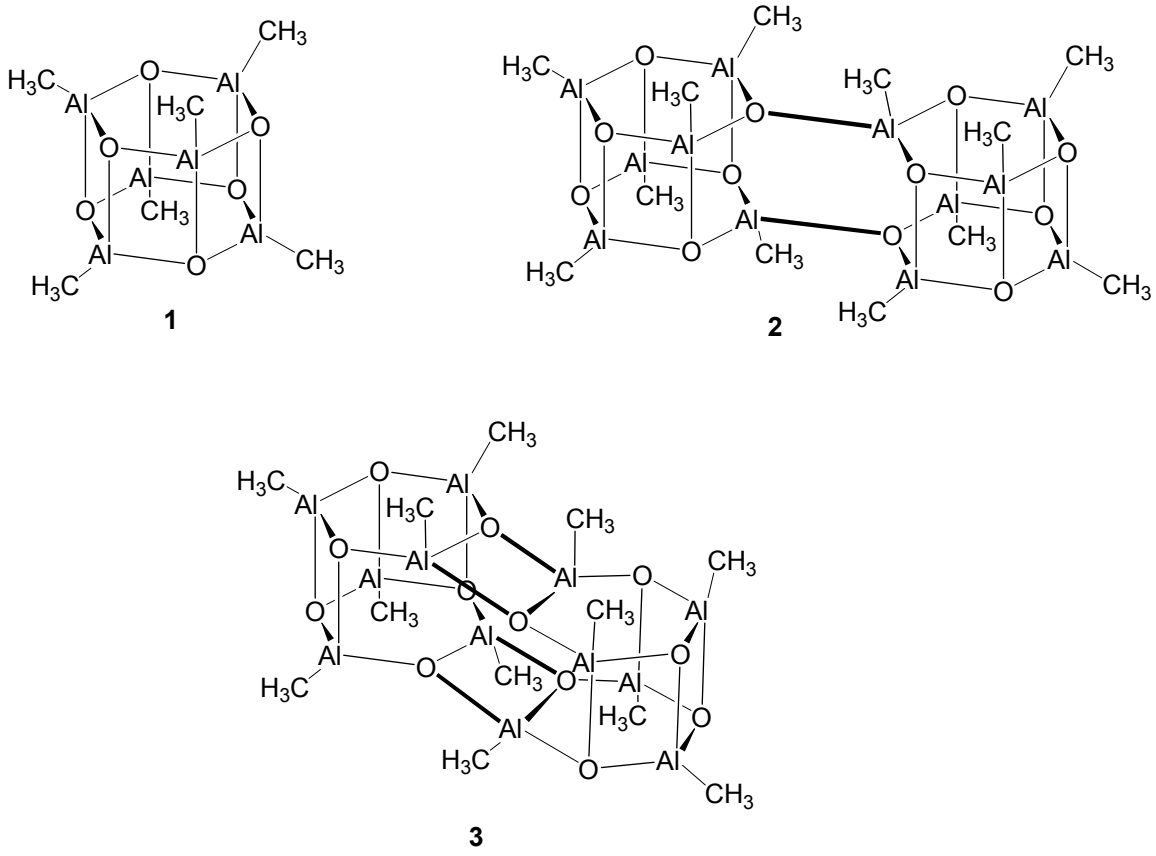

Figure 1.4. Model Structures for Principal MAO Components[42]

High-field, MAS NMR experiments were performed on both MAO_{solid} and MAO_{gel} at high spinning rates. The spectra of MAO_{solid} and MAO_{gel} were not overwhelmingly different, so the only difference between the samples was in their line widths compared with field-swept NMR (Figure 1.5). As in the field-swept experiment, this experiment demonstrated that **1** was not a good model for either MAO_{solid} or MAO_{gel}. However, both **2** and **3** proved to be reasonable models; some combination of the two species could account for the observed experimental spectrum.

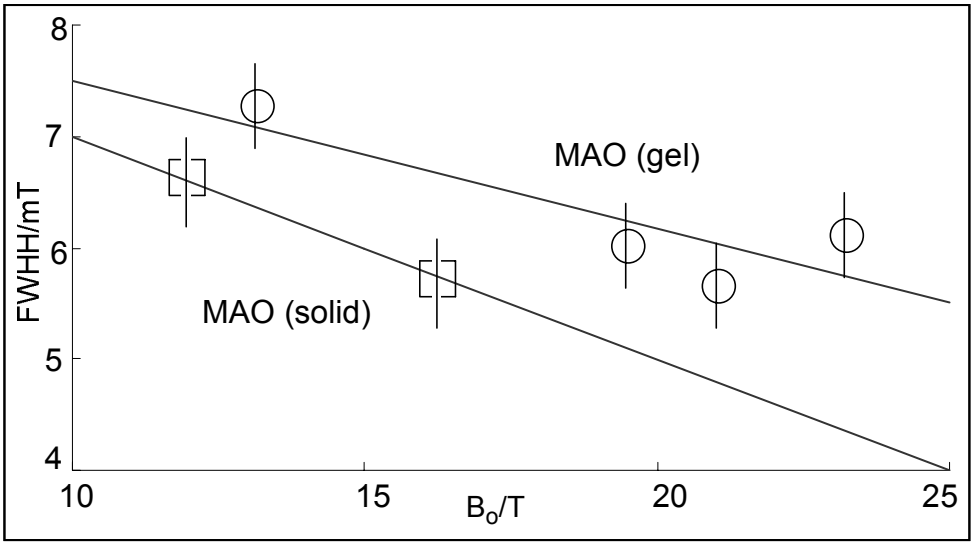

Figure 1.5. Measured Line Widths as a Function of Field Strength[42]

Gel permeation chromatography was also used in an attempt to elucidate the structure of MAO. Cam synthesized MAO from the reaction of $AlMe_3$ and $Al_2(SO_4)_3 \bullet 18$ H_2O in toluene at 70 °C. The reaction was filtered and separated into an A and B sample. MAO A was obtained from the clear filtrate after the toluene was removed. MAO B was obtained from the caramel-like residue that was washed several times with hexane to ensure "complete" removal of $AlMe_3$.[43] GPC analysis of MAO A showed trimethylaluminum and traces of other products in the range of M_w = 400 – 2800.

Although MAO B was not completely soluble in toluene, the GPC of the soluble portion was different from that of MAO A. The GPC spectrum showed six peaks of different molecular weights ranging from 144 - 1580. While it is impossible to verify that the six peaks correspond to six pure components or to adducts formed by association of lower-molecular-weight compounds, the data suggest that the substance contains several discrete compounds. When a second sample of MAO B was analyzed by GPC, only a portion of the compounds present in the first sample were observed. However, a controlled thermal treatment of the sample resulted in the formation of compounds similar to those present in the first sample.[43] These results suggest that the compounds and their relative proportions within a sample of MAO may change during the course of a typical olefin polymerization reaction at elevated temperature.

MAO is usually represented by the general formula $[\text{-OAlMe-}]_n$, which contains at least one bridging μ-oxo group between two aluminum atoms.[44,45] However, as shown above, the structure is not easily elucidated using standard spectroscopic techniques, and a wide range of cyclic, linear, and caged structures have been proposed. Sinn and Kaminsky[4] reported a cyclic structure, containing five aluminum atoms, isolated by fractional precipitation and analyzed by mass spectroscopy and cryoscopy (Figure 1.6).

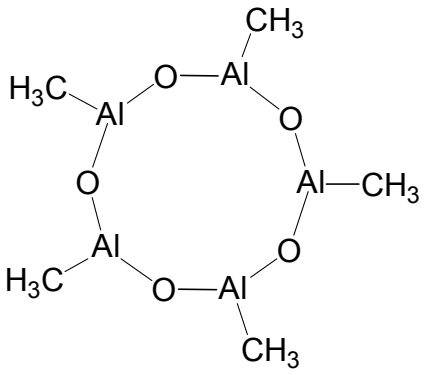

Figure 1.6. Proposed Cyclic Structure of Aluminoxane

This proposed structure would require tri-coordinate aluminum atoms and di-coordinated oxygen, which are rare in Al/O chemistry. Unless oligomerization is hindered by sterically bulky ligands, Al/O compounds tend to maximize their coordination number to four for aluminum and three for oxygen, through bridging ligands and the formation of dimers and trimers.[28] As a result, most authors have proposed structures for MAO which contain four-coordinate aluminum atoms. Double chains, with Al-O crosslinks[33,46] and methyl bridges[40] that allow aluminum and oxygen to be 4- and 3-coordinate, respectively have been proposed (Figure 1.7).

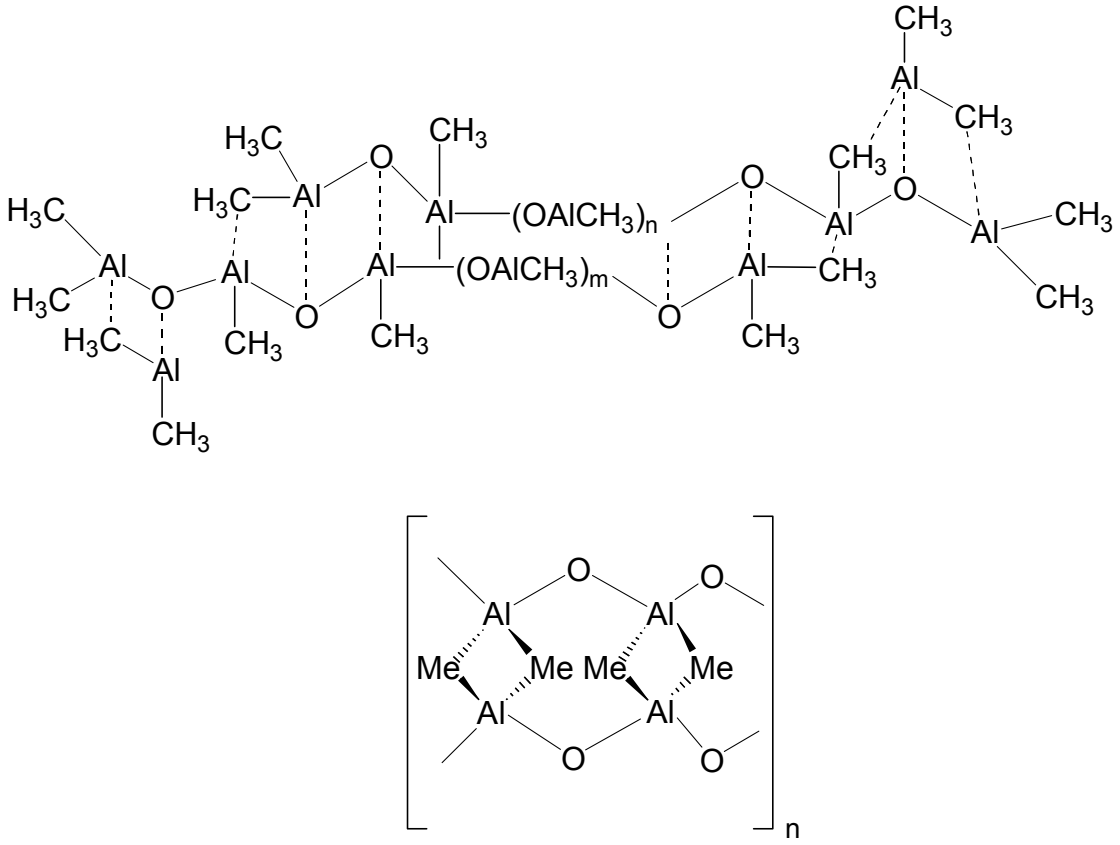

Figure 1.7 Proposed MAO Structures with 4-Coordinate Aluminum Centers

No X-ray structure of any component from a MAO mixture prepared traditionally (hydrolytic and non-hydrolytic) has been reported. However, Atwood determined the X-ray crystal structure of two MAO anions prepared using non-traditional synthetic

methods. The reaction of KO_2 with two equiv of Me_3Al results in large crystals of $K[Al_7O_6Me_{16}]\bullet C_6H_6$.[47] The crystal structure of the $[Al_7O_6Me_{16}]$ anion is shown in Figure 1.8a. The reaction between sodium cacodylate, $Na[AsMe_2O_2]$ and Me_3Al resulted in crystals of $[AsMe_4]_2$ $[Me_2AlO\bullet AlMe_3]_2$.[48] The crystal structure of the dianionic $[Me_2AlO\bullet AlMe_3]_2^{2-}$ is shown in Figure 1.8b. The aluminum atoms in both of

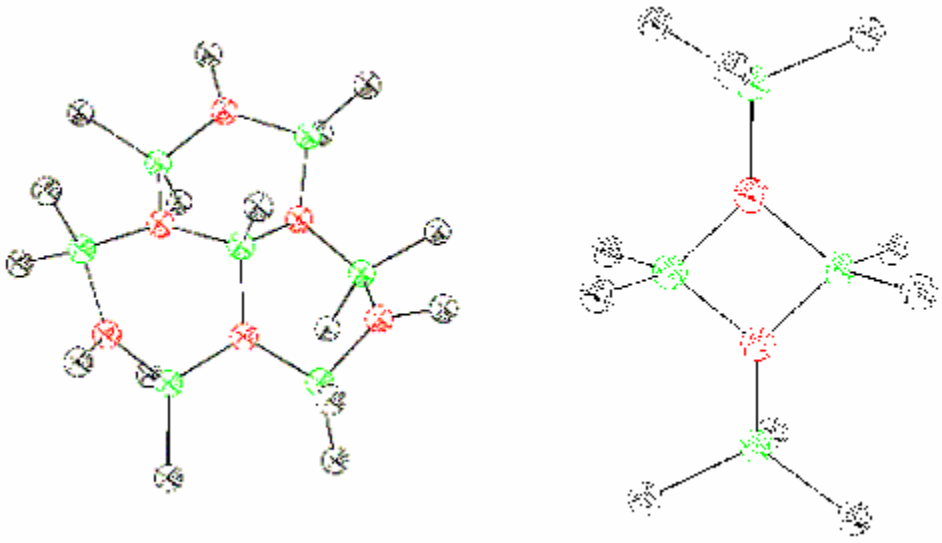

$[Al_7O_6Me_{16}]^-$ $[Me_2AlO\bullet AlMe_3]_2^{2-}$

Figure 1.8. Molecular Structures of Methylaluminoxane[47,48]
O - red, Al - green, C - black.

these structures are four-coordinate while the oxygens are three-coordinate. Barron reported some crystal structures of aluminoxanes that contained t-butyl groups, $[(^tBu)_2Al\{\mu\text{-}OAl(^tBu)_2\}]_2$ (**4**), $[(^tBu)Al(\mu_3\text{-}O)]_6$ (**5**) and $[(^tBu)Al(\mu_3\text{-}O)]_9$, (**6**) with four-coordinate and three-coordinate aluminum and oxygen atoms, respectively (Figure 1.9).[49]

Rytter[50] used a combination of IR, *in situ* IR spectroscopy, polymerization experiments, and density functional theory (DFT) calculations to provide insight into the structure of MAO. Beginning with the different results about the structure of MAO in the

literature,[4,33,35,39,46-49,51] He proposed a cage structure for MAO. DFT calculations demonstrated that cage structures made up of 4- and 6-membered interconnected rings

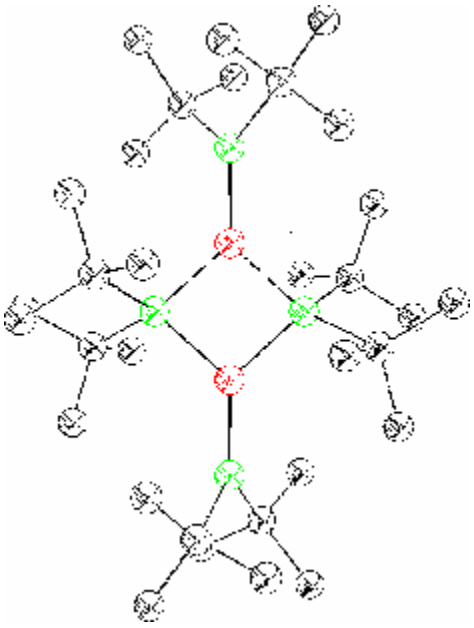

$[(^tBu)_2Al\{\mu\text{-}OAl(^tBu)_2\}]_2$

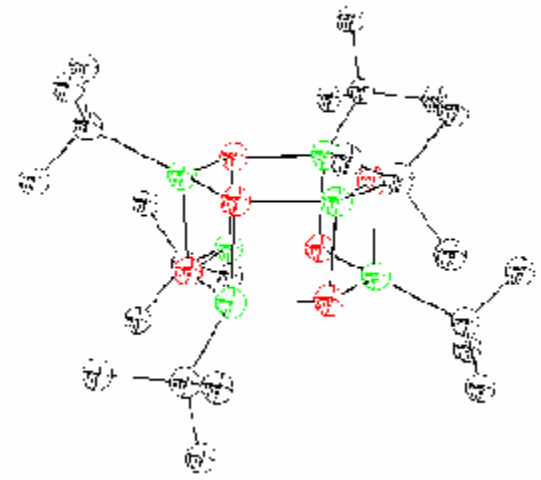

$[(^tBu)Al(\mu_3\text{-}O)]_6$

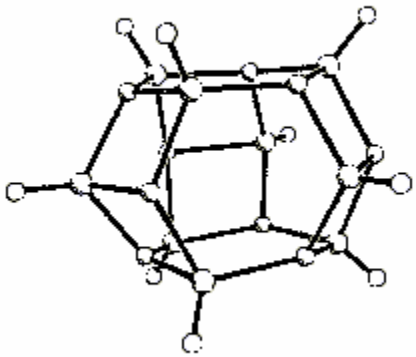

$[(^tBu)Al(\mu_3\text{-}O)]_9$

Figure 1.9. Molecular Structures of Tri-*tert*-butlyaluminoxanes[49]
O - red, Al - green, C - black.

with the general formulas $Me_{6m}Al_{4m}O_{3m}$ (m = 3 predominantly, but possibly 2 and 4) (Figure 1.10), were more stable than proposed linear, cyclic or double-chain structures. Based upon the reported Me-to-Al ratio of 1.5 and molecular weights for MAO, the most stable structures corresponded to m = 3. Thus, three cage structures **7**, **8**, and **9** (Figure 1.11) with the formula $Me_{18}Al_{12}O_9$ were proposed to be major components in MAO solutions. Structures **7**, **8**, and **9** are all based upon the same $(MeAlO)_9$ central cage. A fourth structure, **10** (Figure 1.12) was also suggested as a possible component in MAO solutions although it was based upon a smaller central cage $(MeAlO)_6$.

An important feature of the proposed structures was that while the cages are rigid, the bridging methyl groups are labile and reactive. Experimentally, an IR spectrum of MAO in toluene and cyclohexane was obtained showing several peaks corresponding to bridging (1257 cm^{-1}) and terminal (1219 and 1200 cm^{-1}) methyl groups as well as symmetric (808 cm^{-1}) and asymmetric (697 cm^{-1}) Al-O stretches.[50] In order to demonstrate both the reactivity and importance in polymerization of the bridging methyl groups, reactions with Me_2AlCl and Cp_2*ZrCl_2 were investigated. When a Me_3Al-depleted sample of MAO reacted with Me_2AlCl, *in situ* IR showed that the bridging methyl groups were exchanged with chlorine atoms forming "MAO-Cl" and releasing Me_3Al. When MAO-Cl reacted with Cp_2*ZrCl_2 under polymerization conditions, no polyethylene was produced.

The reaction of a metallocene with MAO is often described to as a simple Lewis-acid base reaction. The role of the Lewis-acidic MAO is the abstraction of a halide or methide affording a "cation-like" polymerization catalyst. As discussed above, both three- and four-coordinate aluminum centers have been proposed for the structure of

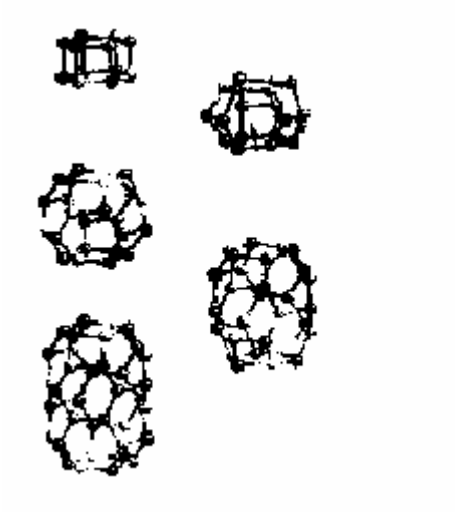

Figure 1.10. Cage Structures $(MeAlO)_{3m}$ (Al – black; O – gray)
Reprinted by permission of John Wiley & Son, Inc.[50]

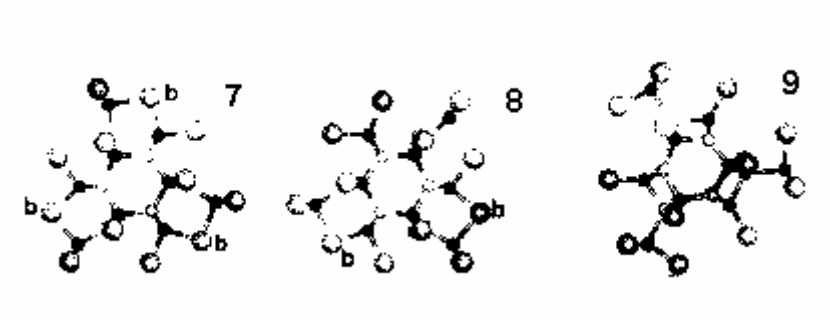

Figure 1.11. Cage Structures with the Formula $Me_{18}Al_{12}O_9$
Reprinted by permission of John Wiley & Son, Inc.[50]

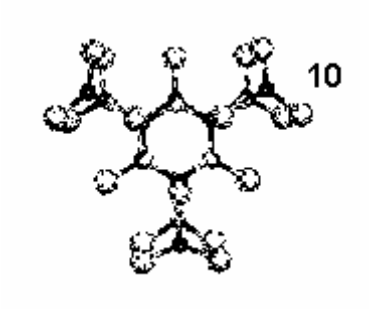

Figure 1.12. Cage Structure Based Upon $(MeAlO)_6$
Reprinted by Permission of John Wiley & Sons, Inc.[50]

MAO. While three-coordinate aluminum centers are strong Lewis acids, an aluminum in a tetrahedral, four-coordinate environment is usually thought not to be Lewis acidic. Compounds **4**, **5**, and **6** allowed Barron[51] to investigate the reactivity difference of aluminoxanes with three- or four-coordinate aluminum centers.

Compound **4** contains two three-coordinate aluminum centers, so it should be sufficiently Lewis acidic for methide abstraction when reacted with Cp_2ZrMe_2. However, ^{1}H NMR analysis of the reaction between Cp_2ZrMe_2 and **4** demonstrated that there was no coordination or abstraction of a methyl group, even with a large excess of **4**. In contrast to this result, the reaction of Cp_2ZrMe_2 with **5**, **6**, or $[(^tBu)Al(\mu_3\text{-}O)]_7$ afforded the methyl transfer products, $[(\eta^5\text{-}C_5H_5)_2ZrMe][(^tBu)_nAl_n(O)_nMe]$ (n = 6, 7, or 9; eq 1.8) and these complexes were active toward the polymerization of ethylene. These results prompted Barron to propose the idea of "*latent Lewis acidity.*" Latent Lewis acidity is defined as the ability of a cage aluminoxane to undergo cage opening, via heteroleptic bond cleavage, to generate a Lewis acidic site.[52]

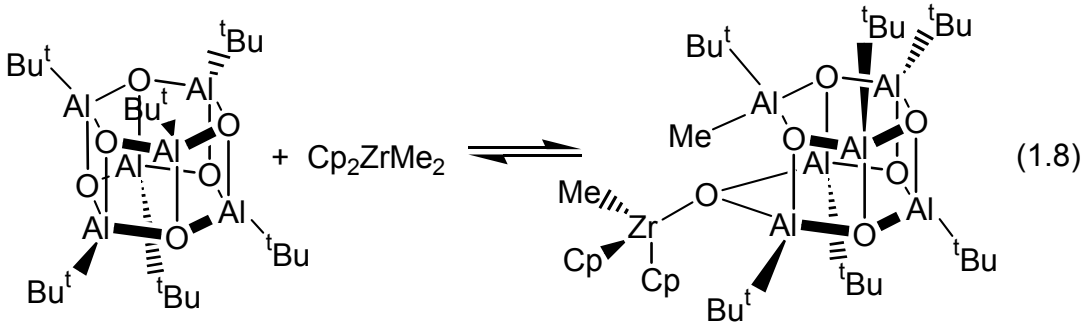

The relative magnitude of the latent Lewis acidity was first proposed to be based upon the relative strain of the cage.[51] Based upon the distortion from an ideal geometry, an estimation of the relative reactivity of the aluminoxane cage structures is shown in eq 1.9.

$$[(^{t}Bu)Al(\mu_3\text{-}O)]_7 > [(^{t}Bu)Al(\mu_3\text{-}O)]_9 > [(^{t}Bu)Al(\mu_3\text{-}O)]_6 \approx [(^{t}Bu)Al(\mu_3\text{-}O)]_8 \quad (1.9)$$

However, when the catalytic rates for the series of aluminoxanes **4**, **5**, and **6** were compared, it was determined that the aluminoxanes reacted in the manner shown in eq 1.10.

$$[(^{t}Bu)Al(\mu_3\text{-}O)]_7 > [(^{t}Bu)Al(\mu_3\text{-}O)]_6 > [(^{t}Bu)Al(\mu_3\text{-}O)]_9 \quad (1.10)$$

The original proposal did not account for any steric hinderance of the Al-O bond (i.e., the steric bulk of the aluminum alkyl group) or the possible strain remaining in the ring opened product. A new approach that accounted for the steric effects in the aluminoxanes was required to develop a reliable predictive measure of latent Lewis acidity. Barron proposed that the relative steric limitations of the aluminoxane in the cage-opening reaction could be determined by reactions with a series of amines with various steric bulk (cone angles).[52] The reaction of **5** with a series of amines demonstrated that it reacted with $^{t}BuNH_2$ ($\theta = 120°$) but not with Et_2NH ($\theta = 140°$). Therefore, Barron proposed that the steric accessibility of the reactive side of **5** is between these two values. At this time only the reactivity of **5** has been reported.

Understanding The Metallocene/Cocatalyst Interaction

Since the early reports of Breslow and Newburg,[9,53] cationic d^0 metal alkyl species Cp_2MR^+ have been implicated as the active components of metallocene olefin polymerization catalysts. In the early 1960s, based upon conductivity and electrodialysis experiments, Shilov proposed that the active species in the soluble Cp_2TiCl_2/AlR_nX_{3-n} system was cationic.[54,55] Breslow et al.[53,56] also proposed a cationic species, most likely the ion pair $[Cp_2Ti(R)][AlR_{n-1}Cl_{5-n}]$ based upon UV-Vis spectroscopic and chemical studies. Titanium is superior to zirconium in UV studies because its ligand-to-metal-

charge-transfer (LMCT) absorptions are in the visible range where there is no interference from solvents or aluminum species. Cossee used this early work to propose a mechanism (Figure 1.13) for the polymerization of ethylene with metallocene/alkylaluminum systems.[57,58] The dual role of the alkylaluminum cocatalyst was to alkylate the transition metal and to activate the resulting $Cp_2M(R)Cl$ species for olefin coordination. The significance of these early studies was questioned when it was realized that adventitious water was present.

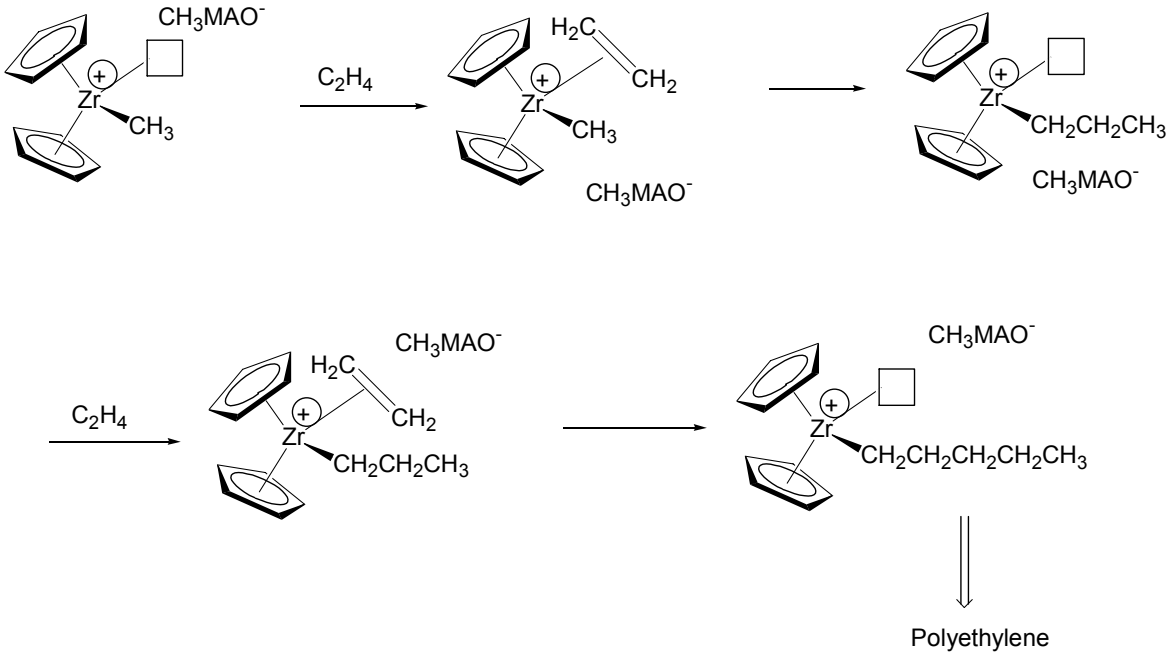

Figure 1.13. Cossee – Arlman Mechanism for the Polymerization of Ethylene[57,58]

Interest in identifying the nature of the active species in soluble Ziegler-Natta polymerization systems was rekindled in the early 1980s by the results of Sinn and Kaminsky. This research can be loosely classified into two areas: (1) investigation of computational and synthetic models and (2) direct spectroscopic measurements of metallocene/MAO mixtures.

Synthetic Models

Bercaw,[59] Marks,[60] and Watson[61] demonstrated that neutral group 3 and lanthanide metal complexes Cp^*_2ScR (R = Me or H) , $Cp^*_2MCH(SiMe_3)_2$ (M = La, Nd, Sm, Lu), and Cp^*_2LuMe, respectively, are active ethylene polymerization catalysts. These compounds are isoelectronic in their monomeric form with $Cp_2M(R)^+$ (M = Ti, Zr) when the *f* electrons are neglected. Importantly, no cocatalyst is needed. Watson expanded on the polymerization results by also demonstrating that $Cp^*_2Lu(R)$ complexes underwent all the key reactions involved in olefin polymerization including olefin insertion (chain propagation), β-H and β-alkyl elimination, and Lu-R bond hydrogenolysis (chain transfer/termination).[62,63]

Eisch reported two important discoveries using $Cp_2TiCl(R)$ (R = Cl or CH_2SiMe_3). First, when Cp_2TiCl_2-$MeAlCl_2$ reacted with the highly substituted surrogate for ethylene, trimethyl(phenylethynyl)silane (**11**), the single insertion product **14** was isolated and its crystal structure determined (eq 1.11).[64] Spectroscopic studies with ^1H, ^{13}C, and ^{27}Al NMR showed that the formation of **14** from **11-13** was the only insertion product. Eisch concluded that the active species formed from **12** and **13** is the methyltitanium cation (**15**, eq 1.12). However, **15** is in equilibrium with a chloride-bridged complex, (**16**, eq 1.13), which has been isolated and a crystal structure determined, and the crucial step in the activation is postulated to be the isomerization of **16** into **15**.

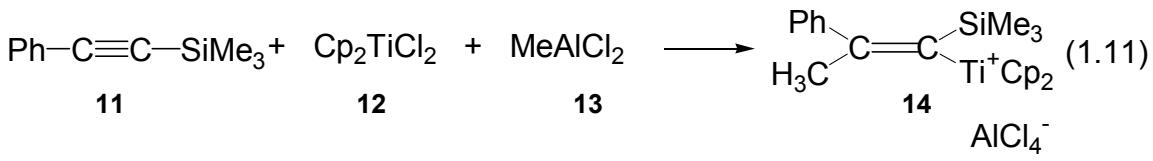

(1.11)

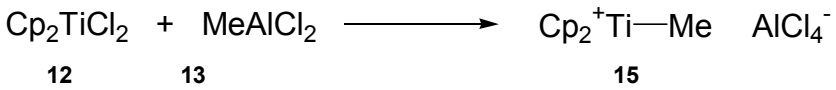

(1.12)

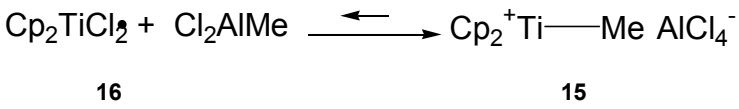

(1.13)

Reacting ((trimethylsilyl)methyl)titanocene chloride (**17**) with $AlCl_3$, Eisch reported direct spectral evidence for the heterolysis of the Ti-Cl bond and the formation of ion pairs (eq 1.14).[65] This alkyltitanium (**18**) species was active for the polymerization of ethylene. Spectral evidence for the formation of **18** was demonstrated using ^{1}H, ^{13}C, and ^{27}Al NMR. In the ^{1}H NMR, the signals of **17** at 2.26 (CH_2) and 6.32 (Cp) ppm are shifted to 3.04 and 6.51 ppm, respectively. The ^{13}C NMR signals of **14** at 2.8 (CH_3), 79.8 (CH_2), and 115.6 ppm (Cp) are shifted to 117.2 and 2.8 ppm. The peak at 79.8 disappears due to the formation of $Me_3SiCH_2AlCl_2$ **19** (eq 1.14) over the time scale needed to obtain a ^{13}C NMR. A peak at 103.3 ppm in the ^{27}Al NMR spectrum provided the best evidence for the formation of **18**. Independent analysis demonstrated that this peak corresponds to the $AlCl_4^-$ ion.[66]

Jordan demonstrated that $[Cp_2Zr(CH_3)(THF)][BPh_4]$ (**20**), an aluminum free cationic metallocene complex, prepared from Cp_2ZrMe_2 and $Ag[BPh_4]$, was a moderately active ethylene polymerization catalyst.[67] This result supported the proposal by Eisch

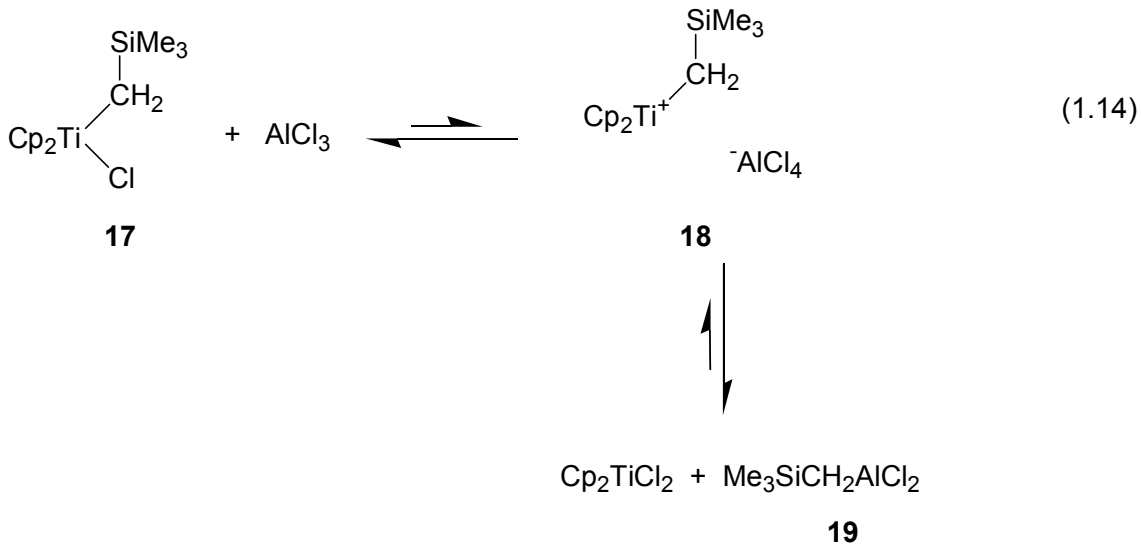

(1.14)

that $Cp_2Ti\text{-}CH_3^+$ was the active species in the $Cp_2TiCl_2/MeAlCl_2$ catalyst. While **20** was an active catalyst, its activity was very low (0.2 g/(mmol of catalyst) min atm at 25 °C and 1-4 atm of ethylene) most likely due the presence of the THF ligand, which competes effectively with ethylene for the open coordination site on zirconium.

Several other examples of aluminum-free cationic complexes have been reported in the literature as olefin polymerization catalysts. Along with **20**, Jordan found that $[(C_5H_4Me)_2Zr(CH_2Ph)(THF)][BPh_4]$, $[(C_5H_4Me)_2Zr(H)(THF)][BPh_4]$, and $[(C_5H_4Me)_2Zr(\eta^3\text{-}C_3H_5)(THF)][BPh_4]$ were all moderately active toward the polymerization of ethylene.[68] Hlatky and Turner[69] reported the polymerization of ethylene with the zwitterionic, base-free catalysts $Cp^*_2Zr^+(m\text{-}C_6H_4)\text{-}B^-(C_6H_4R)_3$ (R = H, Me, Et) and $Cp'_2ZrMe(C_2B_9H_{12})$ (Cp' = Cp* or C_5Me_4Et), while Taube[70] reported ethylene polymerization with $[Cp_2TiMe(L)][BPh_4]$ (L = THF, Et_2O, or MeOPh). Bochmann used two different approaches to make a series of base-free cationic polymerization catalysts. The first approach was protonolysis of $M\text{-}CH_3$ bonds (Figure

1.14).[71,72] Complexes **21a-23a** are all active polymerization catalysts, although catalyst lifetimes are shortened by formation of M-Ph species.

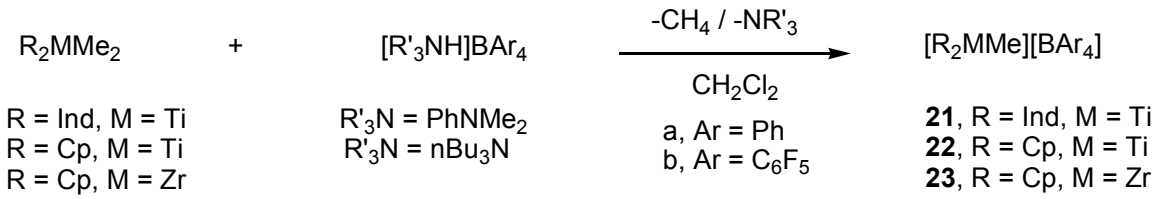

Figure 1.14. Base-Free Cationic Polymerization Catalysts

The second approach was alkide abstraction with trityl salts (Figure 1.15).[73] The fluorinated anions in **24-27** and in **21b-23b** enhance both activity and catalyst lifetimes.

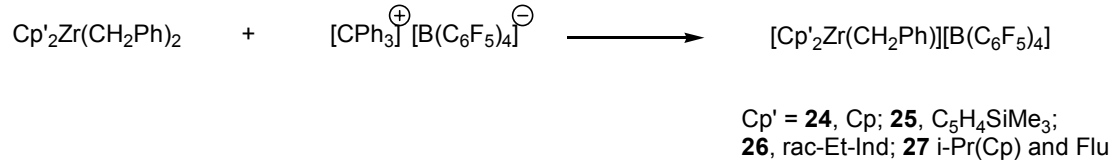

Figure 1.15. Base-Free Cationic Polymerization Catalysts

Marks demonstrated that the Lewis acid tris(pentafluorophenyl)borane[74] could activate dimethylmetallocenes (eq 1.15)[75], and that their NMR spectra showed the

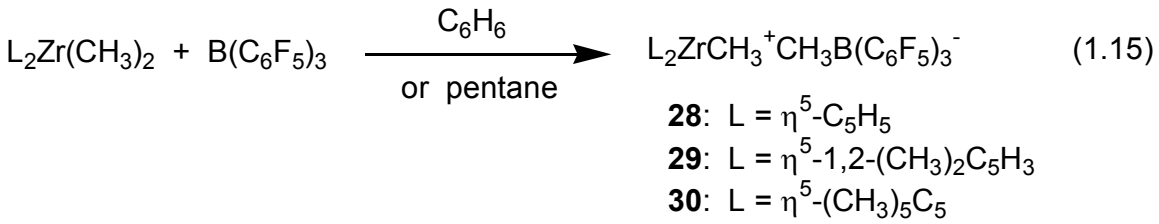

downfield $Zr^{13}CH_3$ signals previously associated with "cation-like" species.[67-71,73,76] This was an important system because it produced a well-defined cationic metallocene, in which the crystal structure could be determined. Furthermore the methide transfer is reversible, as with MAO, and the Lewis acidity of the borane could be modified by changing the borane substituents. Complexes **28-30** were all active homogeneous catalysts for olefin polymerization.

These cationic group 4 metallocene complexes undergo all the key reactions involved in olefin polymerization, including olefin insertion, β-H and β-CH_3 elimination, Zr-R bond hydrogenolysis, and certain types of ligand C-H activation reactions.[76] Thus the analogy between neutral Sc/lanthanide and cationic Ti/Zr catalysts is complete but the Zr catalysts especially are much more active.

A search of the Cambridge Crystallographic Database for metallocene-aluminoxane structures revealed only one such compound. Erker[77] reported a cyclodimeric mixed metal complex $[Cp_2Zr(CH_3)OAl(CH_3)_2]_2$ (Figure 1.16), synthesized via the reaction of $[Cp_2ZrO]_3$ and Me_3Al. While the dimer was not active for the polymerization of ethylene alone (up to 180 °C, 30 atm, 10 h), the addition of MAO [Zr:Al = 1:8] afforded polyethylene. While the nature of the active species is this reaction mixture is unknown, it is likely that the "traditional" $Cp_2Zr\text{-}CH_3^+$ active species is generated and responsible for the activity, and that there is nothing unusual about Erker's compound as a catalyst precursor.

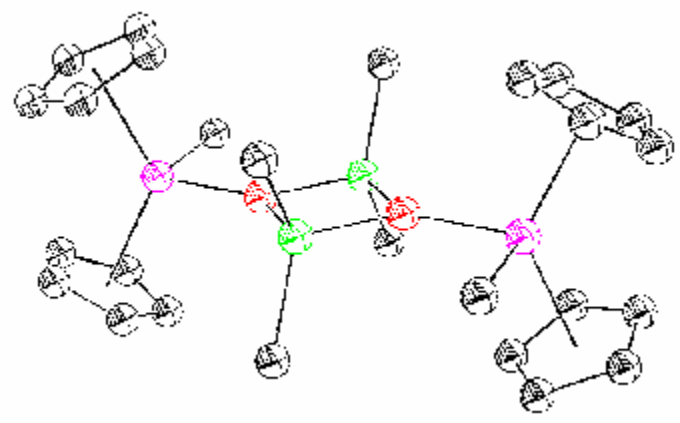

Figure 1.16. Molecular Structure of $Cp_2Zr(CH_3)OAl(CH_3)_2$ dimer[77]
O – Red, Al – Green, Zr – Purple

Direct Spectroscopic Measurements

While all the model systems provided evidence to support the theory that a cationic metallocene complex was the active species in the polymerization of ethylene, more direct methods such as XPS, ^{1}H, ^{13}C NMR, etc., have also been used to provide evidence to support the proposed role of $Cp_2M(R)^+$ ions as the active species.

Gassman reported the first characterization of a highly active homogeneous metallocene polymerization catalyst using a direct spectroscopic method, X-ray photoelectron spectroscopy (XPS), by measuring the binding energy of different zirconium species within catalytic mixtures.[78] Table 1.3 shows the binding energies of dichlorozirconocene, Cp_2ZrCl_2 (**31**) methylchlorozirconocene, $Cp_2Zr(Me)Cl$ (**32**), and dimethylzirconocene, Cp_2ZrMe_2 (**33**) before and after each had reacted with MAO. The reaction with MAO generated three new zirconium derivatives which had the same zirconium(IV) binding energy. The increase in binding energy indicates that these zirconium species are electron deficient in comparison to the three starting materials.

Table 1.3. Binding Energies (Zr $3d_{5/2}$) of Two Distinct Catalytic Species[78]

Compound	Zirconocene (eV)	Catalyst before ethylene addn (eV)	Catalyst after ethylene addn (eV)
31	181.7	182.4	182.1
32	181.2	182.4	182.1
33	180.7	182.4	182.1

Polyethylene was immediately produced when the catalysts were exposed to an atmosphere of ethylene. After the addition of the ethylene, there was no trace of the zirconium species with a binding energy of 182.4 eV. Instead new zirconium species with a binding energy of 182.1 eV were observed. This new material proved to also be active in the polymerization of ethylene.

Marks[79] used CPMAS-NMR to obtain direct spectroscopic evidence for the formation of a cationic metallocene when Cp_2ZrMe_2 was reacted with MAO. Various Al:Zr ratios of MAO:$Cp_2Zr(^{13}CH_3)_2$ (**34**) were combined in toluene, stirred for 1 h, and filtered. The filtrate was evaporated, and the residue was dried under high vacuum. The ^{13}C CPMAS-NMR spectrum obtained for MAO showed a single broad $^{13}CH_3Al$ signal (-6.5 ppm). The spectrum of the **34**/MAO mixture showed two signals representative of $Cp_2Zr(^{13}CH_3)_2$ (31.7 ppm (Zr-CH_3), 111.5 ppm (Zr-Cp)) along with two down-field-shifted signals representative of the "cation-like" $Cp_2Zr(^{13}CH_3)^+$. Marks confirmed these assignments by comparing the chemical shifts to $B(C_6F_5)_3$-activated species.

In order to demonstrate the polymerization activity of these cationic complexes, ethylene was introduced into the **34**/MAO sample and the CPMAS spectra was recorded. With sequential additions of ethylene, the Zr-$^{13}CH_3^+$ peak diminishes relative to the Cp and MAO peaks. A new resonance at 14.5 ppm appeared, corresponding to the terminal $^{13}CH_3$ of an oligomeric chain, while the increase in the relative intensity of the Zr-$^{13}CH_3$ region of **34**/MAO was due to the appearance of the coincident $(CH_2CH_2)_n$ resonances, expected at 32 ppm.[80]

Tritto used both ^1H and ^{13}C NMR to investigate the reaction of titanocene compounds with Me_3Al and MAO in order to obtain evidence for the formation of an active cationic complex.[81-83] When $Cp_2TiMeCl$ (**35**) reacted with Me_3Al, ^{13}C NMR analysis showed that the Cp (115.52 ppm) and Me (49.32 ppm) of **35** had completely disappeared and two new sets of resonances appeared. The first set corresponds to Cp_2TiMe_2 (**36**) (Cp at 113.16 ppm and Me at 46.25 ppm), while the second set corresponds to $Cp_2TiMeCl{\bullet}AlMe_3$ (**37**) (Cp = 117.08 ppm and Me = 60.14 ppm). When

35 was reacted with MAO, a new species with peaks further downfield (Cp at 117.96 ppm and Me at 64.6 ppm)**,** indicating a further decrease in electron density on the metal center.[81] This species was assigned as $Cp_2TiMe^+Cl{\bullet}MAO^-$ and is the only polymerization-active species in the study.

Tritto also used ^{13}C NMR to investigate the $Cp_2Zr(^{13}CH_3)_2$/MAO catalyst system and compare it to the well defined $B(C_6F_5)_3$ activated system. Initially reacting $B(C_6F_5)_3$ with **34** at three B/Zr mole ratios between 0.5 and 2, she found that two distinct species were produced. With B/Zr ratio of 0.5 the resulting cationic species is dimeric $[Cp_2Zr^{13}CH_3]_2(\mu\text{-}^{13}CH_3)^+[^{13}CH_3B(C_6F_5)_3]^-$ (**38** eq 1.16). When the B/Zr ratio is 1, a

$$2\ Cp_2Zr(^{13}CH_3)_2 + B(C_6F_5)_3 \longrightarrow \underset{\mathbf{38}}{[Cp_2Zr(^{13}CH_3)]_2(\mu\text{-}^{13}CH_3)^+[^{13}CH_3B(C_6F_5)_3]^-} \quad (1.16)$$

mixture of **38** and $[Cp_2Zr(^{13}CH_3)]^+[(^{13}CH_3)B(C_6F_5)_3]^-$ (**39**) results. With an excess of $B(C_6F_5)_3$ only **39** is present in the ^{13}C NMR spectrum.[84] Brintzinger found the same trend using ^1H NMR.[85] These results were then used to assign the monomeric and dimeric species that were obtained from reaction of **34** with MAO.

The reaction of **34** and MAO with [Al]/[Zr] = 10 and 20 resulted in the formation of a dimeric cationic species $[Cp_2Zr^{13}CH_3]_2(\mu\text{-}^{13}CH_3)^+[^{13}CH_3MAO]^-$ (**40**, eq 1.17) and a monomeric cationic species $[Cp_2Zr^{13}CH_3]^+[^{13}CH_3MAO]^-$ (**41** eq 1.18).[84] Complexes **40** and **41** exhibit methyl resonances shifted significantly downfield from neutral **34** but only slightly downfield from complexes **38** and **39** (Table 1.4).

$$\underset{\mathbf{34}}{2\ Cp_2Zr(^{13}CH_3)_2} + MAO \longrightarrow \underset{\mathbf{40}}{[Cp_2Zr(^{13}CH_3)]_2(\mu\text{-}^{13}CH_3)^+[^{13}CH_3MAO]^-} \quad (1.17)$$

$$\underset{\mathbf{34}}{Cp_2Zr(^{13}CH_3)_2} + MAO \longrightarrow \underset{\mathbf{41}}{[Cp_2Zr(^{13}CH_3)]^+[^{13}CH_3MAO]^-} \quad (1.18)$$

Table 1.4. ^{13}C NMR Chemical Shifts for Activated Zirconocene Complexes[84]

Zirconocene	Cp (δ, ppm)	Me (δ, ppm)	μ-Me (δ, ppm)	B-Me (δ, ppm)
34	110.45	30.45		
38	113.20, 113.01	38.91, 38.64	23.20, 22.85	11.43
39	114.12	40.61		26.84
40	113.27	39.84	22.54	
41	113.70	40.68		

This downfield shift is attributed again to the electron deficiency of the metal center in the cationic species. These were the first reports of dimeric cationic species with $[MeMAO]^-$ counteranions.

The less commonly used ^{91}Zr NMR has provided direct spectroscopic evidence for the proposed role of $Cp_2M(R)^+$ ions as the active species. Siedle showed that the resulting complex from a mixture of **34** and MAO had two peaks in the ^{91}Zr spectrum, +100 and -100 ppm.[86] The peak at +100 ppm was assigned to a $Cp_2Zr(Me)X$ species, where X is a strongly electron withdrawing group. The model complex that most closely matched the +100 ppm peak and justified the assignment, was Jordan's $[Cp_2ZrMe(THF)][BPh_4]$,[68] ^{91}Zr = 115 ppm. The other possible model, $Cp_2Zr(Me)Cl$, has a ^{91}Zr peak of 32.4 ppm and was not observed in this reaction mixture. The other ^{91}Zr peak at -100 ppm lies in the chemical shift region occupied by compounds of the type $Cp_2Zr(Me)(OR)$ (R = OMe, $OSiMe_2$-*t*-Bu). Thus, the peak at -100 ppm was assigned to a $Cp_2Zr(Me)$-OAl species most probably formed by the cleavage of an Al-O-Al bond of MAO, a process initially proposed by Kaminsky[87] and confirmed by Barron.[51]

Recently, UV-Vis spectroscopy has emerged as a complementary tool for identifying the active species in olefin polymerization.[88-94] The wavelengths of ligand to metal charge-transfer bands (LMCT) of the metallocenes change upon addition of an activator. This technique requires a chromophore such as an indenyl ligand to avoid

interference. Deffieux used UV-Vis spectroscopy to investigate the activation of *rac*-$C_2H_4(Ind)_2ZrCl_2$ (**42**) and *rac*-$C_2H_4(Ind)_2ZrMe_2$ (**43**).[88] The initial absorption band for **42** (λ_{max} = 427 nm) shifted to λ_{max} = 396 nm upon the addition of up to 30 equiv of MAO. The hypsochromic shift was attributed to an increase in electron density on the metal upon exchange of a methyl group for a chlorine. Between 30 and 150 equivalents of MAO a distinct species appeared with λ_{max} = 440 nm, but was inactive toward hexene polymerization. The bathochromic shift was due to the decrease in electron density on the metal, as would be expected during the formation of a cationic metallocene resulting from the abstraction of one of its Cl ligands. With [Al]/[Zr] > 2000, the major species present had λ_{max} = 470 nm, and this species was active toward the polymerization of hexene.

To better understand the identities of the metallocene species with λ_{max} = 440 and 470 nm, similar reactions were investigated starting with **43**. The initial absorption band for **43** (λ_{max} = 367 nm), allowed for the band located at 396 nm to be assigned to *rac*-$Et(Ind)_2Zr(Me)Cl$ (**44**). Activation of **43** with MAO, resulting in complete cation formation, occurs at a low Al:Zr ration ([Al]/[Zr] = 150). This activation is accompanied by a bathochromic shift to λ_{max} = 439 nm and this species was active toward the polymerization of hexene.[88] These results suggest a poisoning effect of the abstracted chloride ligand in the **42**/MAO system at low Al:Zr ratios. However, no information about the structure of the metallocene species with λ_{max} = 470 nm was obtained.

To further characterize the species with λ_{max} = 440 and 470 nm, reactions with Me_3Al-depleted MAO (thermal treatment of commercial MAO) were investigated. The thermal treatment of commercial MAO involved after the removal of solvent,

maintaining the residue at 80 °C under reduced pressure for several hours. When **42** reacted with Me_3Al-depleted MAO, the formation of **44** was first observed as indicated by the band shift from 427 to 396 nm. With [Al]/[Zr] = 150-200 the expected shift to 440 nm was seen, but this species was now active toward the polymerization of hexene, stressing the importance of the associated activator structure on the activity. The further shift in the absorption band to 470 nm was seen with [Al]/[Zr] = 3000, corresponding to the active species formed with commercial MAO.[88]

Based on these results, Deffiuex and Cramail proposed structures for the species absorbing at 440 and 470 nm. Rytter[50] had proposed, based on computational studies, that MAO $Me_{6m}Al_{4m}O_{3m}$ (m = 2-4) has a cage-like structure in which only the labile and reactive bridging methyl groups participate in metallocene activation. Rapid exchange between the active bridging methyl groups of MAO and the chloride ligands of **42** results in chlorine atoms in the bridge positions, rendering MAO-Cl inefficient for the activation of the metallocene. Based up this result the inactive species with λ_{max} = 440 nm corresponds to tight ion pairs formed between cation-like zirconocene and $[MAO\text{-}Cl]^-$ counter ion (Figure 1.17). The addition of large amounts of commercial MAO disrupts

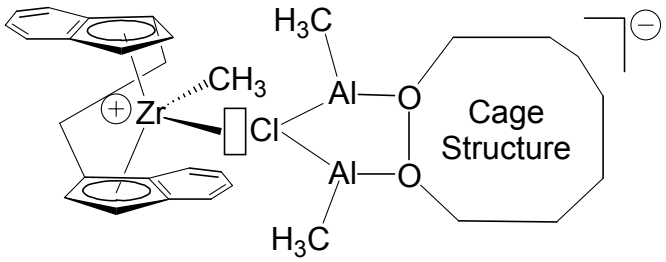

Figure 1.17. Proposed Structure for Cationic Species Absorbing at 440 nm[88]

the interaction between the tight ion pair, resulting in the Me_3Al separated ion pairs (Figure 1.18) active for olefin insertion.[88]

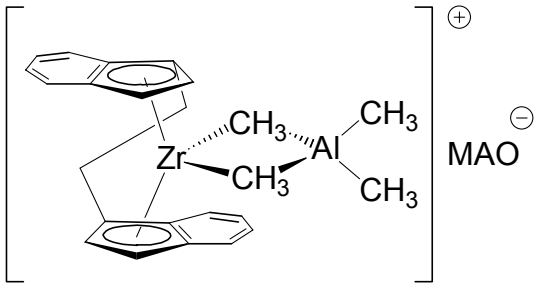

Figure 1.18. Proposed Structure for Active Species Absorbing at 470 nm[88]

Theoretical Studies

The initial computational work that was performed on metallocene polymerization catalysts,[95-99] due partly to limited computer technology, overlooked the importance of the counterions. However, experimental[100-106] and computational[107-109] results have demonstrated that the anionic counterion is an important component in the polymerization process.

Using DFT calculations, Ziegler recently calculated the ion-pair formation energies and ion pair separation energies for the interactions between six group 4 polymerization cations, $(1,2\text{-}Me_2Cp)_2ZrR^+$ (**45**), $(NPMe_3)_2TiR^+$ (**46**), $(Cp)(NPMe_3)TiR^+$ (**47**), $(Cp)(NCMe_2)TiR^+$ (**48**), $(CpSiMe_2NMe)TiR^+$ (**49**), and $(Cp)(OSiMe_3)TiR^+$ (**50**) (R = H, Me, or ^{t}Bu; Figure 1.19) and four non-coordinating anions, $B(C_6F_5)_4^-$ (**51**), $MeB(C_6F_5)_3^-$ (**52**), $MAOMe^-$ (**53**), and $Me_3Al\text{-}MAOMe^-$ (**54**).[110] The calculated ion-pair formation energies were based upon the equation

$$LL'MMe_2 + A \rightarrow [LL'MMe]^+[MeA]^- + \Delta H_{ipf} \qquad (1.18)$$

where L, L' = Cp, NPR_3, NCR_2, $OSiR_3$, $CpSi(Me)_2NR$, A = $B(C_6F_5)_3$, MAO, Me_3Al-MAO and ΔH_{ipf} = enthalpy of ion pair formation. The calculated ion-pair separation energies were based upon the equation

$$[LL'MMe]^+[MeA]^- \rightarrow [LL'MMe]^+ + MeA^- + \Delta H_{ips} \qquad (1.19)$$

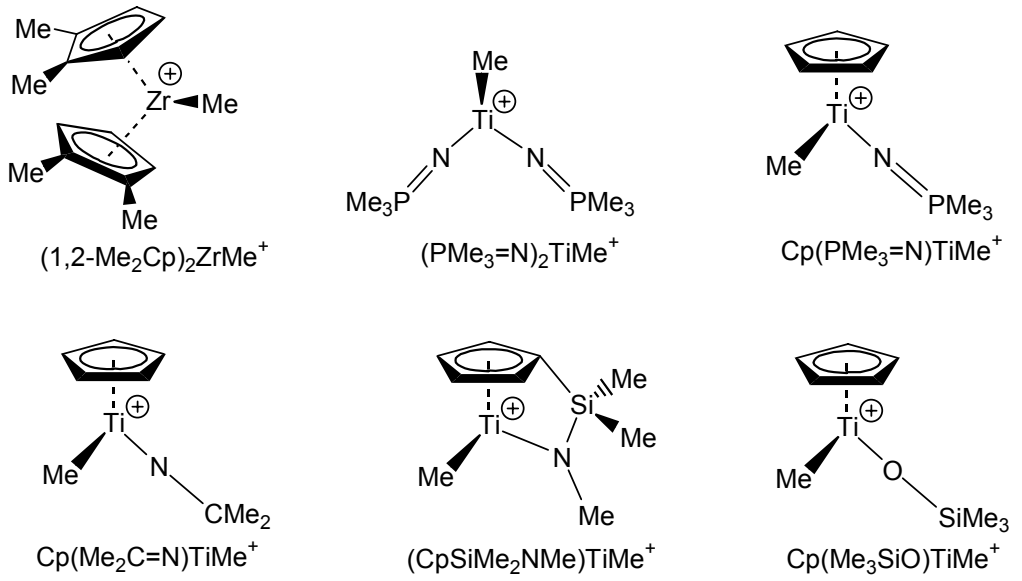

Figure 1.19. Structures of Catalysts[110]

where ΔH_{ips} = enthalpy of ion-pair separation and A = $B(C_6F_5)_3$, MAO, Me_3Al-MAO. The ΔH_{ips} for the $B(C_6F_5)_4^-$ anion was calculated separately based upon eq 1.20.[110]

$$LL'MMe\text{-}B(C_6F_5)_4 \rightarrow LL'MMe^+ + B(C_6F_5)_4^- + \Delta H_{ips} \qquad (1.20)$$

The results of the ion-pair separation calculations demonstrated that among the four counterions **51**, **52**, **53**, and **54**, **51** had the weakest interaction with the cations when R = Me (Table 1.5).

Table 1.5. Ion-Pair Separation Energies (kcal/mol) For Metallocenium Salts[110]

Cation	$B(C_6F_5)_4^-$		$B(C_6F_5)_3Me^-$		$Me_3Al\text{-}MAOMe^-$		$MAOMe^-$	
	gas	soln[a]	gas	soln[a]	gas	soln[a]	gas	soln[a]
45	55.72	23.40	86.98	52.34	87.95	51.82	104.92	63.98
46	58.74	28.91	73.05	41.59	82.50	49.87	102.05	62.05
47	69.86	37.31	84.17	50.86	93.10	55.34	113.91	73.41
48	78.16	43.17	90.08	54.87	99.41	60.20	122.94	80.41
49	73.73	41.54	91.50	56.52	104.32	67.36	129.81	88.24
50	76.84	42.83	91.49	55.46	102.45	64.18	122.02	79.20

a: cyclohexane

The ion-pair separation energies (IPSEs) increased in the order, **51** < **52** < **53** < **54** for each of the catalysts. Ziegler found that when the IPSEs of the six catalysts were compared with one counterion and R = Me, **46** had the lowest value.[110]

The IPSEs were also calculated for the titanium catalysts, **46-50** (R = H, Me, or ^{t}Bu) with the counterion **52** (Table 1.6). The ion-pair separation energies increased in the order ^{t}Bu < Me < H.[110] Two explanations could rationalize the trend that was observed. First, the better electron-donating ability of ^{t}Bu compared to Me and H would enhance the stability of the cationic metal center. Second, the larger R group could have a larger steric interaction with the counterion, thus lowering the separation energy. The same type of trend was seen when catalyst **50** interacted with all four counterions.

Table 1.6. Ion-Pair Separation Energies (kcal/mol) For Different R Groups[110]

Counterion	Catalyst	H		Me		^{t}Bu	
		gas	soln[a]	gas	soln[a]	gas	soln[a]
52	**46**	82.43	45.79	73.05	41.59	72.32	42.46
52	**47**	86.08	50.71	84.17	50.86	80.62	49.00
52	**48**	92.36	55.78	90.08	54.87	85.43	51.04
52	**49**	95.25	58.31	91.50	56.52	88.48	53.16
52	**50**	94.96	57.33	91.49	55.46	83.26	49.65
51	**50**	80.83	45.71	76.84	42.83	66.53	35.63
53	**50**	108.33	68.57	102.45	64.18	95.33	59.42
54	**50**	129.58	85.50	122.02	79.20	101.26	60.87

a: cyclohexane

The ion-pair formation calculations showed that the interaction between **54** and the five titanium catalysts **46-50** was the most favorable followed by **52** and then **53** (Table 1.7).

Table 1.7. Ion-Pair Formation Energies (kcal/mol)[110]

Precatalyst	$B(C_6F_5)_3$		Me_3Al-MAO		MAO	
	gas	soln[a]	gas	soln[a]	gas	soln[a]
$(Me_3P{=}N)_2TiMe_2$	-27.77	-25.88	-15.29	-14.17	-29.62	-24.59
$Cp(Me_3P{=}N)TiMe2$	-26.55	-25.69	-13.55	-10.18	-29.39	-26.49
$Cp(Me_2C{=}N)TiMe_2$	-24.56	-24.40	-11.96	-9.74	-30.52	-28.19
$(CpSiMe_2NMe)TiMe_2$	-14.58	-14.52	-5.47	-5.37	-25.99	-24.29
$Cp(Me_3OSi)TiMe_2$	-14.82	-12.78	-3.85	-1.51	-18.45	-14.77

a: cyclohexane

For catalyst **45** the trend was **52** more favorable than **54** and then **53**. Varying the R group on the catalyst had very little effect on the ion-pair formation energies because steric (destabilizing) and electronic (stabilizing) effects opposed one another. When the ion-pair formation and separation energies for the five titanium catalsyts, R = Me and the same counterion were compared, Ziegler found that the lower the separation energy the more negative ion-pair formation energy. There was however no correlation for the different counterions.[110]

Polymerization Studies

During the last 50 years of research, modifications of many different components (ligand, solvent, metal, cocatalyst etc.) of the polymerization system have been investigated. Directly related to the research discussed above, some general trends about the effect on polymerization of Al/metal ratios, Me_3Al effects and solvent effects have been reported.

High Al/metal ratios are usually required to obtain optimum catalytic activities in metallocene/MAO catalyzed polymerization.[21,28] A typical study of the effect of Al/metal ratio on catalytic activity is shown for Cp_2ZrMe_2/MAO in Table 1.8.[16]

Table 1.8. Al/Zr Ratio and the Effect on Polymerization Activity[16]

Catalyst	[Al]/[Zr]	Polymerization conditions	Activity[a]
Cp_2ZrMe_2	6760	[Zr] = 1.0×10^{-6} M, 60 °C 8 bar [b]	1.4×10^6
Cp_2ZrMe_2	9250	[Zr] = 1.0×10^{-6} M, 70 °C 8 bar [b]	4.4×10^6
Cp_2ZrMe_2	14800	[Zr] = 1.0×10^{-6} M, 70 °C 8 bar [b]	1.2×10^7
Cp_2ZrMe_2	15300	[Zr] = 1.0×10^{-6} M, 70 °C 8 bar [b]	1.5×10^7
Cp_2ZrMe_2	66100	[Zr] = 1.0×10^{-7} M, 70 °C 8 bar [c]	3.0×10^6
Cp_2ZrMe_2	158000	[Zr] = 1.0×10^{-7} M, 70 °C 8 bar [c]	8.9×10^6

a: g-PE/g-zr h.
b: $[Al(CH_3)O]_n$ $n \approx 12$
c: $[Al(CH_3)O]_n$ $n \approx 14$

The Me_3Al content of MAO also influences polymerization activity. Initially, an addition of Me_3Al results in an increase in catalytic activity and a cahnge in the kinetic profile from decay-type to steady-type.[111,112] A stabilizing effect of Me_3Al has been inferred from several similar observations. However, a large excess of Me_3Al results in both a decrease in the activity (Table 1.9) and also in molecular weight, most likely due to chain-transfer to the aluminum center.[33,113]

Table 1.9. Effect of Me_3Al Content on Polymerization Activity[113]

Catalyst	$[Me_3Al]\ 10^2$ (Al)	$[Me_3Al]\ 10^2$ (Al)	Me_3Al/MAO	Activity[a]
Cp_2ZrCl_2	0	5.14	-	250
Cp_2ZrCl_2	2.57	2.57	1	180
Cp_2ZrCl_2	3.43	1.71	2	150
Cp_2ZrCl_2	4.67	0.47	10	150
Cp_2ZrCl_2	5.04	0.1	50	81
Cp_2ZrCl_2	5.09	0.05	100	83
Cp_2ZrCl_2	5.12	0.017	300	12
Cp_2ZrCl_2	5.14	0.05	1000	2

a: kg-PE/g-Zr.h.MPa
polymerization conditions: Al/Zr = 1070, 70 °C, 100 kPa

Changing the polarity of the solvent, also has an effect on the catalytic activity. Higher catalytic activity was observed in dichloromethane as compared to toluene in the *rac*-$C_2H_4Ind_2ZrCl_2$ system for both homopolymerization of 1-hexene and copolymerization of propylene/1-hexene[114,115] and in the $C_2H_4(IndH_4)_2ZrCl_2$ and Cp_2TiPh_2 systems for the polymerization of propylene.[116] This solvent effect is consistent with ion pair separation as an important mechanistic theme.

Recently, Jordan described the synthesis of d^0 metal olefin complexes that are models for the elusive $Cp_2Zr(R)(olefin)^+$ intermediates in metallocene-based polymerization catalysts.[67,117] The reaction of $Cp_2Zr(OCMe_2CH_2CH_2CH{=}CH_2)(Me)$ and $B(C_6F_5)$ results in $Cp_2Zr(OCMe_2CH_2CH_2CH{=}CH_2)^+$ (**55**, Figure 1.20). Compound **55** is

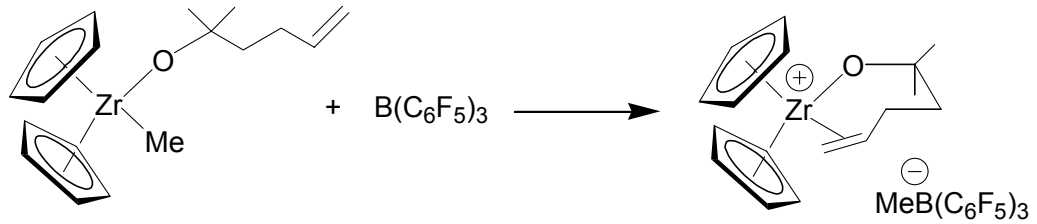

55

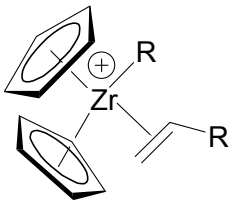

56

Figure 1.20. Model Complex for the Elusive $(C_5R_5)_2Zr(R)(Olefin)^+$ Intermediate[117]

a chelated d^0 olefin complex that models the putative $Cp_2Zr(R)(\alpha\text{-olefin})^+$ (**56**) key intermediate in metallocene-based polymerization. The X-ray structure of **55** (Figure 1.21) demonstrated that Zr-olefin bonding is unsymmetrical and consists of a weak

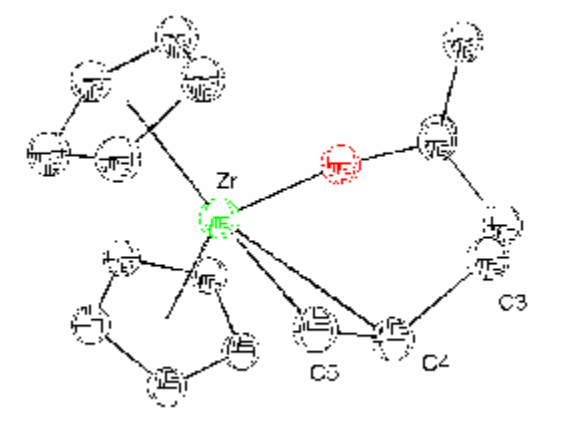

Figure 1.21. Molecular Structure of the $(C_5H_5)_2Zr(OCMe_2CH_2CH_2CH{=}CH_2)^+$ cation[117]
Zr – Green, O – Red

$Zr\text{-}C_{term}$ interaction and a minimal $Zr\text{-}C_{int}$ interaction. The C=C bond is polarized by the Zr-C interaction such that positive charge buildup occurs at C_{int}. Similar polarization and

unsymmetrical bonding effects could contribute to the high insertion reactivity of $Cp_2Zr(R)(olefin)^+$ species.

Chapter Two: Analysis of Metallocene-Methylaluminoxane Methide Transfer Processes in Solution

Introduction

The activation of group 4 metallocene olefin polymerization catalysts with MAO is often described as a simple Lewis acid-base equilibrium (eq 1-2, Cp' = η^5-C_5H_5 or a substituted Cp ligand; M = Ti, Zr, or Hf).[17] Siedle used ^{13}C NMR to demonstrate that the methyl groups exchanged between the MAO and Zr sites. This suggested that the methide abstraction (eq 2.1) is reversible,[79] and if eq 2.1 corresponds to a true equilibrium, then a constant reaction quotient ($Q = K_{eq}$) would be expected (eq 2.2). Using $B(C_6F_5)_2Ph$ as the activator, Marks found that the reaction quotient was constant using ^1H NMR spectroscopy.[118]

$$Cp'_2MMe_2\ (\mathbf{M}) + MAO\ (\mathbf{A}) \rightleftharpoons Cp'_2MMe^+\ Me[MAO]_n^-\ (\mathbf{C}) \qquad (2.1)$$

$$Q = [C] / [M][A] \qquad (2.2)$$

In chapter one, the literature concerning the metallocene/cocatalyst interaction was reviewed. The existing spectroscopic and polymerization data is complex and in particular, *quantitative* data from analyses *in solution* is still rather limited. Some useful qualitative trends, however, have been established by examining metallocene/MAO mixtures in solution using NMR spectroscopy.[81,83,86,119,120]

Marks analysed the residue that remains after evaporating the solvent from a mixture of **34** and MAO using CPMAS-NMR.[79] Varying the amount of MAO (Al:Zr = 5, 10, and 20), and monitoring the disappearance of the signals for **34**, he determined that **34** was completely consumed and that the residue was entirely activated using an Al:Zr ratio of only 12:1.[79] This was some of the earliest evidence that large Al:Zr ratios were not needed to optimize catalytic activities in a typical polymerization experiment.

However, to obtain values for Q that are directly analogous to polymerization data requires analysis in solution at low concentrations, which is challenging when using NMR spectroscopy. While ^{13}C, ^{27}Al, and ^{91}Zr NMR all benefit from outstanding dispersion, they suffer from low sensitivity, whereas in ^{1}H NMR the opposite is true. Both ^{1}H and ^{13}C NMR studies of activated metallocenes are complicated by interference from aluminoxanes at high Al:Zr ratios and by exchange broadening.

Tritto used ^{13}C NMR to investigate mixtures of **34** with either MAO or $B(C_6F_5)_3$.[84,105] Well-resolved signals were assigned to $[(Cp_2ZrMe)_2(\mu\text{-}Me)]^+$ and $[Cp_2ZrMe]^+$ and the $\delta(^{13}C)$ values for the Zr-Me and Cp ligand were nearly identical whether the counteranion was $MeB(C_6F_5)_3$ or MeMAO. The distribution of the cation-like species were then investigated varying temperature, concentration, and reactant stoichiometry (Al:Zr ratio). In these studies, the dimer $[(Cp_2ZrMe)_2(\mu\text{-}Me)]^+$ was present in significant and varying amounts, and the discussion concentrated on the effect of concentration and conditions on monomer-dimer equilibria. In addition, without access to the original integration data, conversion of the concentration data into a useful reaction quotient for methide abstraction as defined by eq 2.1 and 2.2 was not viable.

Babushkin[121] obtained comparable results using both ^{1}H and ^{13}C NMR spectroscopy. His most significant finding was based upon careful analysis of the signals assigned to C_5H_5 in the ^{1}H NMR spectrum. When the Al:Zr ratio (10 – 4000) was varied (holding [Al] constant to rule out medium effects), he concluded that MAO may contain a distribution of aluminum acids with varying capability for methide abstraction.

Recently, Babushkin and Brintzinger[122] used pulsed field-gradient NMR to estimate the size of the Me-MAO^- anion in the activation of dimethyl zirconocene with

MAO. They estimated that 150-200 Al atoms are contained in each Me-MAO$^-$ anion. With typical [Al]:[Zr] ratios of 1000-2000, there are only about 15-20 MAO molecules per zirconium center. Thus, if there is a distribution of Lewis acidic sites within MAO, the actual number of "truly" active sites will be small.

Based upon the complexity of the existing spectroscopic and polymerization data, we concluded that a new method for the study of metallocene-aluminoxane reactions is needed. This chapter describes the synthesis of a series of pentafluorophenyl-substituted metallocenes that were used to investigate the metallocene/aluminoxane interaction. Well resolved ^{19}F NMR signals corresponding to **M** and **C** (eq 2.1) allowed us to determine a value of Q as a function of MAO and metallocene concentrations.

Results and Discussion

Group 4 Metallocene Synthesis

As shown in Figure 2.1, Na[$(C_6F_5)C_5H_4$] (**57**) reacts with various zirconium and hafnium halides to afford the corresponding metallocenes. The synthetic details and characterization for complex **58** are described elsewhere.[123] Complexes **59, 60** and **61** were all prepared via the reaction of **57** with the appropriate metal halide in toluene at 110 °C for 1 h. The corresponding dimethylmetallocenes **62**, **63**, **64**, and **65** were prepared via the reaction of the dichloro-metallocene and 20 equivalents of solid MeLi in toluene solution in the absence of light. Solid MeLi was employed because it was found that reactions with MeLi in ethereal solutions led to methylation of the para-fluorine on the pentafluorophenyl substituent (eq 2.3). Interestingly, however, the reaction of **58** and

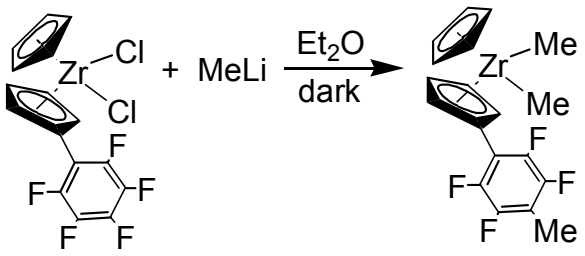

(2.3)

CH_3MgI in ether afforded **62** cleanly without any methylation of the para fluorine.

The reactions were performed in the absence of light due to apparent decomposition. Methylation reactions carried out under ambient light slowly deposit intractable black solids and give poor yields. In an attempt to determine the nature of the decomposition products, independent benzene-d_6 solutions of **62** were placed in both sunlight and fluorescent light. ^{1}H and ^{19}F NMR analysis demonstrated that **62** had decomposed into unidentifiable material.

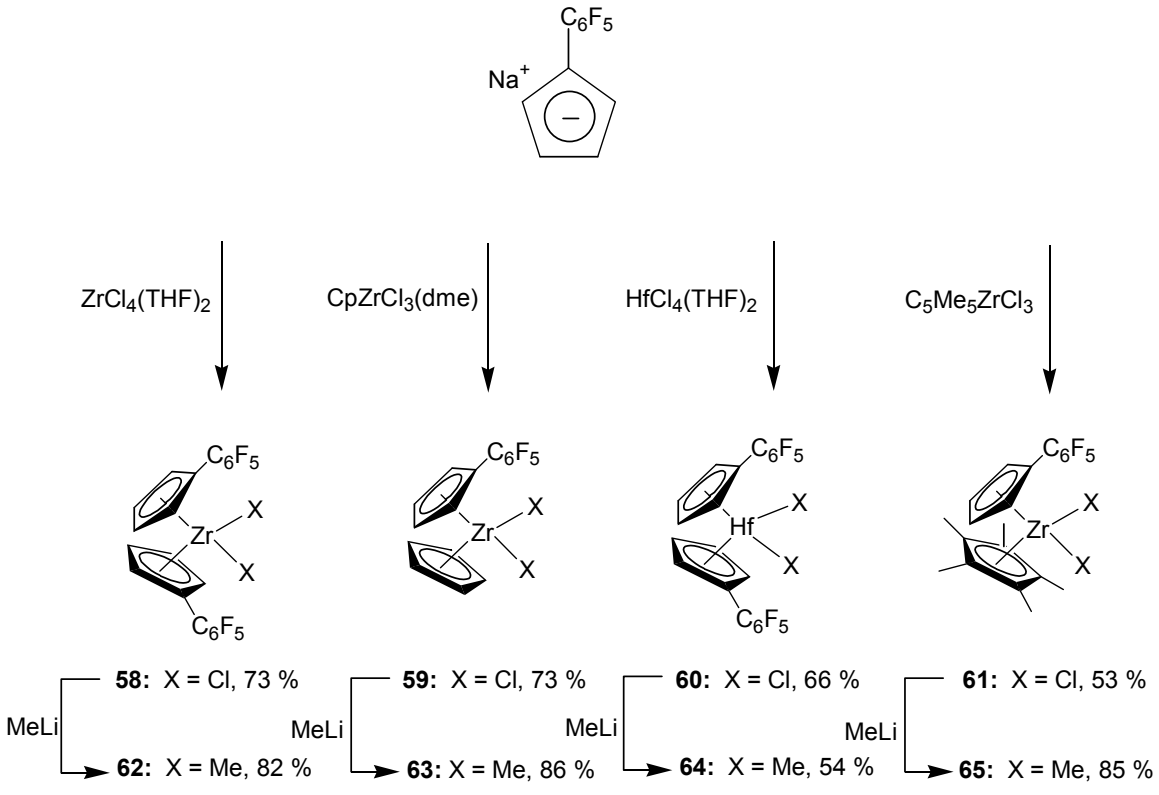

Figure 2.1. Synthesis of Pentafluorophenyl-Substituted Metallocenes

Assignment of Activated Metallocene Spectra

The ^{19}F NMR spectrum of **62** is shown in Figure 2.2a. Reaction of **62** with a slight excess of the well-defined activator $B(C_6F_5)_3$ resulted in the formation of the corresponding "cation-like" species $[(C_6F_5C_5H_4)_2ZrMe]^+[MeB(C_6F_5)_3]^-$ (**66**, eq 2.4).[75,100,124]

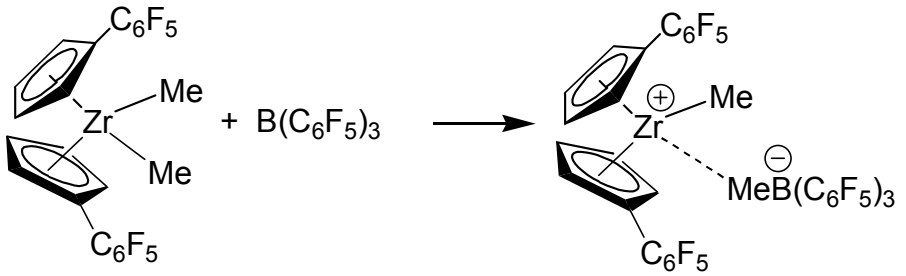

62 **66** (2.4)

The ^{19}F spectrum of **66** (Figure 2.2b) illustrates the expected downfield shifts in each of the three C_6F_5 signals as the metallocene becomes more electron-deficient.[67-71,73,76,125] The conversions of **63** and **64** were analogous. Interestingly, the chemical shift change for the conversion of **62**, **63**, and **64** into the cationic species is nearly uniform (Table 2.1).

Table 2.1. Chemical Shifts of Metallocene vs. Borane Activated Cation

Compound	Ortho-F	Para-F	Meta-F
$[(C_6F_5)C_5H_4]_2ZrMe_2$	-140.92	-156.95	-163.11
$[(C_6F_5C_5H_4)_2ZrMe]^+[MeB(C_6F_5)_3]^-$	-140.54	-151.64	-160.53
$[(C_6F_5)C_5H_4][C_5H_5]ZrMe_2$	-141.08	-157.59	-163.36
$[(C_6F_5C_5H_4)(C_5H_5)ZrMe]^+[MeB(C_6F_5)_3]^-$	-140.82	-152.30	-160.72
$[(C_6F_5)C_5H_4]_2HfMe_2$	-141.04	-156.85	-163.81
$[(C_6F_5C_5H_4)_2HfMe]^+[MeB(C_6F_5)_3]^-$	-140.66	-151.80	-160.70

The ^1H NMR sprectra of **66** shows two equally integrating methyl peaks, one sharp Zr-Me (0.19 ppm) and the other broadened B-Me (0.34 ppm). ^1H NMR spectra of $[(C_6F_5C_5H_4)(C_5H_5)ZrMe]^+[MeB(C_6F_5)_3]^-$ and $[(C_6F_5C_5H_4)_2HfMe]^+[MeB(C_6F_5)_3]^-$ show

an unsymmetrical singlet (0.23 ppm) and two equally integrating broad signals (0.64 and -0.08 ppm), respectively.

Others showed [84,104,126] that treatment of a zirconocene dimethyl with 0.5 equiv of $B(C_6F_5)_3$ resulted in dimeric cations having the general formula $[(Cp'_2ZrMe)_2(\mu\text{-}Me)]^+$. Brintzinger[85] carried out a concentration study (10 to 50 mM $[Zr]_{tot}$) on the reaction of Cp_2ZrMe_2 (**33**) with $B(C_6F_6)_3$ (Zr:B = 2:1) to determine the relative concentrations of the different "cation-like" species in the mixtures. ^1H NMR analysis of the mixtures indicated that four species (unreacted **33**, solvent separated binuclear cation (Dim-S), associated binuclear ion pair (Dim-A), and mononuclear contact ion pair (**28**)) were present (eq 2.5). At high [Zr], Dim-A was the dominant species while the concentrations

$$2\ Cp_2ZrMe_2 + B(C_6F_5)_3 \rightleftharpoons \underset{\textbf{28}}{[Cp_2ZrMe]^+[MeB(C_6F_5)_3]^-} + \underset{\textbf{Dim-A}}{[(Cp_2ZrMe)_2(\mu\text{–}Me)]^+[MeB(C_6F_5)_3]^-} + \underset{\textbf{Dim-S}}{[Cp_2ZrMe)_2(\mu\text{–}Me)]^+\cdots\cdots[MeB(C_6F_5)_3]^-} \quad (2.5)$$

of Dim-S and **28** were small. As the solution became more dilute, Dim-S and **28** became the dominant species while the concentrations of Dim-A was sharply decreased.

Interestingly, treatment of **62** (29 mM $[Zr]_{tot}$) with 0.5 equivalents of $B(C_6F_5)_3$ afforded only the monomeric cation **66** and unreacted **62**. However, treatment of **63** (29 mM $[Zr]_{tot}$) with 0.5 equivalents of $B(C_6F_5)_3$ resulted in the monomeric cation $[(C_6F_5Cp)CpZrMe]^+$ along with a binuclear cation $[(C_6F_5Cp)CpZrMe)_2(\mu\text{-}Me)]^+$ (Table 2.2 and Table 2.3). The difference in the reactivity between **62** and **63** can be

Table 2.2. ^{19}F NMR Chemical Shifts of Cationic Metallocenes in C_6D_6 at 22 °C

Compound	Ortho-F	Para-F	Meta-F
$[(C_6F_5C_5H_4)C_5H_5ZrMe_2$	-141.08	-157.59	-163.36
$[(C_6F_5C_5H_4)(C_5H_5)ZrMe]^+$	-140.78	-152.23	-160.68
$[(C_6F_5Cp)CpZrMe)_2(\mu\text{-}Me)]^+$	-141.08	-153.10	-161.02

Table 2.3. ^{1}H NMR Chemical Shifts of Cationic Metallocenes in C_6D_6 at 22 °C

Compound	C_6F_5Cp	Cp	Zr-CH_3	μ-CH_3	B-CH_3
$[(C_6F_5C_5H_4)C_5H_5ZrMe_2$	6.29 5.58	5.70	-0.27		
$[(C_6F_5C_5H_4)(C_5H_5)ZrMe]^+$	6.20 5.49 5.85	5.84	0.23		0.23
$[(C_6F_5Cp)CpZrMe)_2(\mu\text{-}Me)]^+$	5.85 5.48	5.70	-0.27	-1.05	1.42

attributed to the basicity of the metallocene. Dimer formation is an acid-base reaction (eq 2.5). One acid, $L_2MCH_3^+$, is present and two bases are competing for it. With L = Cp,

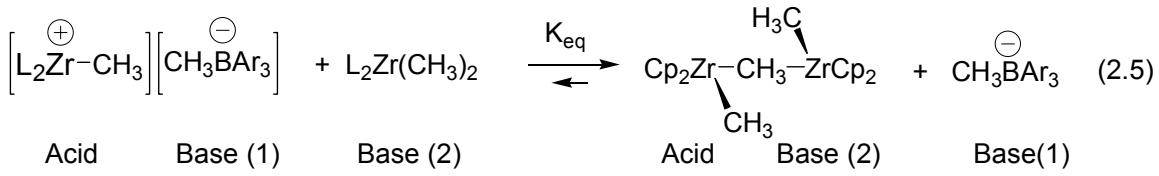

the competition is about even (according to Brintzinger) and $K_{eq} \cong 1$. When L = C_6F_5Cp, the acid is stronger, but the true difference is that the balance between the two bases has shifted. $CH_3B(C_6F_5)_3$ is the same but $L_2Zr(CH_3)_2$ is now a weaker base. So the equilibrium lies more to the left. Upon comparison, it was observed that in our mixtures the amount of the monomeric cation (30 %) was higher then the amount of the binuclear cation (20 %). In contrast Brintzinger reported that at $[Zr]_{tot}$ = 29 mM, the percentage of the solvent separated binuclear cation (28 %) was higher than the monomeric cation (10 %).

When **62** was treated with MAO, the ^{19}F NMR spectrum showed signals for unreacted **62** and three broad signals shifted downfield (Figure 2.2c). The downfield

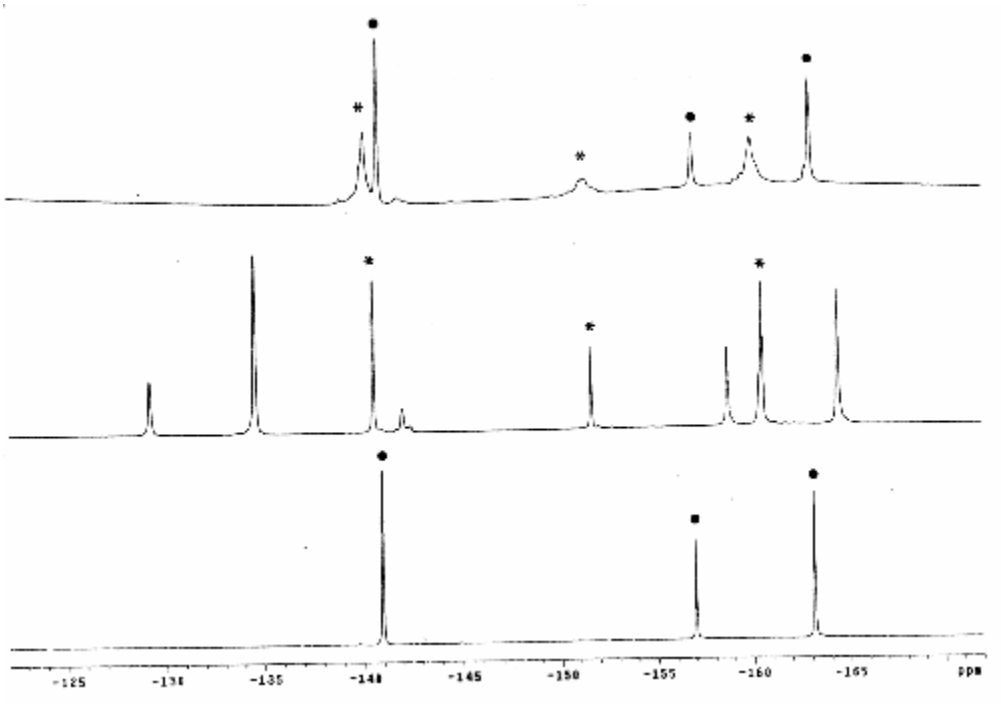

Figure 2.2. ^{19}F NMR of **62** and "Cation-Like" Metallocenes
• $[(C_6F_5)Cp]_2ZrMe_2$ * $[(C_6F_5)Cp]_2ZrMe^+$

signals were assigned to the zirconocenium methylaluminate $[(C_6F_5C_5H_4)_2ZrMe]^+[MeMAO]^-$ (**67**). The chemical shifts of this zirconocenium species were nearly identical to those for the $B(C_6F_5)_3$-activated **66**. Based upon this result, we conclude that the cationic portions of **66** and **67** are structurally equivalent, within the sensitivity of this ^{19}F NMR probe. These results indicate that **62** reacts with MAO according to eq 2.6. Likewise, **63**, **64** and **65** react with MAO to afford

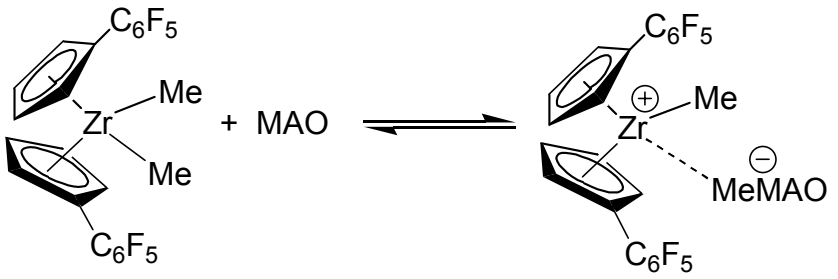

(2.6)

62 **67**

$[(C_6F_5C_5H_4)[C_5H_5]ZrMe]^+[MeMAO]^-$ (**68**), $[(C_6F_5C_5H_4)_2HfMe]^+[MeMAO]^-$ (**69**), and $[(C_6F_5C_5H_4)(C_5Me_5)][ZrMe]^+[MeMAO]^-$ (**70**), respectively (Figure 2.3). Again, the

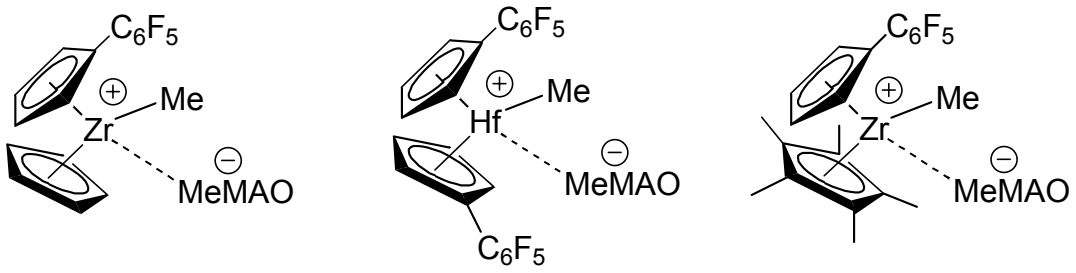

68 **69** **70**

Figure 2.3. Metallocenium Species Observed Upon Treatment of Metallocenes **63, 64,** and **65**

cationic portion of the ^{19}F NMR spectra of **63**/**68** and **64**/**69** were nearly identical to the spectra obtained with activation with $B(C_6F_5)_3$. The reaction between **65** and $B(C_6F_5)_3$ was not investigated, however, based upon the results found in the reactions with **62**, **63**, and **64,** we can conclude the analogous cationic borane complex would be formed.

Broadening of the peaks in the ^{19}F NMR of **67** – **70** arises two ways. First, as discussed in chapter one, MAO is a complex mixture of oligomers[34,35,40,49,127] which could produce an array of aluminate "counter-ion" structures. In some spectra, more defined features are evident in the broad peaks. Further investigation with well-defined aluminum activators and compounds **67** – **70** could help identify the complexes responsible for these peaks. Second, it has been shown previously that chemical

exchange can contribute to line broadening.[104,126] Broadening of the signals assigned to **62** can be seen in Figure 2c and is attributed to the dynamic nature of the abstraction equilibrium (eq 2.6). An EXSY experiment[128] confirmed the reversible nature of eq 2.6. In the EXSY spectrum (Figure 2.4), the off-diagonal peaks indicate that there is chemical exchange between the signals assigned to **62** and **67** on each axis.

Concentration Studies

In order to determine a value for Q (eq 2.2), titration studies with compounds **62 – 65** with MAO were investigated. As discussed in chapter one, the reported molecular weights of MAO samples range between 400 and 3000 g/mol and the complex mixtures are prone to disproportionation reactions.[35-37] Thus, it should be noted that 58 g mol^{-1}, corresponding to the [AlMeO] "repeat unit" of MAO is used as an arbitrary formula weight in all the calculations of [MAO]. This allows for a direct comparison of Q to practical Al:Zr ratios.

In the first series of experiments, the metallocene concentration was held constant (Table 2.4) while the concentration of MAO was varied. Monitoring by ^{19}F NMR, the

Table 2.4. Nominal Metallocene Concentration

Metallocene	Concentration (mM)
$[(C_6F_5)C_5H_4]_2ZrMe_2$	10.2
$[(C_6F_5)C_5H_4][C_5H_5]ZrMe_2$	11.6
$[(C_6F_5)C_5H_4]_2HfMe_2$	3.9
$[(C_6F_5)C_5H_4][C_5Me_5]ZrMe_2$	12.6

titration experiment led to a decrease in the intensity of the signals assigned to **62** – **65** and a corresponding increase in the signals assigned to **67** – **70**, respectively. The equilibrium ratio [**M**]:[**C**] was obtained from the integration of the well-resolved *para*

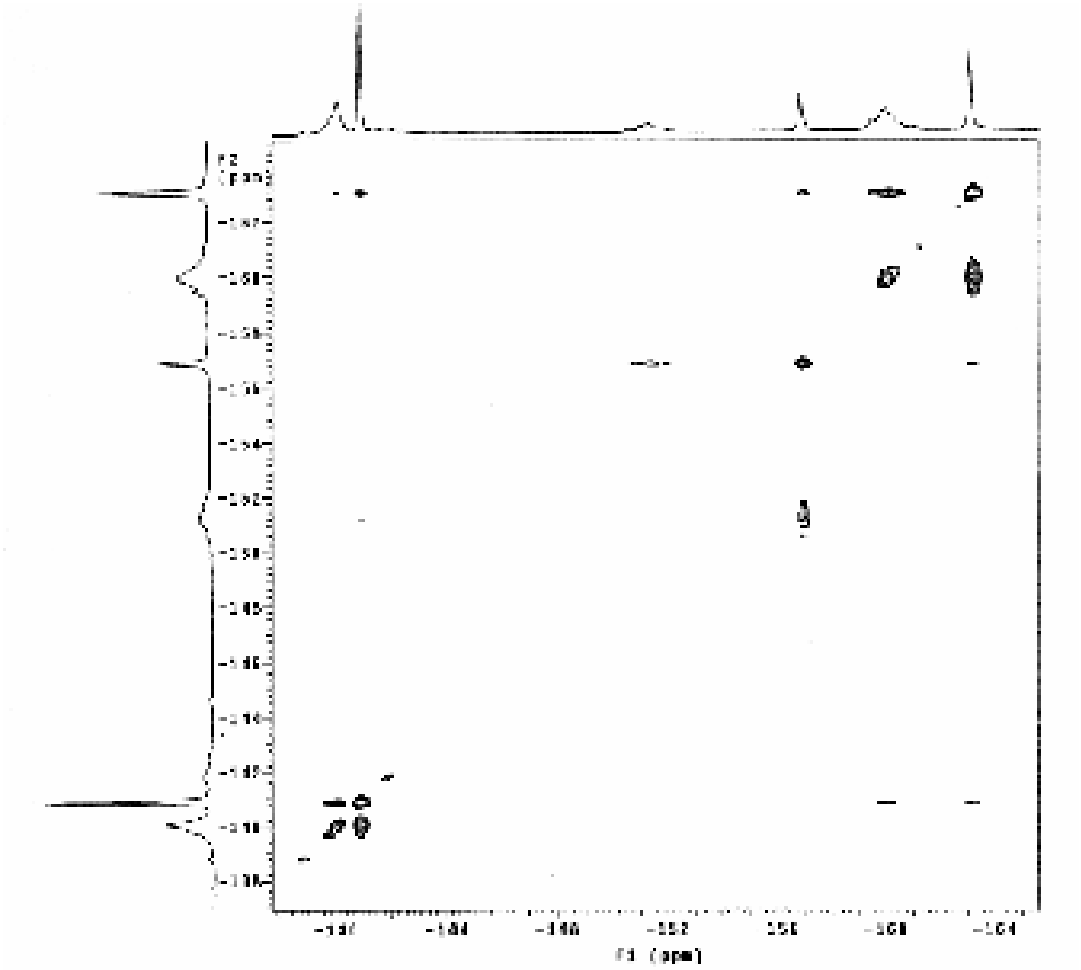

Figure 2.4. ^{19}F - ^{19}F EXSY of **62** with MAO

regions of the ^{19}F NMR spectra. The widest range of MAO concentration that still allowed for the integration of the signals assigned to both **M** and **C** were used. These data allowed us to calculate a reaction quotient (Q) according to eq 2.2. If Q is determined to be constant with respect to $[metallocene]_o$, $[MAO]_o$ and time, then Q is truly an equilibrium constant.

When a toluene solution of **62** was titrated with MAO at 25 °C, we found that as [MAO] increased Q also increased (Figure 2.5). The ^{19}F NMR relative intensities and

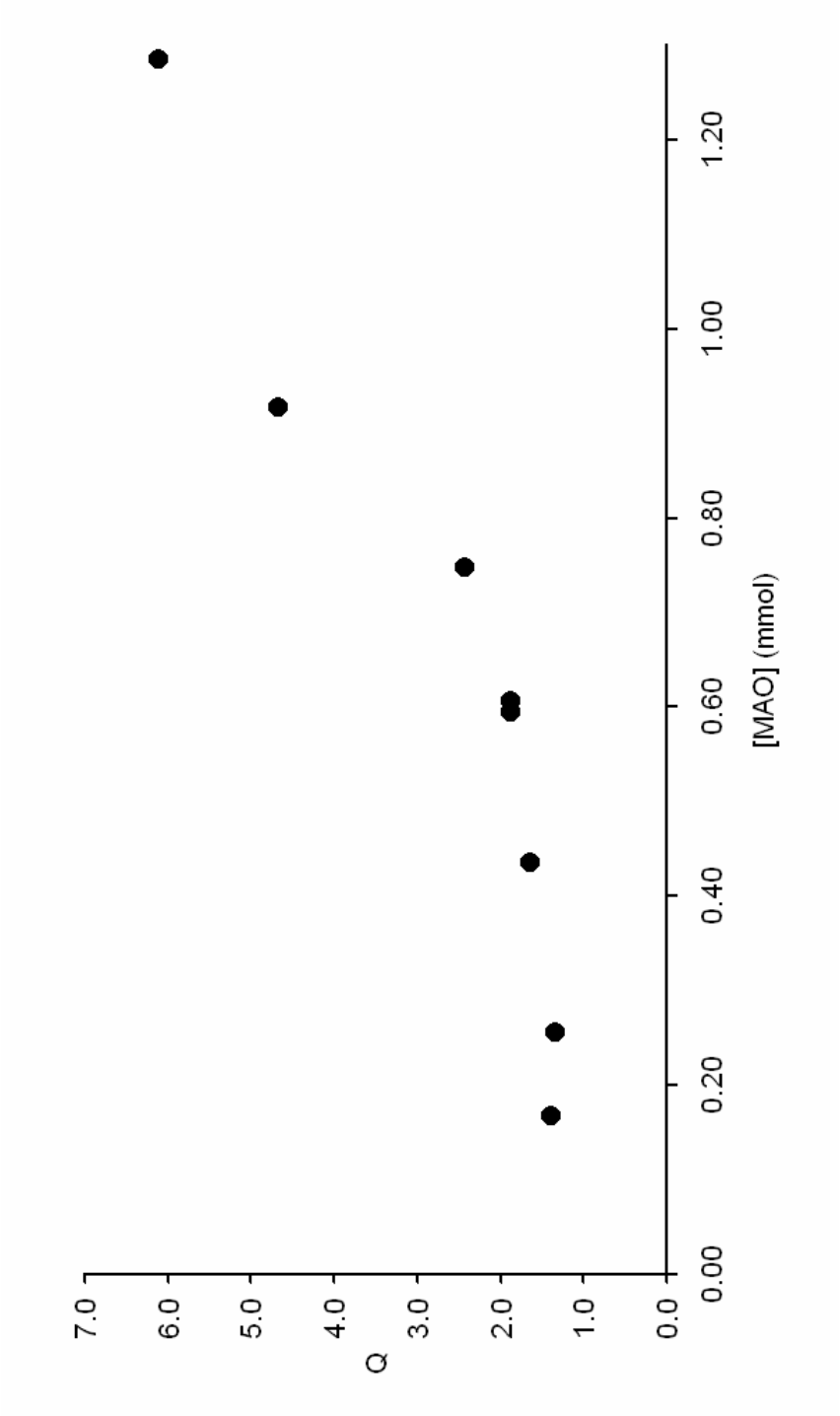

Figure 2.5. Q vs [MAO] for Compound **62**

methide abstraction steady state reaction quotient determinations for the reaction of **62** with MAO are shown in Table 2.5. For **62** Q is within the range $1.0 < Q < 6.0$. When toluene solutions of **63**, **64** and **65** are titrated with MAO and the reaction quotient determined, the same general trend is observed (Figure 2.6). The ^{19}F NMR relative intensities and methide abstraction steady state reaction quotient determinations for the reaction of **63**, **64**, and **65** with MAO are shown in Tables 2.6 through 2.8.

When all the results for the four metallocenes are compiled, three general findings are obtained. First, Q is within the range $0.1 < Q < 40$. An approximate value for Q can also be determined from concentrations in a typical polymerization experiment. Useful catalyst concentrations are micromolar or even less (i.e., $[\mathbf{C}] \approx [\mathbf{M}]_o \approx 10^{-6}$ M) while large excess amounts of MAO (e.g., $[\mathbf{A}] \approx 1000\ [\mathbf{M}]_o \approx 10^{-3}$ M) are typically employed. This allows for an estimation approaching 10^4 for Q. This is truly a rough estimation because in polymerization reactions much of the MAO can be consumed scavenging impurities or "reactivating" dormant species. Different metallocene catalysts can be fully activated at a great range of Al:Zr ratios. Tritto[82] observed an equilibrium ratio of 4.0 for methide abstraction in the $Cp_2TiMeCl$ system (eq 2.7) using ^{13}C NMR at –20 °C.

$$Cp_2TiMeCl + MAO \bullet AlMe_2Cl = [Cp_2TiCl]^+ [MAO \bullet AlMe_3Cl]^- \quad (2.7)$$

Secondly, a comparison of the reaction quotients for the four metallocenes at a fixed aluminoxane concentration indicates that both the substituents on the ligand and the nature of the metal center have an effect on the value of Q. A comparison of **62** ($Q \approx 1.3$) **63** ($Q \approx 4.0$), and **65** ($Q \approx 6.7$) at [MAO] ≈ 0.26 demonstrates the electron-withdrawing ability of the C_6F_5 substituents.[123,129-131] The lowest value of Q for **62**, is attributed to the two C_6F_5 substituents on the Cp rings. When one of the C_6F_5 groups is removed as in **63**,

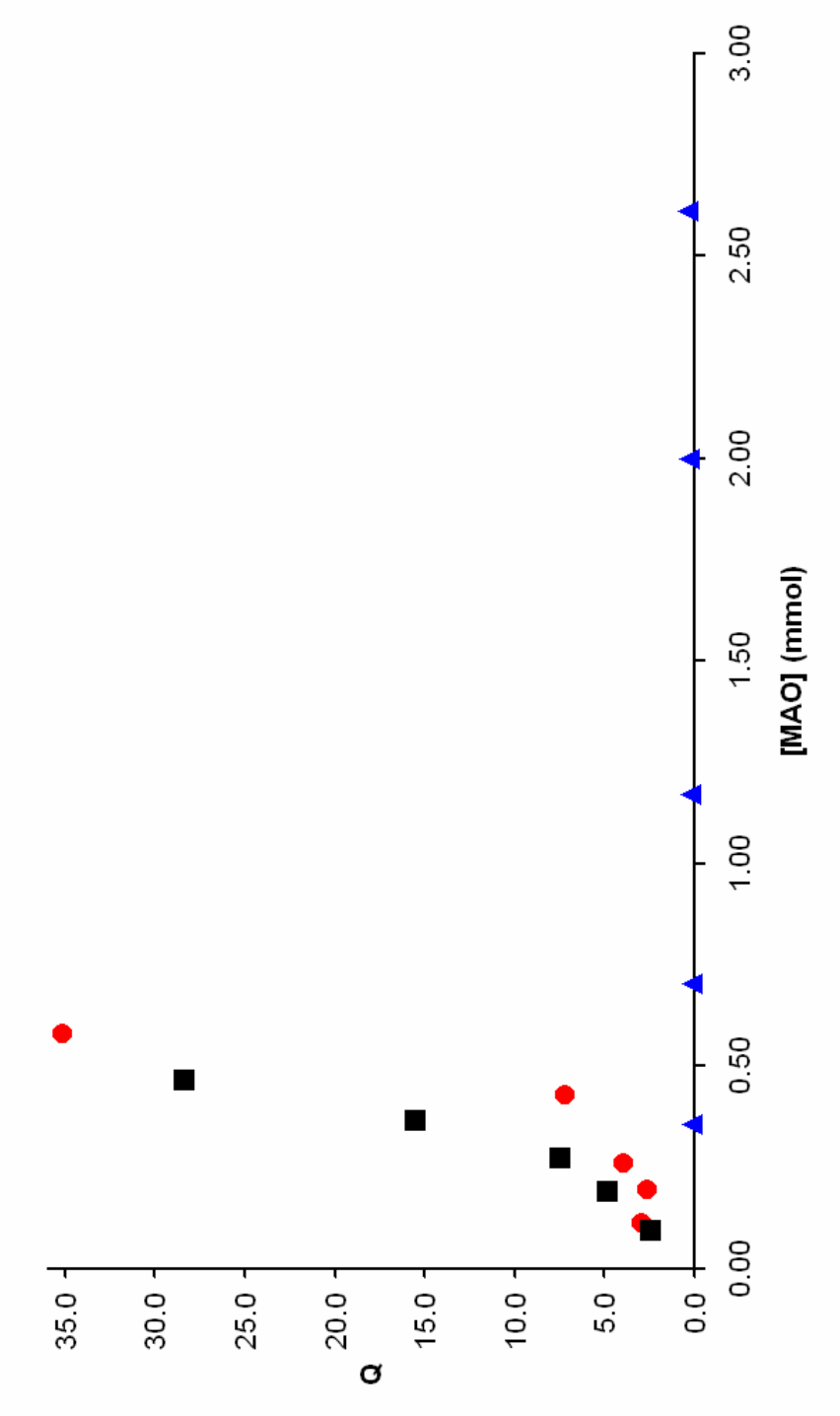

Figure 2.6. Q vs. [MAO] for Compounds **63** (●), **64** (▲), and **65** (■)

the value of Q increases and then when the Cp ligand of **63** is replaced with the more electron-donating Cp* ligand of **65** the Q value increases once again. Comparison of the reaction quotients for **62** ($Q \approx 1.6$) and **64** ($Q \approx 0.32$) at [MAO] ≈ 0.46 M demonstrates the idea that hafnium complexes are more Lewis acidic than corresponding zirconium complexes.[118] This trend in reacivity agrees with the calculated enthalpies of methide abstraction in the $(1,2\text{-}Me_2Cp)_2Zr(CH_3)_2/B(C_6F_5)_3$ and $(1,2\text{-}Me_2Cp)_2Zr(CH_3)_2/B(C_6F_5)_3$ systems.[118]

The third general finding is that as [MAO] increases, Q increases (Figure 2.5 and 2.6) for all four metallocenes. The increase for **64** is not as dramatic as for **62**, **63**, and **65**, but when it is shown individually an increase can be observed (Figure 2.7). However, the value of Q, within experimental errrors, is constant for **64** over the range $0.1 <$ [MAO] < 3.0 M (Figure 2.7). Even when [MAO] was close to saturation, the ^{19}F NMR spectra obtained for **64** indicates low concentration of **69**, thus it was concluded that there was significant error in the determination of Q for **64**. For compounds **62**, **63**, and **65**, Figures 2.5 and 2.6 demonstrate that Q varies noticeably with [MAO]. For the range $0.1 <$ [MAO] < 0.6, the effect of [MAO] on Q is greatest for **65** (a factor of 10), **63** (a factor of 7), and then **62** (a factor of 2). The observation that Q increases with [MAO] increase could result from the fact that MAO is more polar than toluene, and aggregation of MAO around the ion-paired species as a diffuse "solvent effect"[101,132,133] would stablize **C** relative to **M**. However, it would be expected that a "solvent effect" would affect methide abstration from all four metallocenes uniformly.

The observation that Q increases with increasing [MAO] could also be rationalized by (1) more than one MAO molecule may be required to abstract a methyl

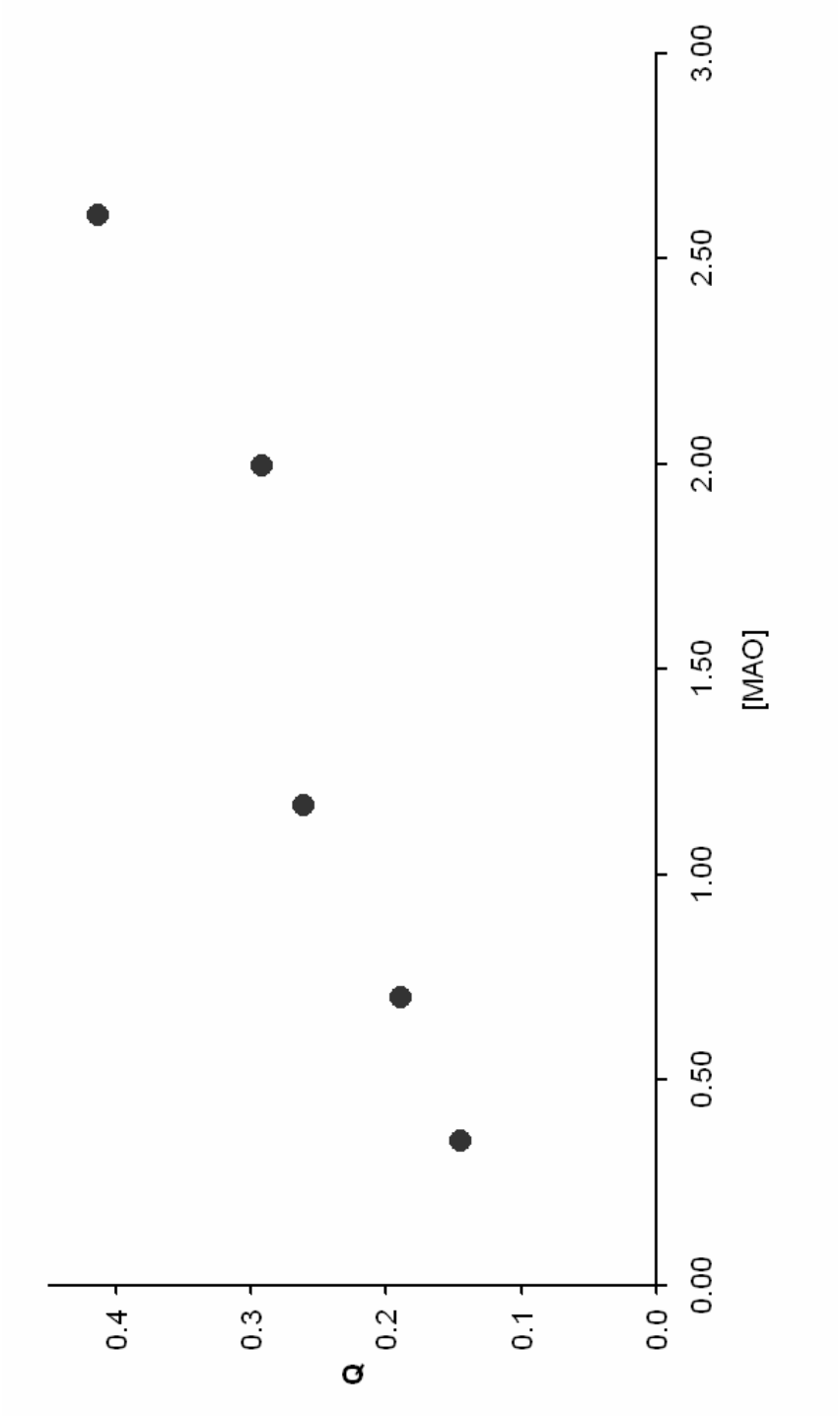

Figure 2.7. Q vs [MAO] for Compound 64

group or (2) MAO forms aggregates with the activated "cationic" species (C). To investigate these possibilities, a parameter corresponding to the number of MAO molecules required was introduced into the stoichiometric equation (eq 2.2). Upon varying the aggregation parameter ($1.0 < a < 3.0$), Q became constant at high [MAO], but not at low [MAO]. Also with $1.5 < a < 3.0$, Q initially decreases with increasing [MAO] and then becomes constant at high [MAO]. Thus, the postulation of multiple Al sites involved in the reaction between the metallocenes and MAO does not rationalize the data any better than the original idea of only one Al site.

In the second experiment, $[MAO]_o$ was held constant (0.35 M) while the initial metallocene concentration $[\mathbf{62}]_o$ was varied ($2.0 < [\mathbf{62}]_o < 5.5$ mM). In contrast to the constant [MAO] experiment, Q was found to decrease with increasing [Zr] (Figure 2.8). Furthermore, the concentration of the "cation-like" species [**C**], is approximately constant throughout the experiment. This observation suggests that there are a limited number of "active" Al sites for the abstraction of a methyl group and they are largely consumed after the first aliquot of **62** is added (Al:Zr = 70 : 1).

Variable temperature (50 to –80 °C) ^{19}F NMR spectroscopy was obtained for a solution of **62** (nominally 30 mM with Al:Zr ~ 35) with MAO. While Tritto reported a dramatic decrease in the "quantity" of cationic products when the temperature was lowered from 25 °C to – 78 °C for the combination of Cp_2ZrMe_2 with 10 equivalents of MAO,[84,105] corroborating an earlier experiment using a mxture of $Cp_2Ti^{13}CH_3Cl$ and 10 equivalents of MAO,[134] it was observed between 50 and – 40 °C that the percentage of **67** was constant (within $\pm$ 10 %). Our total aluminum concentration was ~1.0 M while

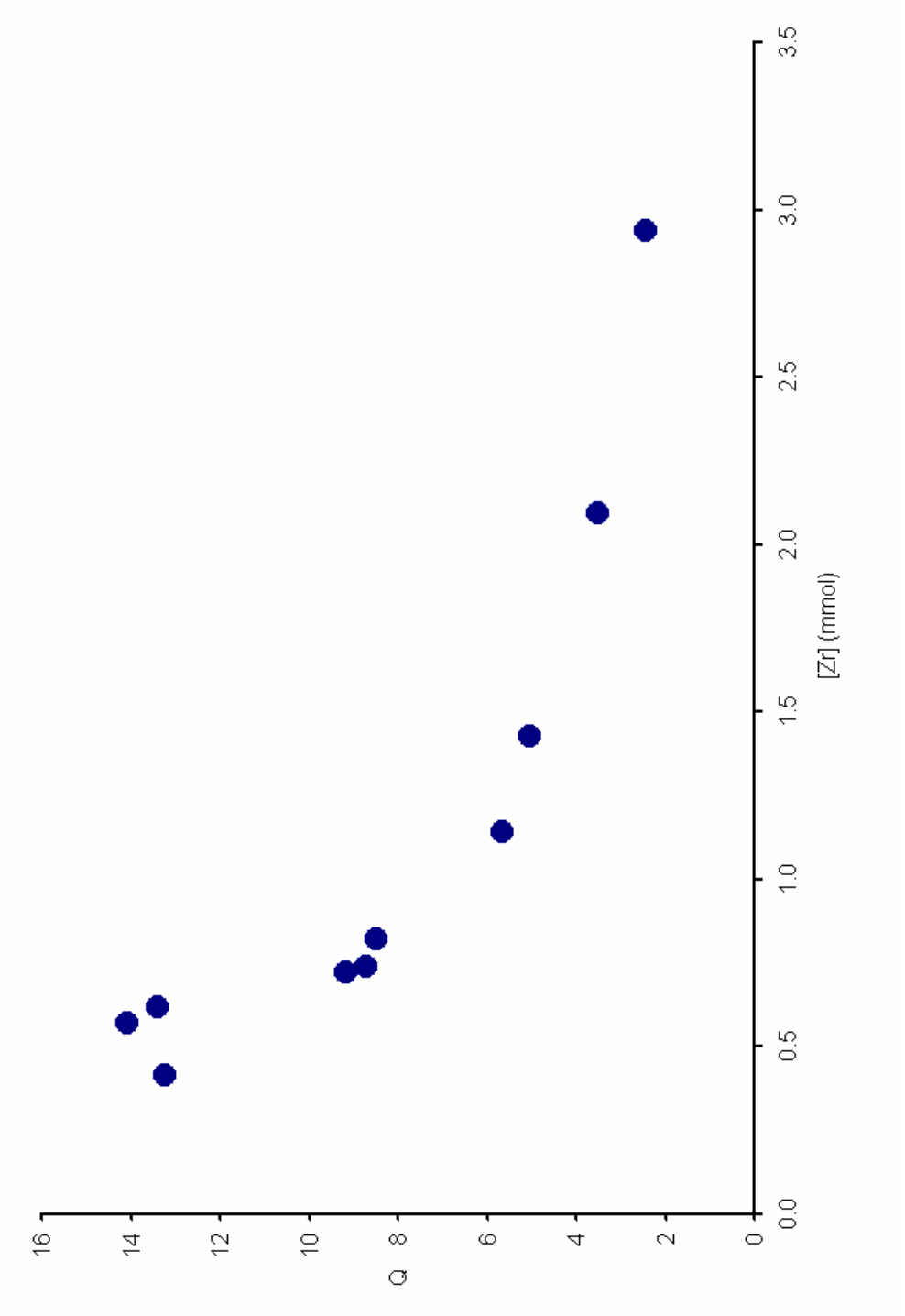

Figure 2.8. Q vs [Zr] for Compound 62

Tritto used a marginally lower (0.7 M) concentration. Below – 40 °C, a decrease in the apparent concentration of 67 was observed, however these data were disregarded due to significant gelation of the sample. In their earlier report, Tritto also noted that their solutions of MAO also became "quite viscous, especially at very low temperatures."[134,135]

Prior explanations (*vide supra*) for the variations in Q with constant [MAO] and constant [Zr] appear to fall short. We now propose a two-part model to account for the observations in our titration studies. First there is a limited number of sites that are "active" toward the abstraction of a methyl group from a metallocene. Second, the Lewis acidity of the aluminum sites of MAO are not uniform.

When a fixed quantity of MAO reacts with a small amount of metallocene, there are enough "active" sites to generate a considerable percentage of the cationic species. However, upon the addition of more metallocene, there is no more "active" aluminum sites Lewis acidic enough to generate more cationic species. Thus, the apparent Q is expressed by a function that is nearly reciprocal in the metallocene concentration (Figure 2.8). The postulation in which a limited number of highly active sites are "titrated" by the metallocene is consistent with the temperature-independence of Q.

The idea of multiple acidic sites in MAO was investigated by Talsi[136] by EPR. He reported that there are two distinctly different acidic sites. Babushkin[121] also proposed a distribution of acidic sites in MAO based upon the analysis of ^{1}H NMR for the reaction between **29** and MAO (Al:Zr ratio ranging from 10 – 4000). First, this explanation can rationalize the data in Figures 2.5 and 2.6. At low [MAO], there is only enough "active" Lewis-acidic sites to activate a small fraction of the metallocene. As [MAO] increases, the number of "active" sites and the concentration of the cationic

species increases proportionally. This results in an increase in Q because while both the [**C**] and [**A**] increase, [**M**] decreases.

It is also apparent from Figures 2.5 and 2.6 that the percentage of "active" sites is metallocene-dependent, and that the "active" aluminum sites must be more acidic than the corresponding activated metallocenium species. The more Lewis basic metallocenes **63** and **65** interact with a different percentage of acidic sites (19-25 and 26-32 "active" Al atoms per 100, respectively) than does **62** (8-10 "active" Al atoms per 100). For **64** with varying [MAO] figure 2.8 demonstrates a nearly constant Q value, which indicates that **64** may be adequately electron-deficient to engage in a more conventional equilibrium with perhaps only a single type of aluminoxane Lewis acidic site. Our data indicates that **64** reacts with 0.5 – 0.75 "active" Al atom per 100.

Future Work

Further experiments in our lab will (1) compare the specific chemical shifts, line widths, and other spectral features with MAO and well-defined aluminoxane activators such as those prepared by Barron, Albemarle, and Hessen/Teuben. These comparisons may advance the goal of learning which aluminoxane structural features are responsible for activation. Those experiments with well-defined activators would be good because we could use both ^{1}H and ^{13}C NMR. (2) Other experiments will probe the limit of aluminoxane acidity by designing a metallocene that is even more electron deficient than our hafnium compound. (3) Other experiments will attempt at higher dilution to see if we can really get an equilibrium constant for a metallocene that we think only interacts with one type of Al site. We may need to combine our approach with Deffieux's UV

approach using a C_6F_5-labelled metallocene that also has a UV or fluorescence tag. (4) Expand these studies to other types of single-site catalysts.

Conclusions

^{19}F NMR spectroscopy is a useful tool for observation of the methide abstraction from metallocenes by MAO. Dimethylmetallocenes and "cation-like" metallocenes are readily distinguished with chemical shifts assigned to well-defined model compounds, and relative concentrations are obtained by integration of their ^{19}F NMR signals. Apparent reaction quotients obtained for methide abstraction are much lower than one might anticipate based on Al:Zr ratios and concentrations actually used in olefin polymerization.[121] The observed effect on Q based upon the concentration of MAO implies that a simple equilibrium model (eq 2.1-2.2) does not describe the methide abstraction by MAO at the concentrations used in our study. MAO acts as though there are only a small number of highly reactive sites toward the abstraction of a methide. Calculations based upon the data suggest that there are between 8-10 "active" Al atoms per 100 for **62**, 19-25 for **63**, 0.50 – 0.75 for **64** and 26-32 for **65**.

Table 2.5. ^{19}F NMR Relative Intensities and Methide Abstraction Steady State Reaction Quotient Determinations for **62** + MAO

	Starting Concentrations		Unit-normalized Integrations		Steady State Concentrations			
Entry	$[\mathbf{M}]_o$ (mM)	$[\mathbf{A}]_o$ (M)	($\mathbf{I}_M$)	($\mathbf{I}_c$)	[**M**] (mM)	[**C**] (mM)	[**A**] (M)	Q
1	11.1	0.60	0.47	0.53	5.3	5.8	0.60	1.9
2	10.9	0.26	0.75	0.25	8.2	2.8	0.26	1.3
3	10.8	0.44	0.61	0.42	6.3	4.5	0.44	1.6
4	10.7	0.75	0.35	0.65	3.8	6.9	0.75	2.4
5	10.5	0.17	0.81	0.19	8.5	2.0	0.17	1.4
6	10.2	0.77	0.34	0.66	4.9	4.8	0.56	1.7
7	10.2	0.25	0.76	0.24	8.1	1.5	0.18	1.1
8	10.1	0.42	0.65	0.35	6.6	3.5	0.42	1.3
9	9.8	0.57	0.51	0.49	4.9	4.8	0.56	1.7
10	9.8	0.43	0.61	0.39	6.9	2.8	0.31	1.3
11	9.8	0.11	0.90	0.10	8.8	1.0	0.11	1.0
12	9.8	0.16	0.83	0.17	8.8	1.0	0.11	1.0
13	9.7	0.61	0.46	0.54	6.6	3.5	0.42	1.3
14	9.7	0.32	0.71	0.29	6.9	2.8	0.31	1.3
15	9.6	0.18	0.84	0.16	8.1	1.5	0.18	1.1
16	7.8	0.92	0.19	0.81	1.5	6.3	9.2	4.7
17	7.6	1.3	0.11	0.89	0.86	6.8	12.8	6.1
18	7.5	0.61	0.47	0.53	3.5	4.0	6.1	1.9

Table 2.6. ^{19}F NMR Relative Intensities and Methide Abstraction Steady State Reaction Quotient Determinations for **63** + MAO

	Starting Concentrations		Unit-normalized Integrations		Steady State Concentrations			
Entry	$[\mathbf{M}]_o$ (mM)	$[A]_o$ (M)	($\mathbf{I}_M$)	($\mathbf{I}_c$)	[**M**] (mM)	[**C**] (mM)	[**A**] (M)	Q
1	13.1	0.59	0.08	0.92	1.0	12.1	0.57	21.1
2	12.6	0.43	0.19	0.81	2.4	10.1	0.42	9.8
3	12.4	0.20	0.59	0.41	7.3	5.1	0.20	3.5
4	12.4	0.11	0.74	0.26	9.2	3.3	0.11	3.2
5	12.3	0.27	0.40	0.60	5.0	7.3	0.27	5.5
6	12.2	0.27	0.49	0.51	6.0	6.2	0.26	4.0
7	11.6	0.44	0.25	0.75	2.9	8.8	0.43	7.2
8	11.5	0.59	0.14	0.86	1.5	10.0	0.58	11.0
9	11.2	0.20	0.66	0.34	7.4	3.8	0.20	2.6
10	11.1	0.12	0.75	0.25	8.3	2.8	0.11	2.9
11	10.9	0.52	0.12	0.88	1.3	9.7	0.51	14.9
12	10.7	0.39	0.21	0.79	2.2	8.5	0.38	9.9
13	10.7	0.26	0.40	0.60	4.3	6.5	0.25	6.0
14	10.4	0.10	0.81	0.19	8.4	2.0	0.10	2.3

Table 2.7. ^{19}F NMR Relative Intensities and Methide Abstraction Steady State Reaction Quotient Determinations for **64** + MAO

	Starting Concentrations		Unit-normalized Integrations		Steady State Concentrations			
Entry	$[\mathbf{M}]_o$ (mM)	$[A]_o$ (M)	($\mathbf{I}_M$)	($\mathbf{I}_c$)	[**M**] (mM)	[**C**] (mM)	[**A**] (M)	Q
1	6.0	1.74	0.82	0.18	4.9	1.07	1.73	0.13
2	5.9	1.42	0.84	0.16	5.0	0.93	1.42	0.13
3	5.7	0.57	0.92	0.08	5.3	0.43	0.57	0.14
4	5.6	1.05	0.89	0.11	4.9	0.61	1.05	0.12
5	5.5	0.54	0.93	0.07	5.1	0.38	0.53	0.14
6	3.4	2.00	0.63	0.37	2.1	1.24	2.00	0.29
7	3.2	2.61	0.48	0.52	1.5	1.66	2.61	0.41
8	3.1	1.17	0.77	0.23	2.4	0.73	1.17	0.26
9	3.1	2.51	0.64	0.36	2.0	1.11	2.50	0.23
10	3.0	0.70	0.88	0.12	2.7	0.35	0.70	0.19
11	3.0	0.35	0.95	0.05	2.9	0.15	0.35	0.14
12	2.9	1.75	0.70	0.30	2.0	0.88	1.75	0.24
13	2.8	0.68	0.87	0.13	2.4	0.38	0.68	0.23
14	2.8	1.39	0.82	0.18	2.3	0.51	1.39	0.16
15	2.7	0.48	0.87	0.13	2.3	0.36	0.48	0.32

Table 2.8. ^{19}F NMR Relative Intensities and Methide Abstraction Steady State Reaction Quotient Determinations for **65** + MAO

	Starting Concentrations		Unit-normalized Integrations		Steady State Concentrations			
Entry	$[\mathbf{M}]_o$ (mM)	$[A]_o$ (M)	($\mathbf{I}_M$)	($\mathbf{I}_c$)	[**M**] (mM)	[**C**] (mM)	[**A**] (M)	Q
1	13.2	0.34	0.24	0.76	3.2	10.1	0.33	9.6
2	13.0	0.19	0.52	0.48	6.8	6.2	0.19	4.9
3	12.9	0.47	0.07	0.93	0.9	12.0	0.46	28.4
4	12.9	0.20	0.59	0.41	7.6	5.3	0.20	3.5
5	12.8	0.47	0.12	0.88	1.6	11.2	0.46	15.9
6	12.8	0.28	0.33	0.67	4.3	8.6	0.27	7.5
7	12.8	0.09	0.81	0.19	10.4	2.4	0.09	2.5
8	12.7	0.37	0.14	0.86	1.8	10.9	0.36	17.2
9	12.7	0.37	0.15	0.85	1.9	10.8	0.36	15.6
10	12.7	0.43	0.16	0.84	2.0	10.6	0.42	12.3
11	12.7	0.28	0.36	0.64	4.5	8.2	0.27	6.7
12	12.6	0.19	0.59	0.41	7.3	5.2	0.18	3.8
13	11.6	0.11	0.70	0.30	8.1	3.5	0.11	4.1
14	11.3	0.16	0.60	0.40	6.8	4.5	0.16	4.2

Experimental Section

General Considerations. All manipulations were carried out with standard nitrogen-atmosphere techniques. MeLi was purchased from Aldrich as a solution in diethyl ether and dried under high vacuum (3 x 10^{-5} torr). For these procedures, it is important to remove as much ether as possible. MAO was received from Albemarle as a 10% toluene solution, filtered, and dried under high vacuum (3 x 10^{-5} torr) for 15 h to remove "free" trimethylaluminum. The same sample of MAO was used for all the experiments described here. $B(C_6F_5)_3$ was obtained as a gift from Albemarle, sublimed (120 °C, 5 x 10^{-6} torr), recrystallized from hexanes, and found to be 99+% pure according to ^{19}F NMR spectroscopy. $[(C_6F_5)C_5H_4]_2ZrCl_2$ (**58**) and $Na[(C_6F_5)C_5H_4]$ were prepared according to our own methods.[123] $CpZrCl_3(DME)$ was prepared according to the method of Lund and Livinghouse.[137] NMR spectra were recorded on a Varian U-400 instrument at 22 °C. ^{19}F NMR spectra are referenced to external C_6F_6 in $CDCl_3$ at –163.0 ppm. Elemental microanalyses were performed by Oneida Research Services (Whitesboro, New York) or Desert Analytics (Tucson, Arizona).

$[(C_6F_5)C_5H_4][C_5H_5]ZrCl_2$ (59). A mixture of $CpZrCl_3(dme)$ (1.50 g, 4.25 mmol), $Na[(C_6F_5)C_5H_4]$ (1.10 g, 4.33 mmol), and toluene (400 mL) was stirred at 110 °C for 2 h. The hot mixture was filtered; the precipitate was rinsed with an additional 100 mL of hot toluene. The yellow filtrate was cooled to 25 °C, and the resulting crystalline product was collected on a filter, washed with hexanes, and dried under vacuum to afford 1.47 g (3.21 mmol, 76 %) of a yellow crystalline solid. ^1H NMR (C_6D_6) δ 6.45 (m, 2 H), 5.89 (s, 5 H), 5.75 (m, 2 H). ^{19}F NMR (C_6D_6) δ -140.06 (d, 2 F), -155.18 (t, ^3J = 22 Hz, 1 F), -

163.14 (m, 2 F). Anal. Calcd for $C_{16}H_9Cl_2F_5Zr$ C, 41.93; H, 1.98. Found: C, 42.05; H, 1.89.

$[(C_6F_5)C_5H_4]_2HfCl_2$ (60). A mixture of $HfCl_4(THF)_2$ (1.50 g, 3.23 mmol), $Na[(C_6F_5)C_5H_4]$ (1.72 g, 6.78 mmol), and toluene (400 mL) was stirrred at 110 °C for 2 h. The hot mixture was filtered; the filter was washed with 50 mL of additional hot toluene. Cooling the yellow filtrate to 25 °C afforded a crystalline product, which was collected on a filter, wahsed with hexane, and dried under vacuum to afford 1.51 g (2.12 mmol, 66 %) of a yellow crystalline solid. ^{1}H NMR (C_6D_6) δ 6.41 (m, 4 H), 5.73 (m, 4 H). ^{19}F NMR (C_6D_6) δ -140.13 (d, 4 F), -154.76 (tt, 2 F), -162.93 (m, 4 F). Anal. Calcd for $C_{22}H_8Cl_2F_{10}Hf$ C, 37.13; H, 1.13. Found: C, 37.79; H, 1.13.

$[(C_6F_5)C_5H_4][C_5Me_5]ZrCl_2$ (61). A mixture of $C_5Me_5ZrCl_3$ (1.50 g, 4.50 mmol), $Na[(C_6F_5)C_5H_4]$ (1.26, 4.96 mmol), and toluene (400 mL) was stirred at 110 °C for 2 h. Cooled the mixture to ambient temperature and filtered. The solvent was removed *in vacuo*, and the resulting solid was washed with hexane, collected on a filter, and dried under vacuum to afford 1.27 g (2.40 mmol, 53 %) of a yellow crystalline solid. ^{1}H NMR (C_6D_6) δ 6.59 (s, 2 H), 5.68 (s, 2 H), 1.73 (s, 15 H). ^{19}F NMR (C_6D_6) δ -139.46 (d, 2 F), -156.03 (tt, 1 F), -163.63 (m, 2 F). Anal. Calcd for $C_{21}H_{19}Cl_2F_5Zr$ C, 47.73; H, 3.62. Found: C, 47.85; H, 3.42.

$[(C_6F_5)C_5H_4]_2ZrMe_2$ (62). A mixture of $[(C_6F_5)C_5H_4]_2ZrCl_2$ (1.00 g, 1.60 mmol), methyllithium (700 mg, 32 mmol), and toluene (35 mL) was stirred at 25 °C in the dark for 18 h. The solvent was evaporated, and the residue was recrystallized from 35 mL of hexanes to afford 770 mg (1.32 mmol, 82 %) of colorless crystals. ^{1}H NMR (C_6D_6) δ 6.32 (m, 4 H), 5.60 (m, 4 H), -0.39 (s, 6 H). ^{19} F NMR (C_6D_6) δ -140.92 (d, 4 F), -156.95

(t, ^{3}J = 22 Hz, 2 F), -163.11 (m, 4 F). Satisfactory elemental analysis could not be obtained in repeated attempts.

[(C$_6$F$_5$)C$_5$H$_4$][C$_5$H$_5$]ZrMe$_2$ (63). A mixture of [(C$_6$F$_5$)C$_5$H$_4$]C$_5$H$_5$ZrCl$_2$ (500 mg, 1.09 mmol), methyllithium (480 mg, 22 mmol), and toluene (20 mL) was stirred at 25 °C in the dark for 18 h. The solvent was evaporated, and the residue was recrystallized from 20 mL of hexanes to afford 391 mg (0.94 mmol, 86 %) of colorless crystals. ^{1}H NMR (C$_6$D$_6$) δ 6.29 (m, 2 H), 5.70 (s, 5 H), 5.58 (m, 2 H), -0.27 (s, 6 H). ^{19}F NMR (C$_6$D$_6$) δ -141.08 (m, 2 F), -157.59 (t, ^{3}J = 22 Hz) 1 F), -163.36 (m, 2 F). Satisfactory elemental analysis could not be obtained in repeated attempts.

[(C$_6$F$_5$)C$_5$H$_4$]$_2$HfMe$_2$ (64). A mixture of [(C$_6$F$_5$)C$_5$H$_4$]$_2$HfCl$_2$ (1.00 g, 1.41 mmol), methyllithium (620 mg, 28 mmol), and toluene (35 mL) was stirred at 25 °C in the dark for 18 h. The solvent was evaporated, and the residue was recrystallized from 35 mL of hexane to afford 508 mg (0.76 mmol, 54 %) of colorless crystals. ^{1}H NMR (C$_6$D$_6$) δ 6.26 (m, 4 H), 5.53 (m, 4 H), -0.59 (s, 6 H). ^{19}F NMR (C$_6$D$_6$) δ -141.04 (m, 4 F), -156.85 (tt, 2 F), -163.81 (m, 4 F). Anal. Calcd for C$_{24}$H$_{14}$F$_{10}$Hf C, 42.97; H, 2.10. Found: C, 42.78; H, 2.05.

[(C$_6$F$_5$)C$_5$H$_4$][C$_5$Me$_5$]ZrMe$_2$ (65). A mixture of [(C$_6$F$_5$)C$_5$H$_4$]C$_5$Me$_5$ZrCl$_2$ (880 mg, 1.66 mmol), methyllithium (550 mg, 25 mmol), and toluene (40 mL) was stirred at 25 °C in the dark for 18 h. The solvent was evaporated, and the residue was recrystallized from 35 mL of hexane to afford 692 mg (1.42 mmol, 85 %) of colorless crystals. ^{1}H NMR (C$_6$D$_6$) δ 6.47 (m, 2 H), 5.37 (m, 2 H), 1.66 (s, 15H), -0.505 (s, 6 H). ^{19}F NMR (C$_6$D$_6$) δ -140.64 (m, 2 F), -158.13 (t, ^{3}J = 22 Hz) 1 F), -163.71 (m, 2 F). Satisfactory elemental analysis could not be obtained in repeated attempts.

Solution Observation of "Cation-Like" Species $(C_6F_5C_5H_4)CpZrMe^+$ $MeB(C_6F_5)_3^-$ and $(C_6F_5C_5H_4)_2ZrMe^+$ $MeB(C_6F_5)_3^-$. In a resealable (J-Young) NMR tube, a solution of $(C_6F_5C_5H_4)CpZrMe_2$ and $B(C_6F_5)_3$ (slightly more than 1 eqiv) was prepared in C_6D_6. NMR spectra showed the coversion into $(C_6F_5C_5H_4)CpZrMe^+$ $MeB(C_6F_5)_3^-$ was complete, with no remaining $(C_6F_5C_5H_4)CpZrMe_2$ but some unreacted $B(C_6F_5)_3$. Data for $[(C_6F_5)C_5H_4)C_5H_5ZrMe^+$ $MeB(C_6F_5)_3^-$: ^1H NMR (C_6D_6) δ 6.20 (br s, 1 H), 5.85 (br s, 1 H), 5.49 (m, 2 H), 5.48 (s, 5 H), 0.23 (broad, unsymmetrical singlet, 6 H). ^{19}F NMR (C_6D_6) δ -134.31 (m, 6 F), -140.82 (m, 2 F), -152.30 (t, ^3J = 21 Hz, 1 F), -158.89 (m, 3 F), -160.72 (m, 2 F), -164.45 (m, 6 F). The same procedure was used to convert $[(C_6F_5)C_5H_4]_2ZrMe_2$ to $[(C_6F_5)C_5H_4]_2ZrMe^+$ $MeB(C_6F_5)_3^-$. Data for $(C_6F_5C_5H_4)_2ZrMe^+$ $MeB(C_6F_5)_3^-$: ^1H NMR (C_6D_6) δ 6.32 (br s, 2 H), 5.95 (br s, 2 H), 5.57 (m, 4 H), 0.33 (br s, 3 H, BCH_3), 0.18 (s, $ZrCH_3$). ^{19}F NMR (C_6D_6) δ -134.54 (m, 6 F), -140.54 (m, 4 F), -151.64 (t, ^3J = 21 Hz), 2 F), -158.71 (m, 3 H), -160.53 (m, 4 F), -164.41 (m, 6 F). The same procedure was used to convert $[(C_6F_5)C_5H_4]_2HfMe_2$ to $[(C_6F_5)C_5H_4]_2HfMe^+$ $MeB(C_6F_5)_3^-$, except that toluene-d_8 was used, and the NMR spectra was collected at -30 °C, otherwise the signals were too broad to assign. Data for $[(C_6F_5)C_5H_4]_2HfMe^+$ $MeB(C_6F_5)_3^-$: ^1H NMR (toluene-d_8) δ 6.20 (br s, 2 H), 5.78 (m, 2 H), 5.48 (m, 4 H, two coincident Cp-H signals), 0.64 (br s, 3 H, B-CH_3), -0.08 (br s, 3 H, Hf-CH_3). ^{19}F NMR (toluene-d_8) δ -134.50 (m, 6 F), -140.00 (m, 4 F), -151.72 (t, ^3J = 22 Hz, 2 F), -158.15 (m, 3 H), -160.31 (m, 4 F), -164.02 (m, 6 F).

Observation of $[\{(C_6F_5C_5H_4)CpZrMe\}_2(\mu\text{-}Me)]^+[CH_3B(C_6F_5)_3]^-$. In a reseable J-Young NMR tube, a solution of **63** (29 mM) and $B(C_6F_5)_3$ (12 mM) was prepared in C_6D_6. ^1H and ^{19}F NMR analyses showed unreacted **63** (50 % of Zr), mononuclear

contact ion pair **68** (30 % of Zr), and a new set of signals accounting for 20% of the Zr present. In the ^{1}H NMR spectrum most of the signals were osbcured by signals arising from **63** and **68**. Only one of the Cp-H signals was well-resolved at 6.42 ppm (2 H). A signal at –1.00 ppm was assigned to the μ-CH_3 group (br, s, 3 H). Based on integration data, we conclude that the terminal CH_3 signal is underneath the signal arising from the $ZrMe_2$ group of **63** at -0.27 ppm. Other data for the dinuclear complex: ^{19}F (C_6D_6) δ -132.5 (m, 6 F, *ortho*-CF of $MeBAr_3$ anion), -153.1 (m, 2 F, *para*-CF of cation), -161.0 (m, 4 F, *meta*-CF of cation), -164.2 (m, 3 F, *para*-CF of $MeBAr_3$ anion), -166.8 (m, 6 F, *meta*-CF of $MeBAr_3$ anion). Based on integration data, we conclude that the remaining signal, assigned to the *ortho*-CF of the cation, is located at –141.1 ppm (4 F), coincident with the *ortho*-CF signal of **63**.

Titration of Dimethyl Complexes with MAO. All weighings were carried out using an analytical balance (± 0.1 mg resolution) in a nitrogen glove box, using caution to minimize exposure of the sample to ambient light. A typical experiment was conducted as follows. A solution of $(C_6F_5C_5H_4)CpZrMe_2$ (3.99×10^{-2} M) in C_6D_6 was prepared by dissolving 50 mg of $(C_6F_5C_5H_4)CpZrMe_2$ in 3.0 mL of C_6D_6 (needed for spectrometer frequency lock and magnetic field homogeneity adjustments). A solution of MAO (0.865 M) in toluene was prepared by dissolving 251 mg of MAO in 5.0 mL of toluene. The calculation of [MAO] uses a formula weight of 58 g mol^{-1}, corresponding to the "repeat unit" of the putative oligomer $[AlMeO]_n$. Actual number-average molecular weights of MAO samples are typically 400 or higher and are subject to complex ligand disproportionation pathways as samples age. Using 58 g mol^{-1} as the formula weight assumes that every aluminum atom is equally effective for methide abstraction and

allows for direct comparison to practical Al:Zr ratios. For detailed discussion, see: Imhoff, Simeral, Blevins, and Beard (ACS Symp. Ser. **2000**, *749*, 177). To each of five J-Young NMR tubes was added 380 mg of the C_6D_6 solution of $(C_6F_5C_5H_4)CpZrMe_2$. Assuming that $(C_6F_5C_5H_4)CpZrMe_2$ forms an ideal solution in C_6D_6 (ρ = 0.95 g mL^{-1}), the density of the C_6D_6 solution of $(C_6F_5C_5H_4)CpZrMe_2$ was 0.97. A 380 mg aliquot of this solution corresponds to 0.400 mL; therefore, 0.016 mmol of $(C_6F_5C_5H_4)CpZrMe_2$ was added. To each of the five NMR tubes, a different amount (e.g. 160, 407, 622, 800, 950 mg) of the MAO solution in toluene was added. Assuming the MAO forms an ideal solution in toluene, the density of the toluene (ρ = 0.865) solution of MAO was 0.915. The added weights of this solution correspond to 0.18, 0.44, 0.68, 0.87, and 1.04 mL, or 0.16, 0.38, 0.59, 0.75, and 0.87 mmol of MAO, respectively. Then, sufficient toluene was added by weight to each tube to bring the total calculated volume to 1.45 mL. The samples were shaken vigorously, allowed to equilibrate for 5 min, and then subjected to ^{19}F NMR analysis. Longer equilbrium times (up to 2 h in the dark at 25 °C) did not change the spectra noticably.

Variable Temperature Study. Small portions of **62** (10.0 mg, 17 μmol) and MAO (35 mg, 610 μmol, Al:Zr = 36) were weighed into a J-Young NMR tube in the glove box. Toluene-d_8 (roughly 0.6 mL) was condensed into the sample. Upon shaking at room temperature, a clear yellow solution was obtained. ^{19}F NMR analysis revealed the ratio of **62**:**64** at the following temperatures: 42:58 at 50 °C, 47:53 at 25 °C, 48:52 at 0 °C, 47:53 at – 20 °C, 46:54 at – 40 °C, 39:61 at – 60 °C, and 27:73 at – 80 °C. Cooling the sample to – 78 °C for 5 minutes using a dry ice-isopropanol bath resulted in faint turbidity and significant gelation of the sample.

Chapter Three: Synthesis of Methylchlorometallocenes

Introduction

The ligand exchange sequence $MCl_2 \rightarrow M(Me)Cl \rightarrow MMe_2$, (and to a lesser extent, other stepwise ligand exchanges) is important in group 4 metallocene catalyzed reactions. While understanding these exchange reactions is important, isolating and characterizing the "mixed" species is necessary to identify it conclusively in metallocene/MAO mixtures, but more difficult than one might imagine.

$Cp_2Zr(Me)Cl$ (**32**)[138] was synthesized by treating $[Cp_2ZrCl]_2O$[139] with two equivalents of Me_3Al (eq 3.1). For this reaction to serve as a general route to

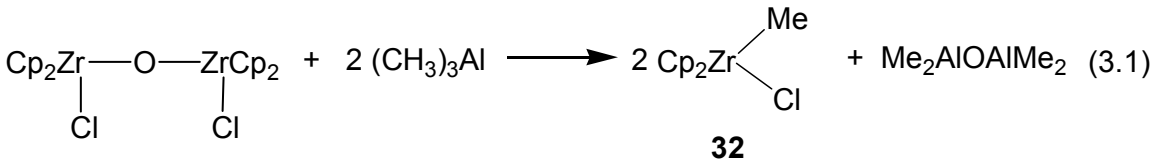

(3.1)

32

methylchlorometallocenes, however, the oxo-bridged starting materials would need to be readily prepared. Several examples, prepared through various methods, of oxo-bridged group 4 complexes are known. Both Wailes[139] and Petersen[140] reported the synthesis of oxo-bridged metallocenes by basic hydrolysis of the dichlorides (eq 3.2-3.3).

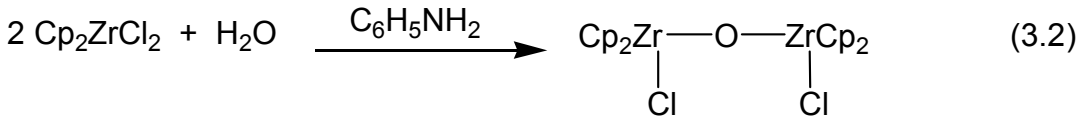

(3.2)

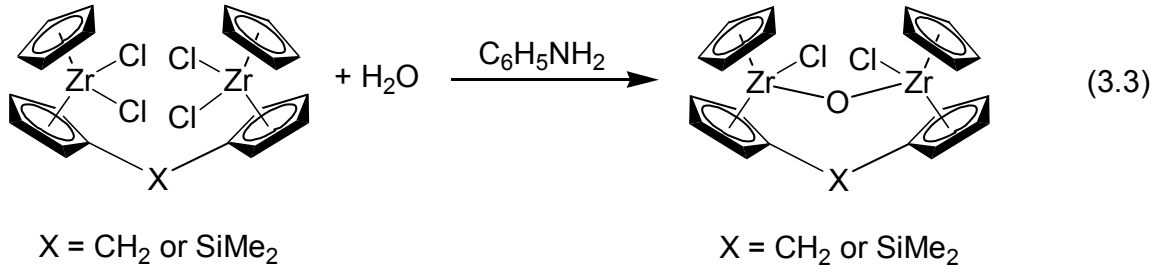

(3.3)

X = CH_2 or $SiMe_2$ X = CH_2 or $SiMe_2$

Atwood[141] and Rausch[142] reported the isolation of $(Cp_2ZrMe)_2O$ and $(Cp_2HfMe)_2O$ from benzene solutions of the dimethylmetallocene, exposed to air for 16 and 45 hours, respectively (eq 3.4). Bercaw[143] demonstrated that $Cp^*_2MH_2$ ($Cp^* = C_5Me_5$; M = Zr, Hf) reacted with water to produce the oxo-bridged hydride complexes $(Cp^*_2MH)_2O$ (eq 3.5). While these oxo-bridged complexes have been reported, no reports of their conversion to corresponding chloromethyl metallocenes have been described.

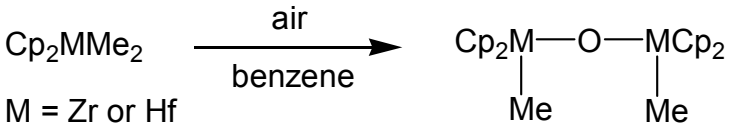

(3.4)

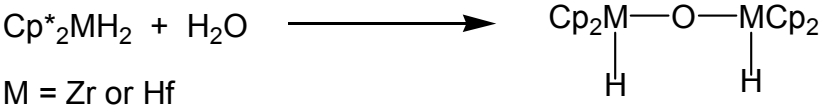

(3.5)

Selective methylation of metallocene dihalides seems a logical approach, but in practice this method is only successful for a few examples. The fundamental problem of selectivity is compounded by the technical difficulty of separating small amounts of dimethyl byproducts or unreacted dihalide. $Cp^*_2Zr(Me)Br$[144] ($Cp^* = C_5Me_5$) was synthesized by the treatment of $Cp^*_2ZrBr_2$ with CH_3MgBr in a toluene/ether solution (eq 3.6). Jordan isolated $Cp_2Zr(Me)X$ (X = F, Br, I),[145] by fractional

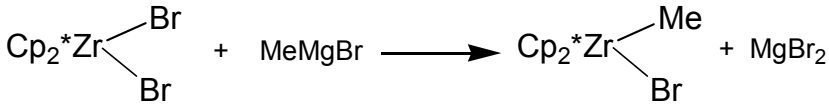

(3.6)

crystallization from the exchange reactions between Cp_2ZrMe_2 and the respective Cp_2ZrX_2. Lisowsky synthesized $(C_9H_7)_2Zr(Me)Cl$ (**71**) from the reaction of $(C_9H_7)_2ZrCl_2$ with trimethylaluminum and NaF (eq 3.7).[146] This synthetic strategy merits further

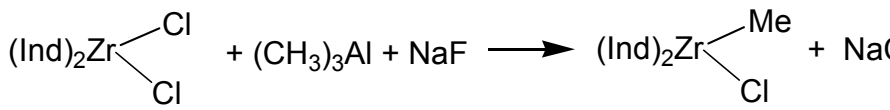

(3.7)

71

discussion. Ordinarily the reaction of **31** and Me_3Al affords an equilibrium mixture **32** and $(AlMe_2Cl)_2$ (eq 3.8). When the reaction of **59** with Me_3Al was

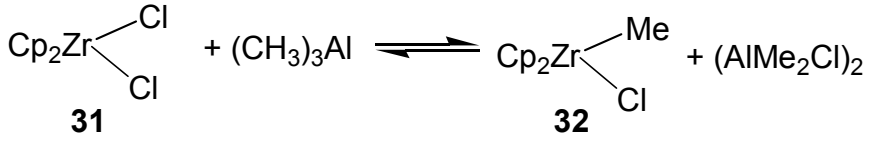

31 **32** (3.8)

investigated, we found that the reaction was reversible. In an NMR tube, over 85 % of **59** was converted into the chloromethyl product (eq 3.9). However when a preparative scale

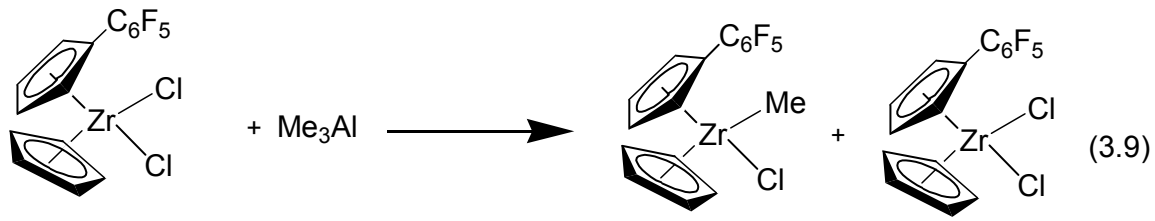

59 85% 15 % (3.9)

reaction was performed, and a vacuum applied to remove the solvent, the distrubution of dichloro- and chloromethylmetallocene was 50/50. Even with a large excess of Me_3Al, it is difficult to remove the $(AlMe_2Cl)_2$ without inconvenient high vacuum pumping, and even then the reaction is driven toward the dichloride upon remolval of Me_3Al which is more volatile than $(AlMe_2Cl)_2$. With the addition of NaF, the $(AlMe_2Cl)_2$ is probably trapped as the fluoride (eq 3.10) but fluoride does not displace ligands at Zr (eq 3.11-3.12).

$$AlMe_2Cl + NaF \rightarrow AlMe_2F + NaCl \text{ or } [AlMe_2FCl]^-Na^+ \quad (3.10)$$

$$MCl_2 + NaF \text{ or } AlMe_2F \rightarrow M(Cl)F \quad (3.11)$$

$$M(Me)Cl + NaF \text{ or } AlMe_2F \rightarrow M(Me)F \quad (3.12)$$

By trapping $AlMe_2Cl$ the alkylation proceeds completely even though only one equivalent of Me_3Al is used. Interestingly, only the synthesis of **71** was attempted via this method.[146]

Another approach to chloromethylmetallocenes begins with readily prepared dimethyls. Again, selectivity and product isolation are the main synthetic obstacles. Much of the work in this area focussed on finding mild chlorinating agents. Both $Cp_2Zr(Me)Cl$[147] and Cp*CpZr(Me)Cl[148] were synthesized by treating the corresponding dimethylzirconocene with $PbCl_2$ (eq 3.13).

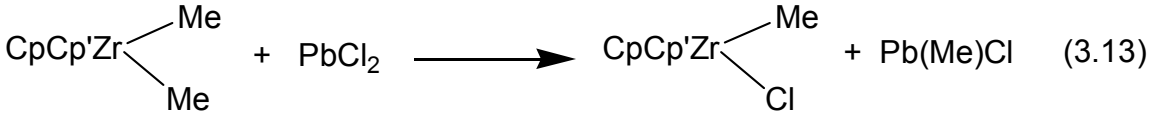

Cp' = C_5H_5 or C_5Me_5

In our ongoing investigation into the reactions of metallocenes with MAO and alkylaluminum halides, we needed a sample of $[(C_6F_5)C_5H_4]_2Zr(Me)Cl$ (**72**) to assign all the NMR signals. In this chapter, the development of a general method for the preparation of chloromethylmetallocenes is discussed. First we demonstrate the scope of the method for several substrates. We also present an analysis of the organic byproducts that are common for all the metallocenes investigated.

Results and Discussion

Synthesis of Metallocenes

As previously discussed, several oxo-bridged complexes have been reported. Although only $[Cp_2ZrCl]_2O$ was converted into a chlormethylmetallocene, the accessibility of oxo-bridged species in general led us to pursue this synthetic route. The first step was to prepare $[(C_6F_5)C_5H_4]_2ZrCl]_2O$ (**73**). All the procedures employed

however failed to produce the desired product, **73**. Without **73** in hand, its subsequent reaction with Me_3Al could not be investigated.

Next we studied selective chlorination. When $[(C_6F_5)C_5H_4]_2ZrMe_2$ (**62**) reacted with one equivalent of $PbCl_2$ at 90 °C for 50 h, a mixture of products formed. Based upon the ^{19}F NMR integration, the three products were **72** (65 %), **58** (5 %), and **62** (30 %) (eq 3.14). Finally, we considered selective alkylation as a route for **72**. The reaction of **58** with a Grignard reagent or methyllithium failed because a mixture of **72** and **62** resulted, which we could not separate efficiently. Despite the failure with $PbCl_2$, we believed that it should be possible to find an organic halogenating agent because the reactivity of the C-Cl bond is readily tuned by substituent effects.

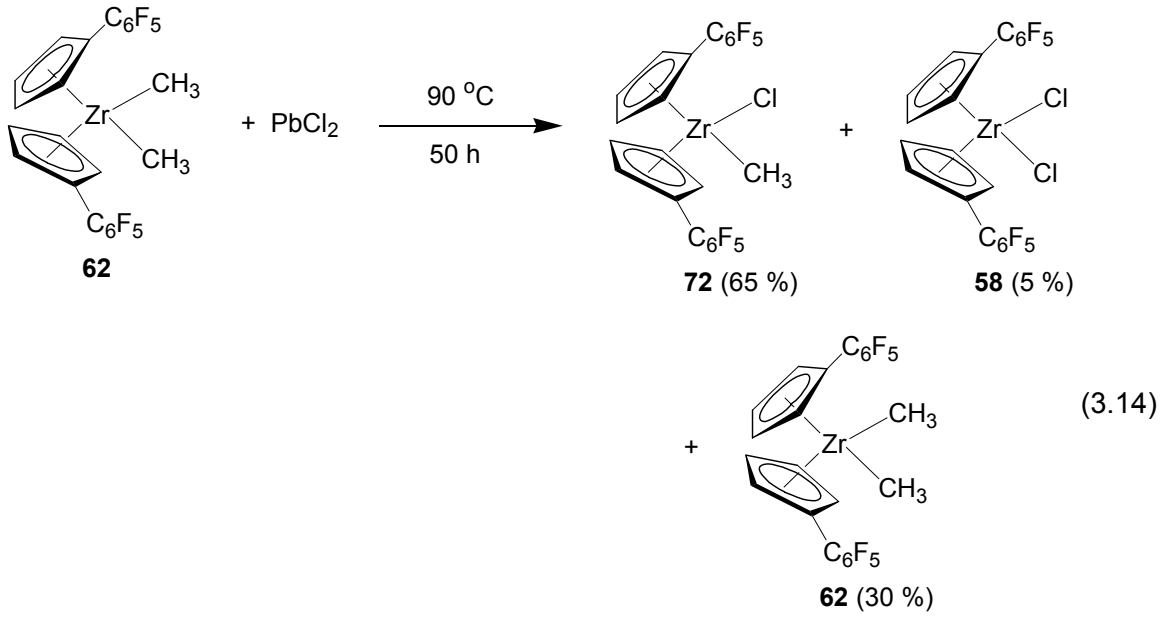

(3.14)

Compound **72** was synthesized by the reaction of **62** and one equivalent of triphenylmethyl chloride, Ph_3CCl, at 60 °C in benzene for 15 h (eq 3.15). The progression of the reaction was monitored by ^{19}F NMR. On a NMR scale, the reaction proceeded to 100 % conversion after only 3 h. However, upon scaling the reaction up, it

was discovered that stirring the reaction overnight (~15 h) at 60 °C was necessary for 100 % conversion. The introduction of additional solvent upon increasing the reaction scale may have retarded a second order reaction thus requiring more time for complete conversion. Compound **72** was isolated after recrystallization from hexane as an air- and moisture-sensitive yellow solid in 85 % yield.

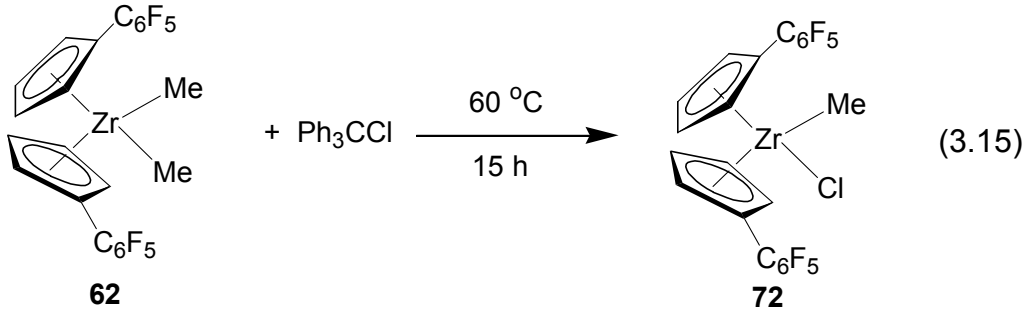

62 **72** (3.15)

Unlike previously discussed synthetic routes that appear to only work for individual compounds, this method is more general. A series of methylchloro metallocenes, previously reported **32** and **71** along with new compounds **72**, $[(C_6F_5)C_5H_4]C_5H_5Zr(Me)Cl$ (**74**), and $[(C_6F_5)Cp]_2Hf(Me)Cl$ (**75**) were all synthesized selectively from the respective dimethylmetallocene and one equivalent of Ph_3CCl (Table 3.1). All compounds were obtained in purity of > 95 %, as determined by NMR spectrocsopic analysis.

The reactions of five additional dimethylmetallocenes, $(C_5Me_5)(C_5H_5)ZrMe_2$ (**76**), $(C_5Me_5)(C_5H_5)HfMe_2$ (**77**), $[(Me_3Si)C_5H_4]_2ZrMe_2$ (**78**), $[(C_6F_5)C_5H_4][C_5Me_5]ZrMe_2$ (**63**), rac-$C_2H_4(C_9H_7)_2ZrMe_2$ (**79**) and a constrained geometry catalyst, $[(C_5Me_4)SiMe_2(N^tBu)]ZrMe_2$ (**80**) with one equivalent of Ph_3CCl were also investigated (Table 3.2). Unlike the compounds in table 3.1, which were isolated as pure compounds, each of the chloromethyl compounds corresponding to **63** and **76**-**80** could not be isolated

Table 3.1. Chemical Shifts for Isolated Monomethylmetallocenes

Metallocene	% Yield	^{1}H NMR	^{19}F NMR
$(C_5H_5)_2Zr(Me)Cl$ (**32**)[a]	80	δ 5.73 (s, Cp); 0.439 (s, CH_3)	
(C9H7)2Zr(Me)Cl (**71**)b	78	δ 7.3–6.8 (m, C_6H_4); 5.83-5.73 (m, C_5H_3); -0.34 (s, CH_3)	
$[(C_6F_5)C_5H_4]_2Zr(Me)Cl$ (**72**)[a]	85	δ 6.46 (m, C_6F_5Cp); 6.32 (m, C_6F_5Cp); 5.68 (m, C_6F_5Cp); 5.55 (m, C_6F_5Cp); 0.26 (s, CH_3)	δ -140.44 (ortho-F); -155.78 (para-F); -162.98 (meta-F)
$[(C_6F_5)C_5H_4]C_5H_5Zr(Me)Cl$ (**74**)[a]	88	δ 6.45 (m, C_6F_5Cp); 6.26 (m, C_6F_5Cp); 5.75 (s, Cp); 5.66 (m, C_6F_5Cp); 5.46 (m, C_6F_5Cp); 0.34 (s, CH_3)	δ -140.61 (ortho-F); -156.38 (para-F); -163.22 (meta-F)
$[(C_6F_5)Cp]_2Hf(Me)Cl$ (**75**)[b]	64	δ 6.39 (m C_6F_5Cp); 6.29 (m, C_6F_5Cp); 5.62 (m, C_6F_5Cp); 5.50 (m, C_6F_5Cp); 0.065 (s, CH_3)	δ -140.58 (ortho-F); -155.86 (para-F); -163.01 (meta-F)

a: 60 °C, 15 h, benzene; b: 90 °C, 15 h, toluene;

in pure form. $(C_5Me_5)(C_5H_5)Zr(Me)Cl$ (**81**) and $(C_5Me_5)(C_5H_5)Hf(Me)Cl$ (**82**) were both prepared in > 90% (eq 3.16) as demonstrated by ^{1}H NMR. Attempts to crystallize or

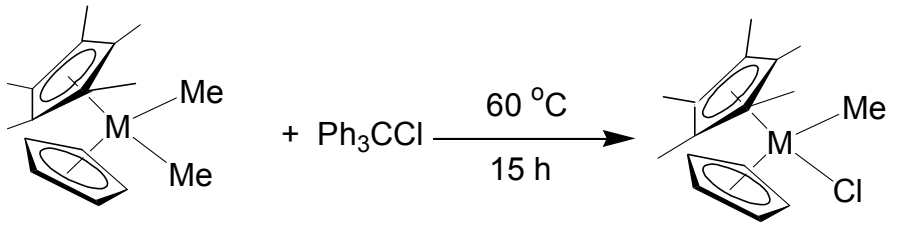

(3.16)

76: M = Zr
77: M = Hf

81: M = Zr
82: M = Hf

sublime **81** and **82** proved unsuccessful, resulting in a mixture of the dimethyl-, monomethyl-, and dichlorometallocenes representing a reduction in purity. Brintzinger found that CH_3 and Cl groups exchange (0.01 M C_6D_6 solutions; catalytic amount of MAO [Al]:[Zr] < 0.1) according to equation 3.17. He used the K_{eq} of eq 3.17 to evaluate

$$L_2MCl(CH_3) + L'_2M(CH_3)_2 \rightleftharpoons L_2MCl_2 + L'_2M(Cl)(CH_3) \qquad (3.17)$$

Metallocene (mmol)	Ph_3CCl (mmol)	Solvent	Temperature	Reaction Time	MMe_2	M(Me)Cl	MCl_2
65, (3.1×10^{-2})	(3.1×10^{-2})	Benzene-d_6	Rt – 60 °C[d]	2 days[b]	10 %	85 %	5 %
76, (4.7×10^{-2})	(4.7×10^{-2})	Benzene-d_6	60 °C	2 days[a]	50 %	50 %	0 %
76, (4.7×10^{-2})	(4.7×10^{-2})	Toluene-d_8	95 °C	18 h[b]	0 %	95 %	5%
76, (6.2×10^{-2})	(6.2×10^{-2})	Toluene	95 °C	18 h[b]	0 %	91 %	9 %
77, (2.8×10^{-2})	(2.8×10^{-2})	Toluene-d_8	95 °C	2 days[b]	3 %	96 %	1 %
77, (4.9×10^{-2})	(4.7×10^{-2})	Toluene	95 °C	2 days[b]	3 %	91 %	6 %
78, (2.8×10^{-2})	(2.8×10^{-2})	Benzene-d_6	RT – 55 °C[c]	1 day[b]	2 %	98 %	0 %
78, (2.4)	(2.4)	Benzene	55 °C	15 h[b]	0 %	100 %	0%
79, (3.2×10^{-2})	(3.2×10^{-2})	Toluene-d_8	RT	5.5 h[b]	2 %	89 %	9 %
80, (2.9×10^{-2})	(2.9×10^{-2})	Benzene-d_6	RT	< 5 min	2 %	91 %	7 %

a: Reaction stopped before complete
b: Reaction complete
c: Reacted at 55 °C for 2.5 h
d: Reacted at 60 °C for 20 h

Table 3.2 Reaction Conditions and product Distribution For the Formation of Several Alkylhalometallocenes

electronic substituent effects. Here we find this exchange reaction to be a nuisance, as it leads to impurity in the desired compounds. The factors influencing exchange rates remain poorly understood, but MAO does catalyze the process. Thus, the combination of > 90% selectivity and the equilibrium between the different species does not allow for a pure sample to be isolated.

$[(Me_3Si)C_5H_4]_2Zr(Me)Cl$ (**83**) and $[(C_6F_5)C_5H_4][C_5Me_5]Zr(Me)Cl$ (**84**) were also selectively prepared (eq 3.18 and 3.19); however, they were too soluble to recrystallize from hexane, which had worked well for compounds in Table 3.1. Attempts to isolate **83** and **84** via sublimation were also unsuccessful.

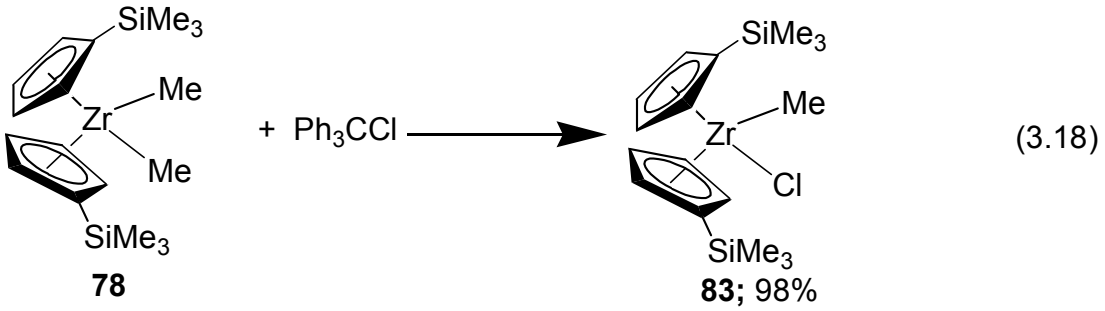

78 **83;** 98% (3.18)

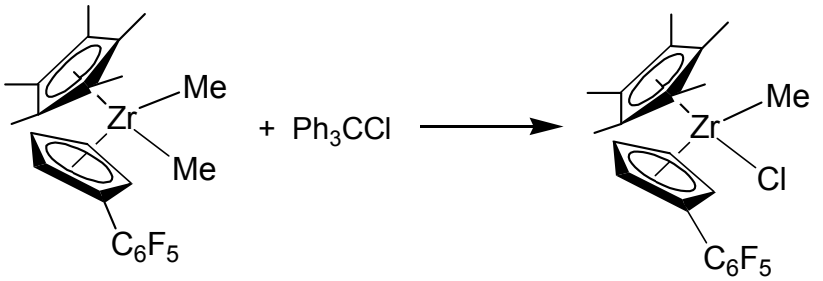

65 **84**; 85 % (3.19)

The reaction of **80** with one equivalent of Ph_3CCl was conducted in an NMR tube and monitored by ^1H NMR. After 45 min, the spectra showed that the reaction had begun. Further analysis by ^1H NMR demonstrated that the reaction was complete after

5.5 h. The formation of $[(C_5Me_4)SiMe_2(N^tBu)]Zr(Me)Cl$ (**85**) was however not selective. Three compounds, **80**, **85** and $[(C_5Me_4)SiMe_2(N^tBu)]ZrCl_2$ were present in 2, 89, and 9 %, respectively (eq 3.20). The reaction of **79** with Ph_3CCl was also monitored by ^1H NMR and found to be complete instantaneously. While rac-$C_2H_4(Ind)_2Zr(Me)Cl$ (**86**) was produced, the reaction was not selective and three compounds were again present, **79** (2%), **86** (91%), and rac-$C_2H_4(Ind)_2ZrCl_2$ (7%) (eq 3.21). The NMR data for compounds **81 - 86** are listed in Table 3.3.

Table 3.3. Data for Monomethylmetallocenes

Compound	Selectivity[c]	^1H NMR	^{19}F NMR
$(C_5Me_5)(C_5H_5)Zr(Me)Cl$ (**81**)[a]	94 %	0.10 (s, Zr-Me); 1.69 (s, C_5Me_5); 5.74 (s, C_5H_5)	
$(C_5Me_5)(C_5H_5)Hf(Me)Cl$ (**82**)[a]	96 %	0.026 (s, Hf-Me); 1.83 (s, C_5Me_5); 5.79 (s, C_5H_5)	
$[(Me_3Si)C_5H_4]_2Zr(Me)Cl$ (**83**)[a]	100 %	0.25 (s, $SiMe_2$); 0.47 (s, Zr-Me); 5.61, 5.85, 5.99, 6.34 (m, C_5H_4)	
$[(C_6F_5)C_5H_4][C_5Me_5]Zr(Me)Cl$ (**84**)[b]	85 %	0.044 (s, Zr-Me); 1.69 (s, C_5Me_5); 5.48, 5,68, 6.36, 6.65 (s, C_5H_4)	δ -140.22 (o) -157.12 (p) -163.67 (m)
$[(C_5Me_4)SiMe_2(N)^tBu]Zr(Me)Cl$ (**85**)[b]	91 %	0.17 (s, Zr-Me); 0.39, 0.44 (s, $SiMe_2$); 1.37 (s, ^tBu); 1.88, 1.89, 2.02, 2.05 (s, $CpMe_4$)	
rac-$C_2H_4(Ind)_2Zr(Me)Cl$ (**86**)[a]	89 %	-0.498 (s, Zr-Me); 2.87 (m, C_2H_4); 5.50, 5.89, 6.35, 6.38 (d, C_5H_2); 6.92-7.37 (m, C_6H_4)	

a: toluene-d_8; b: benzene-d_6
c: $MMe_2 + Ph_3CCl$

Based upon the poor selectivity during the preparation of **81** and **82**, a milder halogen source was investigated. The reaction of **33** with one equivalent of benzyl

bromide, $C_6H_5CH_2Br$ was conducted in a J-Young NMR tube with benzene-d_6 and monitored by ^1H NMR (eq 3.22). An NMR spectrum was collected after 3 hours at room temperature and in contrast to the reaction with one equivalent of Ph_3CCl, no reaction had occurred. The temperature was raised to 75 °C and the reaction only began after reacting for 18 hours. After 19 days, only 73% conversion into the monomethylmetallocene, was observed. While the reaction was very slow, it was selective for the formation of $Cp_2Zr(Me)Br$ (**87**). When the reaction conditions were altered (55 °C and 10 equivalents of $C_6H_5CH_2Br$), the formation of **87** was complete in 4 days. Increasing the temperature again to 95 °C in toluene-d_8, the formation of **87** was complete in 15 h. However, when the reaction was performed at 95 °C, the selectivity appeared to decrease with the formation of **87** (86 %) along with Cp_2ZrBr_2 (6 %) and unreacted **33** (8 %).

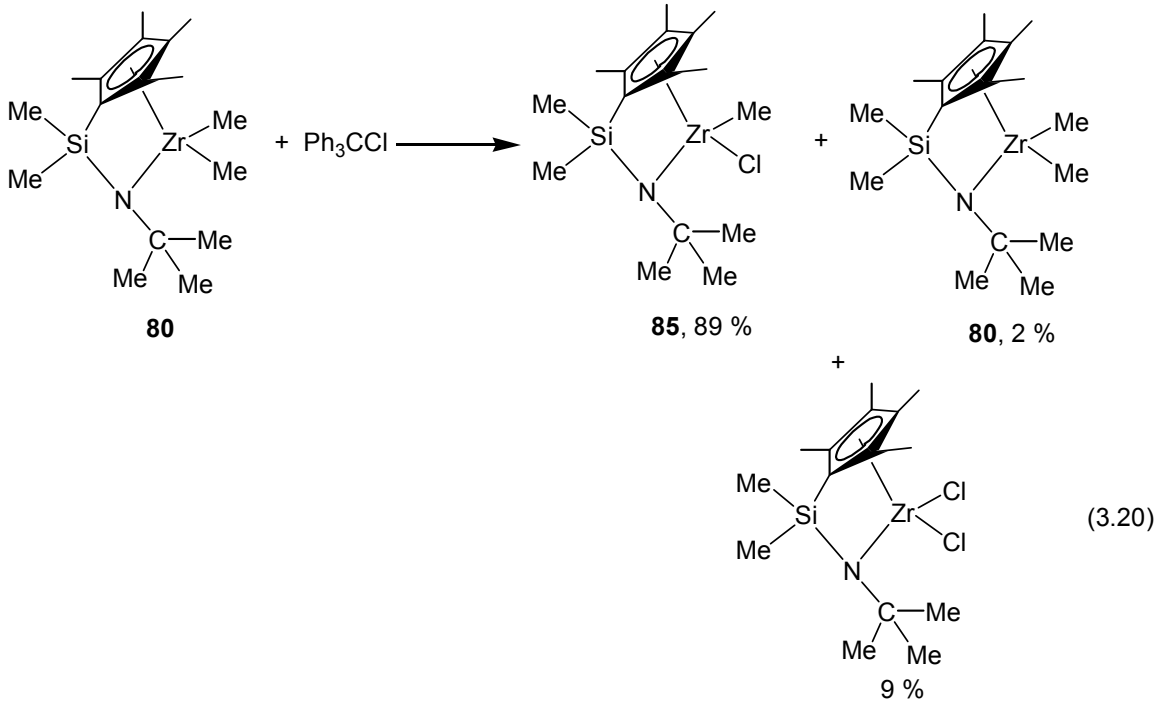

80 **85**, 89 % **80**, 2 % 9 % (3.20)

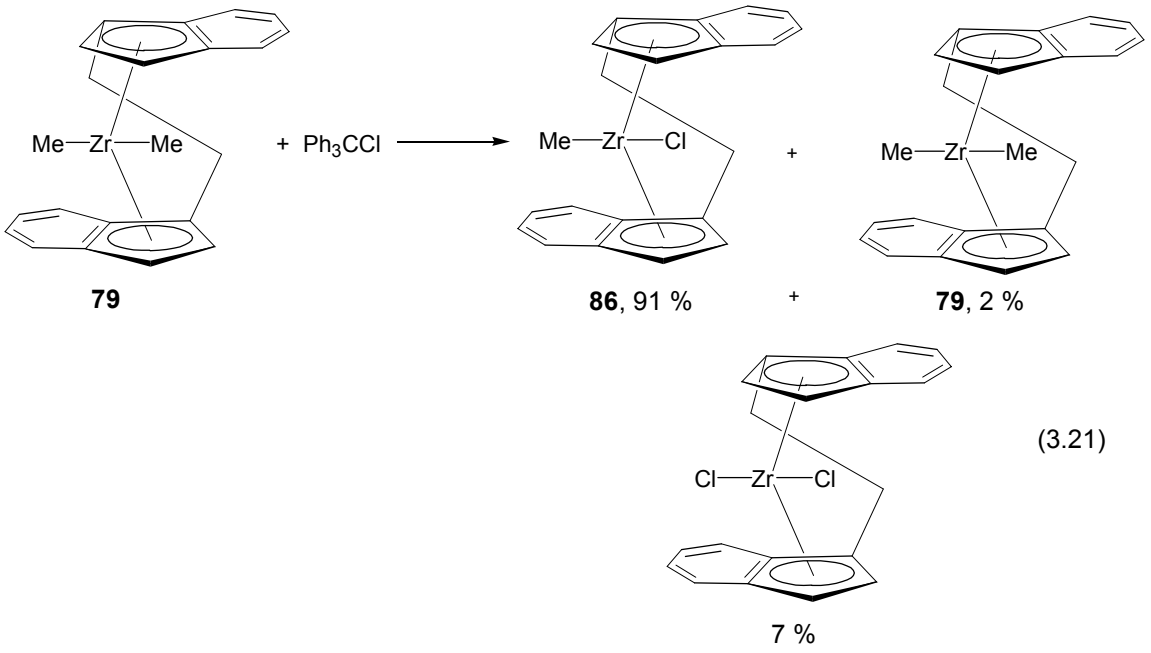

(3.21)

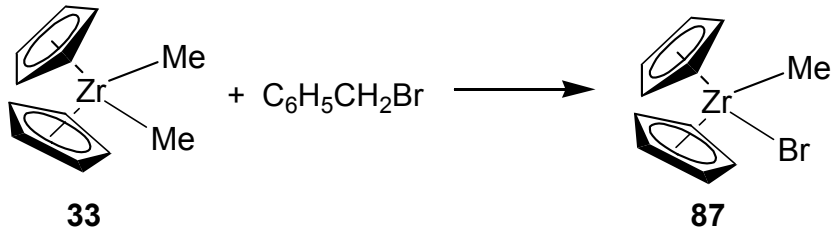

(3.22)

Due to the success of the reaction of **33** and $PhCH_2Br$, reactions with **79** and **80** were also investigated. Our interest in the alkylhalo derivative of **79** stems from conversations with Professor Eugen Chen of Colorado State University. Chen investigated the reaction of **79** and $HN(CH_3)_3Cl$ (eq 3.23).[149] However, a mixture of **86** (70 %) and rac-$C_2H_4(Ind)_2ZrCl_2$ (30 %) was produced. The reaction of **79** with one

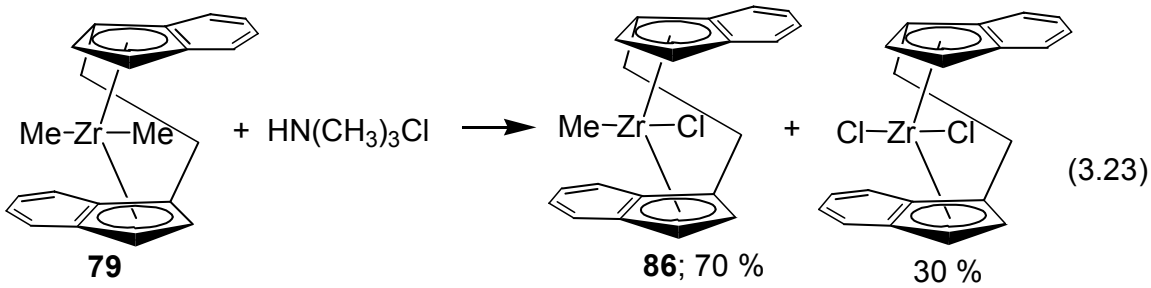

(3.23)

equivalent of $C_6H_5CH_2Br$ was performed in a J-Young NMR tube with benzene-d_6 (eq 3.24). An NMR spectrum was collected after 4 hours at room temperature and in contrast

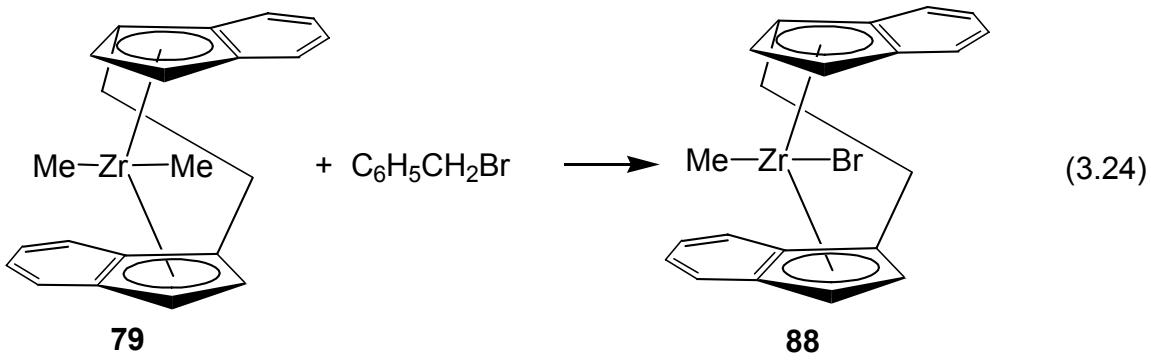

(3.24)

79 **88**

to the reaction with one equivalent of Ph_3CCl, which was instantaneous, no reaction was evident. The temperature was raised to 70 °C, and after 48 hours the reaction had initiated. After a total of 5 days at 70 °C, the reaction was complete, producing rac-$C_2H_4(Ind)_2Zr(Me)Br$ (**88**). When the reaction temperature was increased to 95 °C in toluene-d_8 the reaction again had a 48 hour initiation period. After the initiation period, the reaction was complete in an additional 18 hours. In addition to the peaks for **88**, an additional peak, 0.18 ppm was also present. Analysis of the spectrum has ruled out both Ind-Zr cleavage and formation of a Zr-CH_2Ph species as well as hydrolysis to give CH_4. At this time the peak is still unassigned and further experimentation would be needed.

The reaction of **80** with one equivalent of $C_6H_5CH_2Br$ was also performed in a J-Young NMR tube in toluene-d_8 at 95 °C (eq 3.25). The reaction had an initiation period of 36 hours and after 12 days it was only 78 % complete. The reaction was stopped and a new experiment was performed with 10 equivalents of $C_6H_5CH_2Br$ at 95 °C in toluene-d_8. There was still a long initiation period (18 h), but the reaction was complete after only 48 hours.

Since **83** could not be separated from the byproducts of the reaction with Ph_3CCl, we thought that the reaction of **78** with $C_6H_5CH_2Br$ could produce $[(Me_3Si)C_5H_4]_2Zr(Me)Br$ and that the $C_6H_5CH_2CH_3$ byproduct could be easily removed under vacuum. A J-Young NMR tube reaction of **78** and one equivalent of C_6H_5CHBr

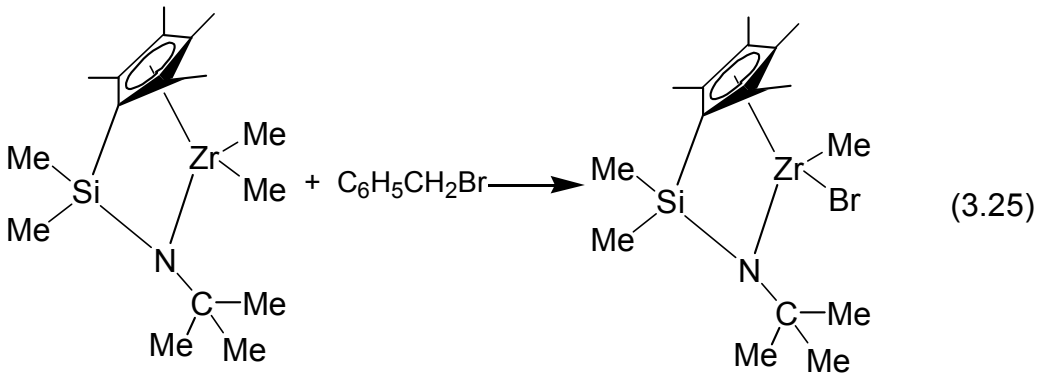

80 (3.25)

in benzene-d_6 was initially investigated at room temperature. An NMR spectrum collected after 24 hours indicated that the reaction had not initiated. The reaction temperature was raised to 65°C and after 72 hours the reaction had still not initiated. The reaction temperature was again raised (95 °C) and 24 h later the reaction had initiated. The reaction progessed very slowly and after 9 weeks it had progressed to 97 % completion and with > 95 % selectivity for the bromomethyl derivative.

Analysis of Organic Byproducts

Upon first glance one might envision a simple exchange reaction between the metal complex and Ph_3CCl (eq 3.26). Instead, several organic byproducts were observed.

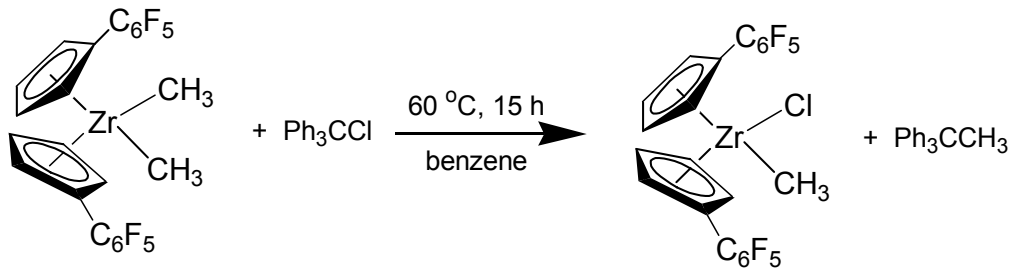

62 **72** (3.26)

The ^{1}H NMR spectrum obtained after a short reaction time (~1 h) showed signals assigned to the starting dimethylmetallocene, triphenylmethyl chloride, and the chloromethyl product. An additional small signal at 2.03 ppm also appeared, assigned to the methyl group of triphenylethane, Ph_3CCH_3.[150] The aromatic signals for triphenylethane (7.00-7.14 ppm) are not resolved from the aromatic signals of the triphenylmethyl chloride. After several hours, additional resonances began to appear in the ^{1}H NMR spectrum. Two signals at 2.08 and 2.15 ppm, were assigned to $(C_6H_5)_2(CH_3C_6H_4)CCH_3$ (Figure 3.2). The third organic compound that appears to be formed in the reaction is triphenylmethane, identified in the ^{1}H NMR by the peak at 5.5 ppm which is representative of the methine hydrogen.[151] Further evidence for the formation of triphenylmethane, triphenylethane, and diphenyl(tol)ethane was obtained from GC/MS analysis. The three products had molecular ion peaks of 244, 258, and 272 m/z, respectively.

The formation of three organic byproducts suggests that a radical process is occurring during the formation of the desired chloro-methyl metal complexes. We propose a chain sequence (Figure 3.1). The reaction between triphenylmethyl radical and **62** could produce a metallocene radical. The metallocene radical could then react with an equivalent of triphenylmethylchloride producing **72** (Figure 3.1). During this process, small concentrations of methyl radical could be formed and undergo further reactions to produce the observed byproducts (Figure 3.2).

Several control experiments were investigated to obtain more evidence about the possible formation of triphenylmethyl radical. Triphenylmethyl chloride was heated to

60 °C in C_6D_6 for 18 h both in the presence and absence of zirconocene dichloride. ^1H NMR analysis indicated no reaction occurred in either mixture.

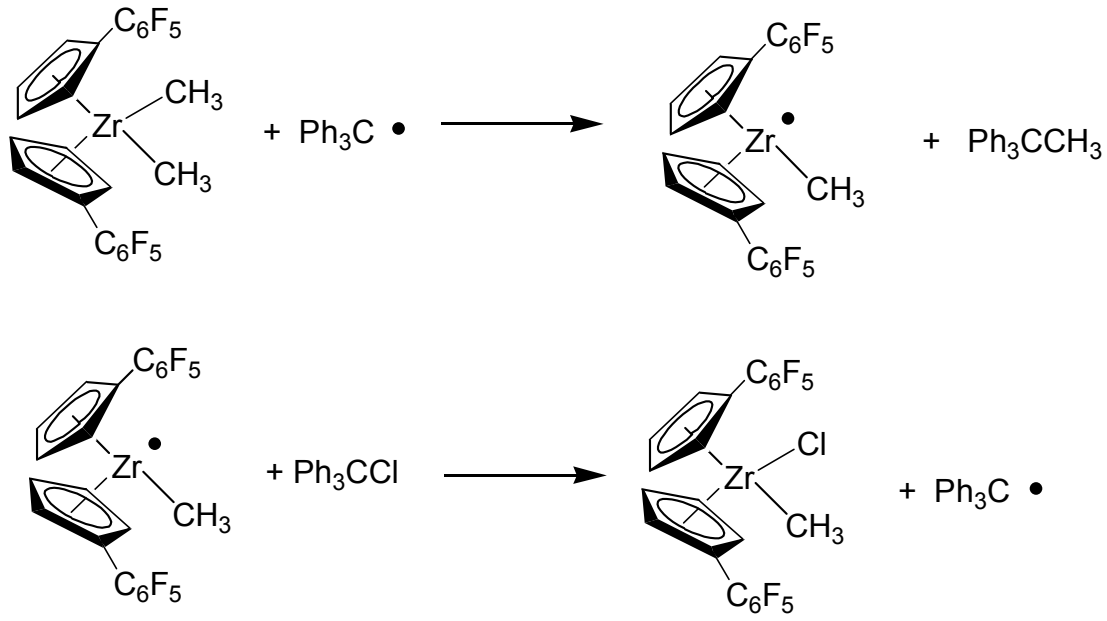

Figure 3.1. Proposed Radical Mechanism

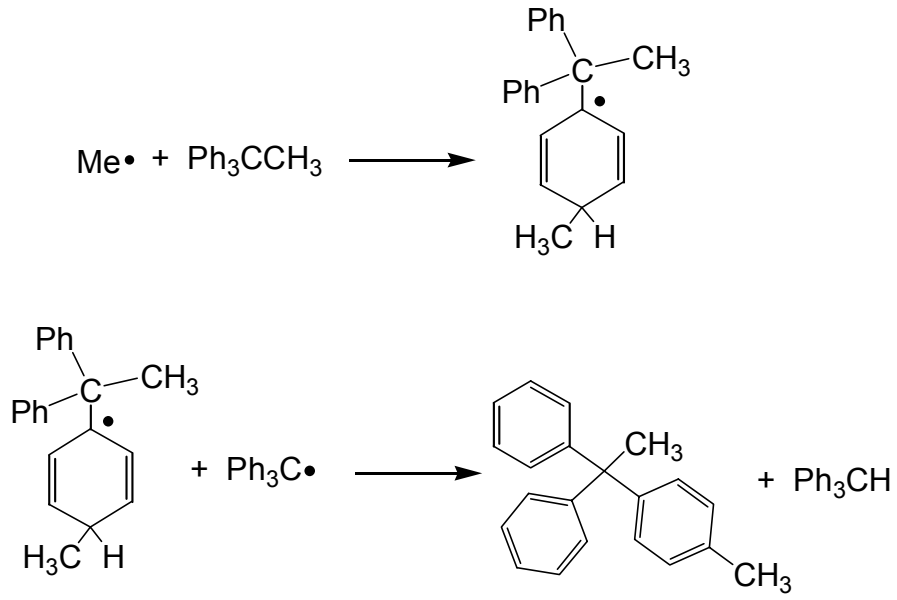

Figure 3.2. Proposed Radical Mechanism for Formation of Organic Byproducts

Finally, 1-diphenylmethylene-4-triphenylmethyl-2,5-cyclohexadiene $[(C_6H_5)_3C(C_6H_5)C(C_6H_5)_2]$[152], was synthesized and reacted with **62** at 25, 60, and 90 °C

(eq 3.27). While the ^{1}H NMR demonstrated that the dimer decomposed upon heating, no reaction with **62** was observed in either the ^{1}H or ^{19}F NMR.

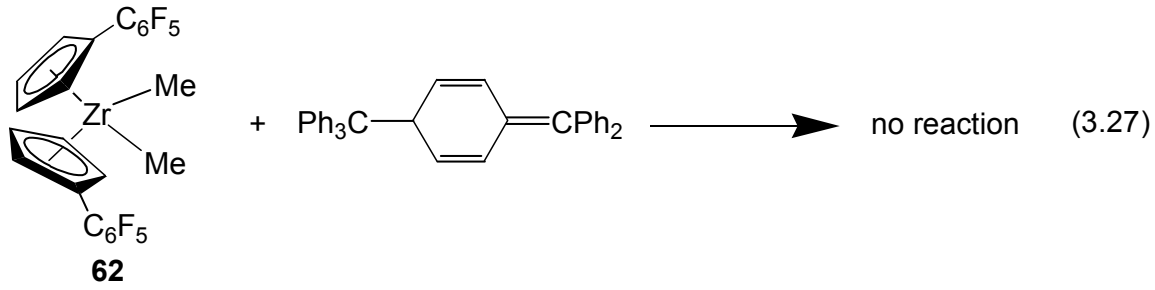

62

Future Work

While the desired chloro-methyl metallocenes were prepared via the reaction between Ph_3CCl and a dimethylmetallocene, the mechanism for their formation is not understood. Some initial reactions were also performed with benzyl bromide to produce bromo-methyl metallocenes. The initiation period associated with these reaction suggests a complex mechanism. Further experimentation could provide information that will allow for the postulation of reaction mechanism for both synthetic routes.

Conclusion

We present a facile synthesis for chloro-methyl metallocenes of group 4. Eleven metallocene dimethides (ligands were Cp, substituted Cp, indenyl, and one "ansa-amido" compound were tested. Five metallocenes (generally the more electron-deficient examples) are highly selective (> 95%) conversion into the chloro-methyl derivative and could also be isolated in moderate to high yield. Another 2 metallocenes showed good selectivity in NMR-scale reactions, but upon scaling up the reactions, the products were too soluble to separate from the triphenylmethane byproduct. The remaining 4 metallocenes reacted unselectively. A preliminary NMR-scale study of benzyl bromide as the halogen source showed high selectivity for the formation of the bromo-methyl

compound, but reaction times were too long to be practical. Long initiation times and analysis of the organic byproducts suggest that the reaction of metallocene dimethyl species with alkyl halides proceeds by a free-radical chain process although an exact mechanism was not elucidated.

Experimental Section

General Considerations. All manipulations were carried out using standard nitrogen-atmosphere techniques. Ph_3CCl was purchased from Aldrich and further purified by sublimation (115 °C, 3 x 10^{-5} torr). $(C_5H_5)_2ZrCl_2$ was purchased from Aldrich. $[(C_6F_5)C_5H_4]_2ZrMe_2$, $[(C_6F_5)C_5H_4]C_5H_4ZrMe_2$, $[(C_6F_5)C_5H_4](C_5(CH_3)_5)ZrMe_2$ and $[(C_6F_5)C_5H_4]_2HfMe_2$ were prepared according to our own methods.[153] $[(Me_3Si)C_5H_4]_2ZrCl_2$[154,155] and $(C_9H_7)_2ZrCl_2$[156] and were prepared according to literature methods. rac-$C_2H_4(Ind)_2ZrMe_2$ was a gift from Dr. E. Y. X. Chen. $(C_5H_5)_2ZrMe_2$, $[(Me_3Si)C_5H_4]_2ZrMe_2$, and $(C_9H_7)_2ZrMe_2$ were prepared via the reaction of the corresponding dichloride and solid methyllithium in toluene. NMR spectra were recorded on a Varian U-400 instrument at 22 °C. ^{19}F NMR spectra are referenced to external C_6F_6 in $CDCl_3$ at –163.0 ppm. GC/MS analysis was performed on a VG Quattro 7770. Elemental microanalyses were performed by Desert Analytics (Tucson, Arizona).

$(C_5H_5)_2Zr(Me)Cl$ (31).[138] A swivel-frit reaction apparatus was charged with a mixture of Cp_2ZrMe_2 (188 mg, 0.749 mmol), Ph_3CCl (211 mg, 0.756 mmol) and benzene (15 mL). The mixture was stirred at 60 °C for 18 h. The solvent was removed *in vacuo*, and the residue was recrystallized from hexane to afford 138 mg (0.597 mmol, 80%) of pale yellow crystals. ^1H NMR (C_6D_6) δ 5.73 (s, 10 H), 0.439 (s, 3 H). Data matched literature values.

$(C_9H_7)_2Zr(Me)Cl$ (71).[146] A swivel-frit apparatus was charged with a mixture of $(C_9H_7)_2ZrMe_2$ (96 mg, 0.273 mmol), Ph_3CCl (75 mg, 0.270 mmol) and toluene (30 mL). The mixture was stirred at 90 °C for 18 h. The solvent was removed *in vacuo* and the residue was washed with hexane. The product was collected on a frit to afford 79 mg (0.211 mmol 78 %) of white solid. ^1H NMR spectroscopic analysis indicated that 2 % of $(C_9H_7)_2ZrCl_2$ was present. ^1H NMR (C_6D_6) δ 7.3–6.8 (m, 4 H, C_6H_4); 5.83-5.73 (m, 3 H, C_5H_3); -0.34 (s, 3 H, CH_3).

$[(C_6F_5)C_5H_4]_2Zr(Me)Cl$ (72). A swivel-frit apparatus was charged with a mixture of $[(C_6F_5)C_5H_4]_2ZrMe_2$ (500 mg, 0.857 mmol), Ph_3CCl (250 mg, 0.899 mmol) and benzene (15 mL). The mixture was stirred at 60 °C for 18 h. The solvent was removed *in vacuo*, and the residue was recrystallized from hexane to afford 441 mg (0.730 mmol, 85 %) of yellow crystals in two crops. ^1H NMR (C_6D_6) δ 6.46 (m, 2 H), 6.32 (m, 2 H), 5.68 (m, 2 H), 5.55 (m, 2 H), 0.26 (s, 3H). ^{19}F NMR (C_6D_6) δ -140.44 (m, 4 F), -155.78 (tt, 2 F), -162.98 (m, 4 F). Anal. Calcd for $C_{23}H_{11}ClF_{10}Zr$ C, 45.74; H, 1.84. Found: C, 45.90; H, 1.55.

$[(C_6F_5)C_5H_4][C_5H_5]Zr(Me)Cl$ (74). A swivel-frit apparatus was charged with a mixture of $[C_6F_5)Cp]CpZrMe_2$ (644 mg, 1.54 mmol), Ph_3CCl (434 mg, 1.56 mmol) and benzene (25 mL). The mixture was stirred at 60 °C for 18 h. The solvent was removed *in vacuo* and the residue was recrystallized from hexane to afford 592 mg (1.35 mmol, 88 %) of yellow crystals in two crops. ^1H NMR (C_6D_6) δ 6.45 (m, 1 H), 6.26 (m, 1 H), 5.75 (s, 5 H), 5.66 (m, 1 H), 5.46 (q, 1 H), 0.340 (s, 3 H). ^{19}F NMR (C_6D_6) δ -140.61 (m, 2 F), -156.38 (t, 1 F), -163.22 (m, 2 F). Satisfactory elemental analysis could not be obtained in repeated attempts.

[(C$_6$F$_5$)C$_5$H$_4$]$_2$Hf(Me)Cl (75). A swivel-frit apparatus was charged with a mixture of [(C$_6$F$_5$)C$_5$H$_4$]$_2$HfMe$_2$ (183 mg, 0.273 mmol), Ph$_3$CCl (76 mg, 0.273 mmol) and benzene (15 mL). The mixture was stirred at 60 °C for 18 h. The solvent was removed *in vacuo*. The product was sublimed (110 °C, 3 x 10^{-5} torr) to afford 120 mg (0.174 mmol, 64%) of white crystals. ^{1}H NMR (C$_6$D$_6$) δ 6.39 (m, 2 H), 6.29 (m, 2 H), 5.62 (m, 2 H) 5.50 (m, 2 H) 0.065 (s, 3 H) ^{19}F NMR (C$_6$D$_6$) δ -140.58 (m, 4 F), -155.86 (t, 2 F), -163.01 (m, 4 F) Anal. Calcd for C$_{23}$H$_{11}$ClF$_{10}$Hf C, 39.96; H, 1.60. Found: C, 39.59; H, 1.33.

(C$_5$Me$_5$)(C$_5$H$_5$)Zr(Me)Cl (81). A J-Young NMR tube was charged with (C$_5$Me$_5$)(C$_5$H$_5$)ZrMe$_2$ (15 mg, 4.7 x 10^{-2} mmol), Ph$_3$CCl (13 mg, 4.7 x 10^{-2} mmol) and Toluene-d$_8$ (1 mL). The tube was placed in a 95 °C oil bath for 18 h. ^{1}H NMR (Toluene-d$_8$) δ 5.74 (s, 5 H), 1.69 (s, 15 H), 0.10 (s, 3 H). ^{1}H NMR analysis indicated the formation of (C$_5$Me$_5$)(C$_5$H$_5$)Zr(Me)Cl (95 %) and (C$_5$Me$_5$)(C$_5$H$_5$)ZrCl$_2$ (5 %).

(C$_5$Me$_5$)(C$_5$H$_5$)Hf(Me)Cl (82). A J-Young NMR tube was charged with (C$_5$Me$_5$)(C$_5$H$_5$)HfMe$_2$ (11 mg, 2.8 x 10^{-2} mmol), Ph$_3$CCl (7.9 mg, 2.8 x 10^{-2} mmol) and toluene-d$_8$ (1 mL). The tube was placed in a 95 °C oil bath for 2 days. ^{1}H NMR (Toluene-d$_8$) δ 5.79 (s, 5 H), 1.83 (s, 15 H), 0.25 (s, 3 H). ^{1}H NMR analysis indicated the formation of (C$_5$Me$_5$)(C$_5$H$_5$)Hf(Me)Cl (96 %), (C$_5$Me$_5$)(C$_5$H$_5$)HfMe$_2$ (3 %) and (C$_5$Me$_5$)(C$_5$H$_5$)HfCl$_2$ (1 %).

[(Me$_3$Si)C$_5$H$_4$]$_2$Zr(Me)Cl (83). A swivel-frit apparatus was charged with a mixture of (Me$_3$SiC$_5$H$_4$)$_2$ZrMe$_2$ (936 mg, 2.36 mmol), Ph$_3$CCl (692 mg, 2.48 mmol) and benzene (35 mL). The mixture was stirred at 60 °C for 18 h. The solvent was removed *in vacuo* and the residue was taken up in hexane. Attempts to recystallize product failed. Attempts to sublime the product also failed. ^{1}H NMR (C$_6$D$_6$) δ 6.34 (m, 2 H), 5.99 (m, 2

H), 5.85 (m, 2 H), 5.61 (m, 2 H), 0.473 (s, 3 H), 0.246 (s, 18 H). ^{1}H NMR analysis indicated the formation of 100 % $[(Me_3Si)C_5H_4]_2Zr(Me)Cl$ it just could not be separated from the organic byproducts.

$[(C_6F_5)C_5H_4][C_5Me_5]Zr(Me)Cl$ (84). A swivel-frit apparatus was charged with a mixture of $[(C_6F_5)C_5H_4][C_5Me_5]ZrMe_2$ (230 mg, 0.472 mmol), Ph_3CCl (138 mg, 0.495 mmol) and toluene (15 mL). The mixture was stirred at 90 °C for 18 h. The solvent was removed *in vacuo* and the residue was taken up in hexane. Attempts to recrystallize or sublime the product failed. ^{19}F NMR analysis indicated the formation of $[(C_6F_5)C_5H_4][C_5Me_5]Zr(Me)Cl$ (85 %), $[(C_6F_5)C_5H_4][C_5Me_5]ZrMe_2$ (10 %), and $[(C_6F_5)C_5H_4][C_5Me_5]ZrCl_2$ (5 %). Data for **84**: ^{1}H NMR (toluene-d_8) δ 6.65 (m, 1H), 6.36 (m, 1 H), 5.68 (m, 1 H), 5.48 (m, 1 H), 1.69 (s, 15 H), 0.044 (s, 3 H). ^{19}F NMR (C_6D_6) δ-140.22 (m, 2 F), -157.12 (t, J = 21.44 Hz, 1 F), -163.67 (m, 2 F).

$[(C_5Me_4)SiMe_2(N^tBu)]Zr(Me)Cl$ (85). A J-Young NMR tube was charged with $[(C_5Me_4)SiMe_2(N)^tBu]ZrMe_2$ (11 mg, 3.2 x 10^{-2} mmol), Ph_3CCl (8.8 mg, 3.2 x 10^{-2} mmol) and C_6D_6 (1 mL). ^{1}H NMR analysis indicated the formation of $[(C_5Me_4)SiMe_2(N)^tBu]Zr(Me)Cl$ (89 %), $[(C_5Me_4)SiMe_2(N)^tBu]ZrMe_2$ (2 %), and $[(C_5Me_4)SiMe_2(N)^tBu]ZrCl_2$ (9 %). Data for **85**: ^{1}H NMR (C_6D_6) δ 2.05 (s, 3 H), 2.02 (s, 3 H), 1.89 (s, 3 H), 1.88 (s, 3 H), 1.37 (s, 9 H) 0.43 (s, 3 H), 0.39 (s, 3H), 0.17 (s, 3 H).

rac-$C_2H_4(Ind)_2Zr(Me)Cl$ (86). A J-Young NMR tube was charged with rac-$C_2H_4(Ind)_2ZrMe_2$ (11 mg, 2.9 x 10^{-2} mmol), Ph_3CCl (8.2 mg, 2.9 x 10^{-2} mmol) and C_6D_6 (1 mL). ^{1}H NMR analysis indicated the formation of rac-$C_2H_4(Ind)_2Zr(Me)Cl$ (91 %), rac-$C_2H_4(Ind)_2ZrMe_2$ (2 %), and rac-$C_2H_4(Ind)_2ZrCl_2$ (7 %). Data for **86**: ^{1}H NMR

(C_6D_6) δ 6.92 - 7.37 (m, 4 H), 6.38 (d, 1 H), 6.35 (d, 1 H), 5.89 (d, 1 H), 5.50 (d, 1 H), 2.87 (m, 4 H), -0.49 (s, 3 H).

$Cp_2Zr(Me)Br$ (88). A J-Young NMR tube was charged with Cp_2ZrMe_2 (12 mg, 4.8 x 10^{-2} mmol), $C_6H_5CH_2Br$ (82.0 mg, 4.8 x 10^{-1} mmol) and Toluene-d_8 (1 mL). The tube was placed in a 95 °C oil bath overnight. ^1H NMR analysis indicated the formation of $Cp_2Zr(Me)Br$ (86 %), Cp_2ZrBr_2 (6 %), and Cp_2ZrMe_2 (8 %). Data for **88**: ^1H NMR (Toluene-d_8) δ 5.76 (s, 10 H), 0.20 (s, 3 H).

rac-$C_2H_4(Ind)_2Zr(Me)Br$ (89). A J-Young NMR tube was charged with rac-$C_2H_4(Ind)_2ZrMe_2$ (53 mg, 1.4 x 10^{-1} mmol), $C_6H_5CH_2Br$ (24.3 mg, 1.4 x 10^{-1} mmol) and C_6D_6 (1 mL). The tube was placed in a 70 °C oil bath for 5 days^1H NMR analysis indicated the formation of rac-$C_2H_4(Ind)_2Zr(Me)Br$ (95 %) and rac-$C_2H_4(Ind)_2ZrBr_2$ (5 %). Data for **89**: . ^1H NMR (C_6D_6) δ 6.92 - 7.37 (m, 4 H), 6.56 (d, 1 H), 6.38 (d, 1 H), 5.82 (d, 1 H), 5.54 (d, 1 H), 2.72 (m, 4 H), -0.62 (s, 3 H).

$[(C_5Me_4)SiMe_2(N^tBu)]Zr(Me)Br$. A J-Young NMR tube was charged with $[(C_5Me_4)SiMe_2(N)^tBu]ZrMe_2$ (8.7 mg, 2.4 x 10^{-2} mmol), Ph_3CCl (40 mg, 2.4 x 10^{-1} mmol) and toluene-d_8 (1 mL). The tube was placed in a 95 °C oil both for 48 h. ^1H NMR analysis indicated the formation of $[(C_5Me_4)SiMe_2(N)^tBu]Zr(Me)Br$ > 98%. The remaining 2% was unreacted $[(C_5Me_4)SiMe_2(N)^tBu]ZrMe_2$. Data for the bromomethyl derivative: ^1H NMR (C_6D_6) δ 2.03 (s, 3 H), 2.00 (s, 3 H), 1.88 (s, 3 H), 1.87 (s, 3 H), 1.36 (s, 9 H) 0.42 (s, 3 H), 0.38 (s, 3H), 0.17 (s, 3 H).

$[(Me_3Si)C_5H_4]_2Zr(Me)Br$. A J-Young NMR tube was charged with $[(Me_3Si)C_5H_4]_2ZrMe_2$ (21 mg, 5.3 x 10^{-2} mmol), $C_6H_5CH_2Br$ (9.1 mg, 5.3 x 10^{-2} mmol) and C_6D_6 (1 mL). The tube was reacted at room temperature for 24 h and no reaction

occurred. The tube was placed in a 65 °C oil bath for 72 h and still no reaction had occurred. The tube was placed in a 95 °C oil bath for 9 weeks and the reaction progressed to 97 % complete with 100 % selectivity (no dibromide was present) based on integrations. ^{1}H NMR (C_6D_6) δ 6.39 (m, 1 H), 6.08 (m, 1 H), 5.93 (m, 1 H), 5.70 (m, 1 H), 0.35 (s, 3 H), 0.27 (s, 18H).

Preparation of Alkylhalometallocene Using Ph_3CCl in an NMR Tube. A typical experiment was conducted as follows. A J-Young NMR tube was charged with $(C_5Me_5)(C_5H_5)ZrMe_2$ (15.0 mg, 4.66 x 10^{-2} mmol), Ph_3CCl (13.0 mg, 4.66 x 10^{-2} mmol) and toluene-d_8. The mixture was reacted at 95 °C and ^{1}H NMR spectrum were collected as time elapsed. The reaction was complete after 15 h. ^{1}H NMR (toluene-d_8) δ 5.74 (s, 5 H); 1.69 (s, 15 H); 0.10 (s, 3 H).

Preparation of organic residue for Mass Spectrometry Analysis. The organic residue was dissolved in hexane and filtered through alumina to remove any residual metal complex. The solvent was removed *in vacuo* and the remaining oily material injected onto the GC/MS. The residue separated into three distinct products on the column. The three products had molecular ion peaks of 244, triphenylmethane 258, triphenylethane and 272 m/z, diphenyl(tol)ethane.

Chapter Four: Reactions of Metallocenes with Alkylaluminum Halides

Introduction

In most industrial and academic settings, the metallocene derivatives used as olefin polymerization catalysts are not dimethyl compounds but usually dichlorides and sometimes dialkoxides and diamido compounds, Cp_2MX_2 where X = Cl, OR, or NR_2.[9,53,157-160] These derivatives, especially the dichlorides, are usually the easiest to prepare and handle, because in most cases they are not especially air-sensitive. MAO then acts to exchange the labile ligands such as chloride for methyl and to abstract a ligand from the inner coordination sphere of the transition metal to generate catalytically active "cationic metallocene" species. Numerous prior studies have helped to identify some of the different pathways involved.[10,53,79,161,162] Some, like Eisch's study with titanocene complexes, used simple, well-defined aluminum alkyl compounds, although even there, ligand scrambling at aluminum could be an important complication.[64,65,163] Other prior studies, notably Deffieux's UV-Vis study,[88-90] used MAO, but the limitations of the UV-Vis technique mandate confirmation of their conclusions by a technique with better spectroscopic resolution and better quantitative accuracy. In spite of all the prior studies, the relationship among the different exchange and abstraction steps remains unclear.

In previous chapters, we described the use of ^{19}F NMR to quantify the methide abstraction in Cp_2MMe_2/MAO mixtures. In this chapter we explore the Cl/CH_3 exchange with Me_3Al and MAO in addition to the activation paythways in the MCl_2/MAO system. Along the way we needed to develop a chemical shift scale so we could follow reactions with MAO using ^{19}F NMR. One particular challenge was understanding the effect of

weak M-Cl---AlR_3 interactions on chemical shift. Reactions of several pentafluorophenyl-substituted metallocenes with a series of alkylaluminum compounds will provide insight into these questions: (1) Is ^{19}F NMR suitable for examining ligand exchange processes that occur when metallocene dichlorides are treated with alkylaluminum compounds? For example, is it possible to correlate a specific change in ^{19}F chemical shift with each ligand exchange? (2) Can we use ^{19}F NMR probes to understand better the nature of MCl---AlR_3 interactions in solution? (3) Are metallocene dichlorides more or less effectively activated by an equivalent amount of MAO, compared to dimethyl metallocenes? (4) What pathway converts metallocene dichlorides into active catalytic species upon treatment with MAO?

Results And Discussion

Interpreting Chemical Shifts in C_6F_5-Substituted Metallocenes

The ^{19}F NMR chemical shifts for the 12 pentafluorophenyl-substituted metallocenes used in this study are listed in Table 4.1. This data establishes a $\delta(^{19}F_p)$ scale that helps us to assign spectra of metallocene-organoaluminum mixtures.

Table 4.1. ^{19}F NMR Chemical Shifts

Metallocene	ortho	para	meta
$(C_6F_5Cp)_2ZrCl_2$ (**58**)	-138.31	-153.39	-161.28
$(C_6F_5Cp)_2Zr(Me)Cl$ (**72**)	-139.28	-154.62	-161.82
$(C_6F_5Cp)_2ZrMe_2$ (**62**)	-139.76	-155.79	-161.95
$(C_6F_5Cp)CpZrCl_2$ (**59**)	-138.87	-154.02	-161.95
$(C_6F_5Cp)CpZr(Me)Cl$ (**74**)	-139.46	-155.23	-162.06
$(C_6F_5Cp)CpZrMe_2$ (**63**)	-139.92	-156.43	-162.20
$(C_6F_5Cp)_2HfCl_2$ (**60**)	-138.97	-153.60	-161.76
$(C_6F_5Cp)_2Hf(Me)Cl$ (**75**)	-139.43	-154.70	-161.85
$(C_6F_5Cp)_2HfMe_2$ (**64**)	-139.88	-155.69	-162.65
$(C_6F_5Cp)Cp^*ZrCl_2$ (**61**)	-138.30	-154.87	-162.47
$(C_6F_5Cp)Cp^*Zr(Me)Cl$ (**84**)	-139.06	-155.96	-162.51
$(C_6F_5Cp)Cp^*ZrMe_2$ (**65**)	-139.48	-156.97	-162.55

The comparison of $\delta(^{19}F_{para})$ for three dichloro-metallocenes, **58**, **59**, and **61** quantifies the electronic substituent effects of the C_6F_5, C_5H_5, and C_5Me_5 ligands. As the electron-density increases on the metal center (replacing [(C_6F_5)Cp] (**58**) with Cp (**59**) or Me_5Cp (**61**)) there is a corresponding upfield shift of the NMR signal (Table 4.2). From the NMR data, it can be concluded that one C_6F_5 group is equal in magnitude to 3-4 methyl groups but opposite in sign. Electrochemical analysis of C_6F_5-substituted ferrocenes showed that each C_6F_5 had the effect of 2-3 CH_3 groups, but opposite in sign.[123]

Table 4.2. Ligand Effect on δ $^{19}F_{para}$ of (Ligand)$(C_6F_5Cp)ZrCl_2$

Ligand	Metallocene	δ ($^{19}F_{para}$)	Shift Relative to Cp
C_6F_5	58	-153.39	0.63
Cp	59	-154.02	0.00
Me_5Cp	61	-154.87	-0.85

Another trend in $\delta(^{19}F_{para})$ is observed during stepwise methylation from **61** $\rightarrow$ **84** $\rightarrow$ **65** (eq 4.1, where Cp' = [(C_6F_5)Cp] and Cp* = C_5Me_5). Shifts in the *ortho* and *meta* resonances of the C_6F_5 group are also observed (Table 4.3). Comparison of the ortho, meta, and para regions demonstrated that the ortho shift is not linear, the meta shift is not sensitive, while the para shift is linear. In fact, analysis of all the compound in Table 4.1 shows that each conversion ($MCl_2 \rightarrow$ MClMe or MClMe $\rightarrow MMe_2$) is accompanied by a change in δ ($^{19}F_{para}$) of 1.0 to 1.2 ppm (upfield). From these data, we conclude that the ligand effects in the MX_2 moiety and the Cp substituent effects are independent.

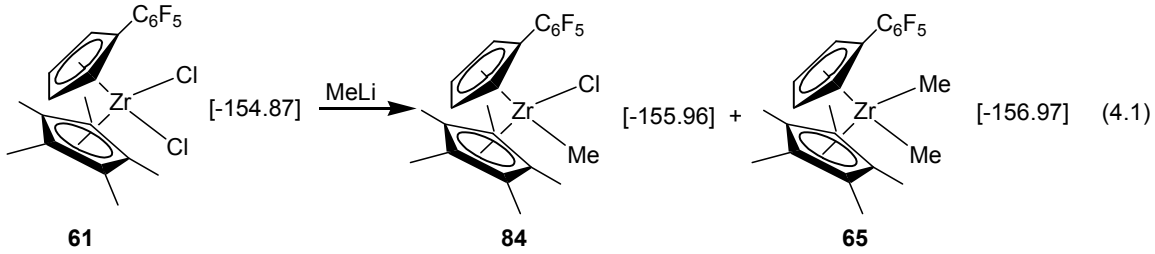

61 **84** **65**

Table 4.3. $\Delta\delta$ of $(C_6F_5Cp)Cp^*ZrRR'$

Metallocene	Ortho	Para	Meta
61 → 84	- 0.76	- 1.09	- 0.04
84 → 65	- 0.42	- 1.01	- 0.04

When **61** is combined with an excess of Me_3Al (eq 4.2), $\delta(^{19}F_{para})$ suggests formation of a $ZrCl\bullet\bullet\bullet AlMe_3$ or $ZrCl\bullet\bullet\bullet AlMe_2Cl$ interaction, analogous to those reported for titanocene dichloride.[64,65,81-83] Barron also characterized such an interaction crystallogaphically, $(\eta^5\text{-}C_5H_5)_2Zr(Cl)(\mu\text{-}Cl)Al(^tBu)_3$ from the reaction between Cp_2ZrCl_2 and $Al(^tBu)_3$.[51] ^1H NMR analysis showed a downfield shift of the complexed $Al(^tBu)_3$ (1.39 ppm) compared to the uncomplexed $Al(^tBu)_3$ (1.07 ppm). The $\delta(^{19}F_{para})$ of starting **61** is shifted downfield ($\Delta\delta$ = 0.41 ppm), while the product **84** exhibits a larger shift ($\Delta\delta$ = 0.44) possibly because the electron-releasing effect of the methyl ligand enhances the $ZrCl\bullet\bullet\bullet Al$ interaction. Normally one would not rely on such a small chemical shift difference except in situations like this where both species are present in the same mixture. Separate experiments demonstrated $\delta(^{19}F_{para})$ of **62** and **63** were unchanged ($\Delta\delta(^{19}F_{para}) < 0.02$) by added Me_3Al, ruling out a $ZrMe\bullet\bullet\bullet AlMe_3$ contact.

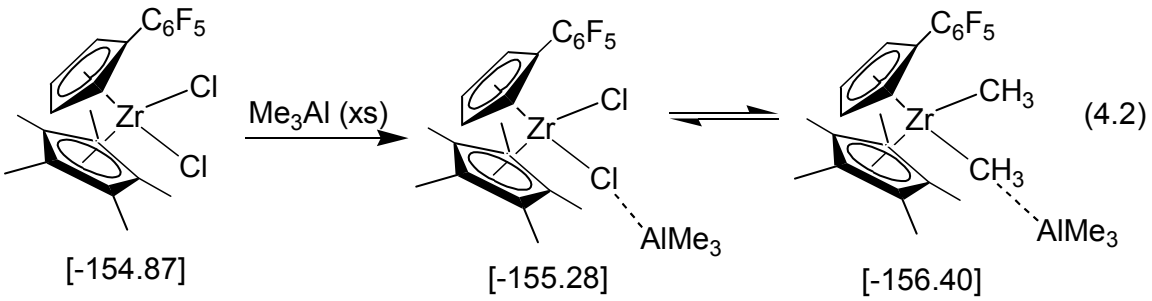

(4.2)

Alkylation Reactions with MAO

Kaminsky[4,16] originally proposed that MAO exchanges both chorine atoms from a dichloride producing a dimethylmetallocene before activation. This pathway has been generally accepted and even incorporated into the Cossee-Arlman mechanism for the

polymerization of ethylene.[57,58] However, there is still a question about the "true" pathway of activation. Deffieux followed the alkylation of *rac*-$[C_2H_4(Ind)_2]ZrCl_2$ using solution UV-Vis spectroscopy. His results (see details in chapter 1) suggested that only one chlorine atom was exchanged for a methyl while the second chlorine atom was abstracted, producing a cationic complex.[88,89,91] Cam[164] investigated the reaction of **31** with MAO using ^{1}H NMR, and found that only **32** was formed (eq 4.3). Cam proposed

$$\underset{\textbf{31}}{Cp_2ZrCl_2} + MAO \longrightarrow \underset{\textbf{32}}{Cp_2Zr(Me)Cl} + MAO \bullet Al(Me)_2Cl \qquad (4.3)$$

that Me_3Al was the methylating agent in this reaction. They also reported that the experimental data was insufficient to prove the formation of a cationic species. This is not surprising because in ^{1}H NMR, the chemical shift difference among the various Cp signals are so small that even a moderate rate of chemical exchage causes signals to coalesce.

Using our ^{19}F chemical shift database as a guide, we investigated reactions of Me_3Al and MAO with metallocene dichlorides. Metallocene **59** proved to be only sparingly soluble in C_6D_6 preventing a truly quantitative study. However, treatment with Me_3Al converted 86 % of the soluble material to **74** while the remaining 14 % was unreacted **59** (eq 4.4). No formation of **63** was evident. The concentration ratio was

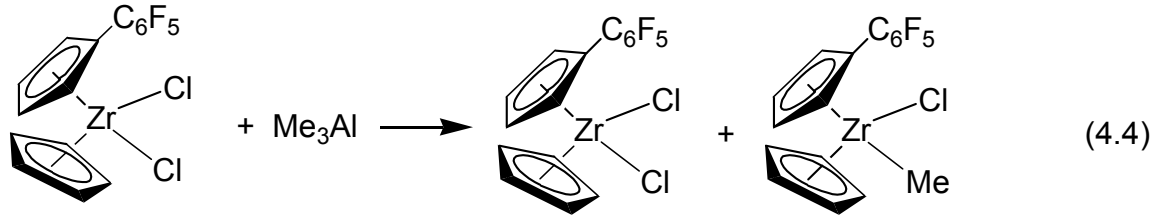

59 **59:** 14 % **74:** 86 % (4.4)

constant (within experimental error; **59**, 13 % and **74**, 87 %) over a 2.5 hour period so we concluded that the reaction had reached equilibrium. This route was briefly investigated as a possible route for the preparation of the chloromethylmetallocenes. However, the reaction of **59** with Me_3Al is also reversible. When a preparative scale reaction was performed and a vacuum applied to remove the solvent, the distribution of the isolated product proved to be dichloro- and chloromethylmetallocene in a 50/50 ratio. ^{19}F NMR analysis of a C_6D_6 solution of **61** (more soluble in C_6D_6) and Me_3Al (Al:Zr = 10) demonstrated the formation of **84** (55%) along with unreacted **61** (45%). Again, no formation of the corresponding dimethylmetallocene, **65** was evident.

To further confirm the limited methylating ability of Me_3Al, the reaction of a methyl-chloro derivative (**72**) with Me_3Al was performed on an NMR scale. ^1H and ^{19}F NMR analysis demonstrated that no ligand exchange reaction had occurred, however there was a downfield shift of the para signal (-154.62 to –154.40). We conclude that the residual Me_3Al in MAO is not the agent for the complete methylation of the dichlorometallocene in polymerization reactions. Our results indicate instead that if MAO exchanges both chloride ligands before the abstraction of a methyl group, then the aluminoxane component of the MAO mixture must be responsible for the second alkylation exchange step.

To verify the alkylating effect of the aluminoxane component of MAO, a C_6D_6 solution of **58** was combined with a benzene-d_6 solution of MAO (eq 4.5, Al:Zr = 20). ^{19}F NMR analysis demonstrated the formation of a “cation-like” complex along with **72**. No signals representative of **62** were evident. The cation-like complex was tentatively

assigned to **67** because the ^{19}F shifts were identical to those observed upon activation of **62**.

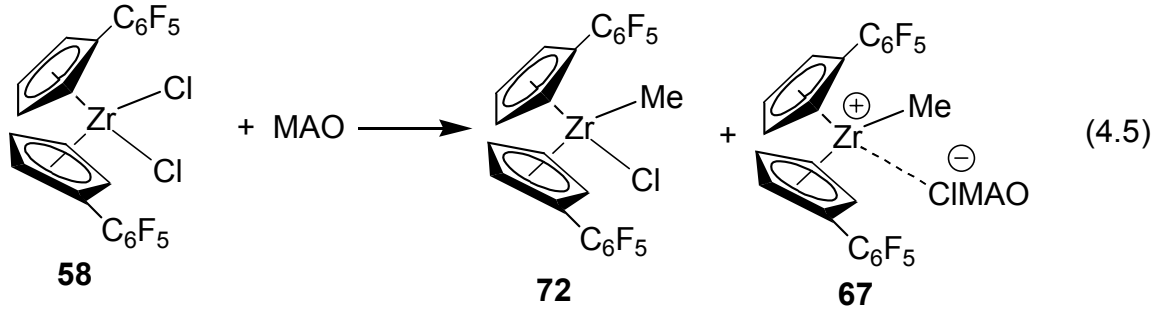

(4.5)

In contrast, when the intermediate **72** was treated with MAO (Al:Zr = 25) and analyzed by ^{19}F NMR, three compounds (unreacted **72** (63 %), dimethyl **62** (12 %) and cation **67** (25 %)) were evident in the spectrum. A second ^{19}F NMR spectrum obtained after 4 h indicated that the reaction had already reached equilibrium (**72** (65%), **62**, (11 %), and **67** (24%)). The formation of **62** within the reaction mixture was presumably due to the exchange of a methyl group between MAO and **67** (eq 4.6). This was an interesting result because the reaction of **58** with MAO (eq 4.5) produced no dimethylmetallocene even though we had previously shown (eq 2.5) that the metallocene dimethyl and the cation-like species should both be present at the concentrations of Al and Zr used.

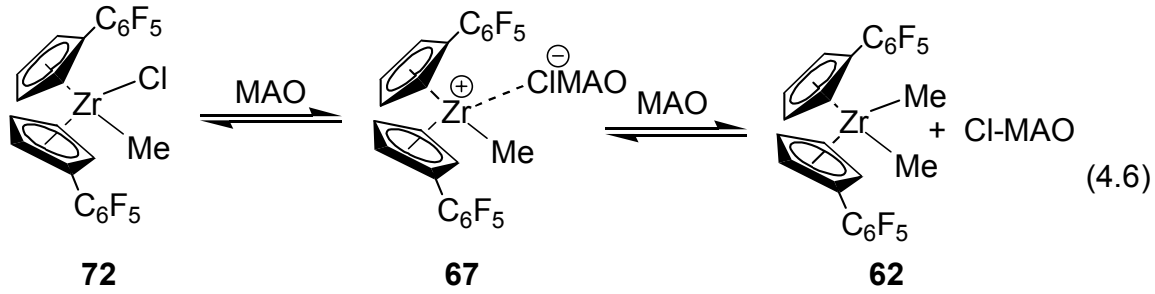

(4.6)

Upon the initial exchange of chlorine with a methyl, MAO becomes chlorinated (Cl-MAO). Our initial thought was that the chlorination effectively "poisoned" MAO.

Cl-MAO could no longer exchange a methyl for chlorine inhibiting the formation of the dimethylmetallocene. In other words, at Al : Zr, 20 : 1, all the exchangeable methyl groups of MAO had been consumed. However, when **58** was treated with twice as much MAO (Al:Zr = 50) the same results were observed. Given that no **58** remained when Al:Zr = 25, doubling the amount of MAO should have compensated for the "poisoning" effect and **62** should have been observed. An alternative explanation is that a "chloride-bridged" (MCH_3^+ $ClMAO^-$) ion pair is formed, which is much tighter than the corresponding methyl-bridged (MCH_3^+ $MeMAO^-$) species, preventing methyl transfer from MAO to give the dimethyl metallocene.

When **61** was treated with MAO (Al:Zr = 25) and analyzed by ^{19}F NMR, three compounds (monomethyl **84** (22.9 %), dimethyl **70** (14.1 %), and cation **65** (63.0 %) were observed (eq 4.7). The difference in reactivity between **58** and **61** with MAO can

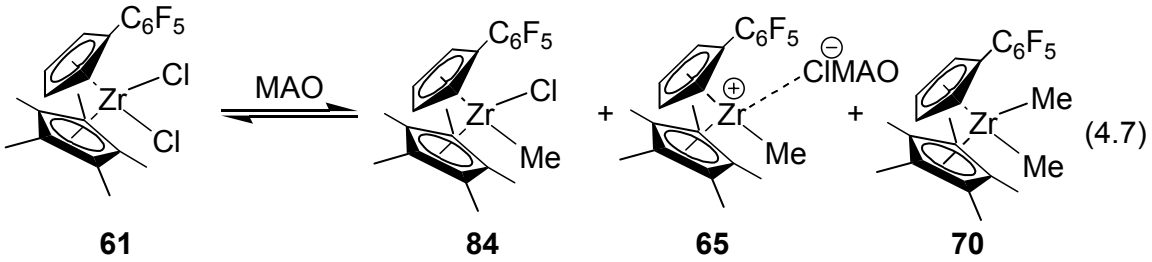

be attributed to both steric and electronic effects. **58** has a more electron-deficient, accessible metal center. Upon formation of the "cation-like" metallocene, the ion pair is tightly coordinated. In contrast, **61** contains the bulky electron-donating Cp* ligand. Upon formation of the "cation-like" metallocene, the ion pair is more easily separated, and transfer of CH_3 from MAO to form **65** can proceed. In future work, reactions with well-defined aluminoxanes (see below) could also provide evidence to clarify the difference in reactivity of MAO with our metallocenes, **58 – 65**, **72**, and **74**.

Me$_3$Al as a Cation Stabilizer

Bochmann[104] reported that the reaction of Cp'$_2$MMe$_2$ [M = Zr or Hf; Cp' = C_5H_5, $Me_2Si(Ind)_2$, $C_2H_4(Ind)_2$, or $Me_2C(Cp)(Flu)$], $[CPh_3]^+[B(C_6F_5)_4]^-$, and $AlMe_3$ afforded the heterodinuclear complexes $[Cp'_2M(\mu\text{-}Me)_2AlMe_2]^+$ (**89-93**, eq 4.8). Bochmann suggested that as MAO contains a significant amount of Me_3Al, and as Al:Zr ratios

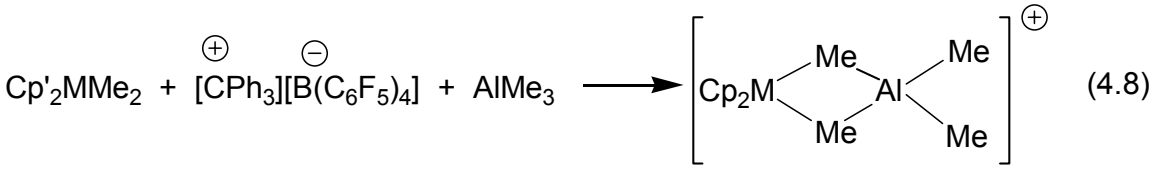

(4.8)

89: M = Zr; Cp' = C_5H_5
90: M = Hf, Cp' = C_5H_5
91: M = Zr, Cp' = $Me_2Si(Ind)_2$
92: M = Zr, Cp' = $C_2H_4(Ind)_2$
93: M = Hf, Cp' = $Me_2C(Cp)(Flu)$

in practical polymerization reactions usually range between 10^3 to 10^4, the cationic zirconium species formed could be **89** and not $[Cp_2ZrMe]^+$. Others found that catalysts formed with MAO as the cocatalyst are longer-lived than catalysts formed with organoborane activators. The $AlMe_3$ adducts were proposed as "stabilized" catalyst resting states.

When we treated our dimethylmetallocenes with MAO, we observed the formation of a monomeric cationic species (*vide supra*). Given the significant $\delta(^{19}F_{para})$ range (4 ppm) for the different ligand sets (Me_2, MeCl, and Cl_2), we proposed that we could distinguish between a monometallic and heterobimetallic cationic species with ^{19}F NMR. When a benzene-d_6 solution of **62** was treated with MAO (Al:Zr = 61) the formation of a cationic species (**67**) was confirmed by ^{19}F NMR spectroscopy. Upon the addition of one equivalent (based upon the metallocene) of Me_3Al, no change was

evident in the ^{19}F NMR spectrum. Even upon the addition of a large excess of Me_3Al there was no change in the ^{19}F NMR spectrum (eq 4.9). There are three potential

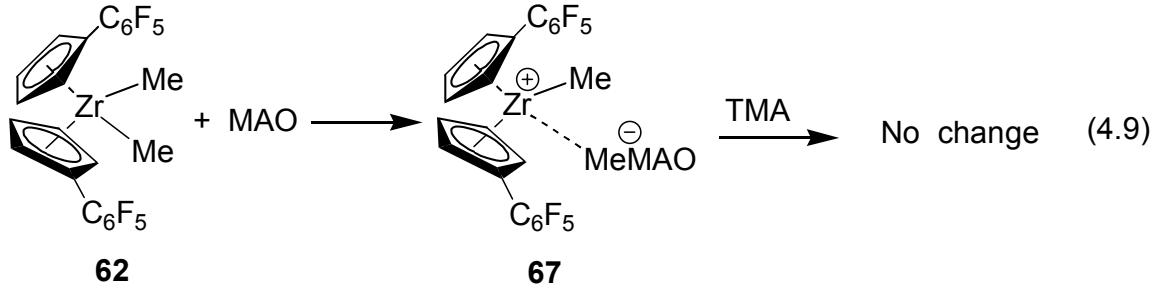

62 **67**

explanations for our findings. First, there are no Al-Zr interactions upon the addition of Me_3Al. In other words, our metallocenes simply do not form heterobimetallic Me_3Al adducts. Second, the fluorine substituents are too far removed from the Al-Zr interactions to observe a shift in the ^{19}F NMR spectrum. Third, if our sample of MAO contains residual Me_3Al,[165] then Me_3Al adducts could make up all of our activated species (**67**-**70**). Barron[166] reported that "depleted MAO" contained about 10 % Me_3Al. Because we already know that there is a smaller percentage of "competent" sites for the abstraction of a methyl group, there could be enough Me_3Al in "depleted MAO" to account for all of our activated species (**67**- **70**).

The formation of a heterodinuclear complex, of the general formula $Cp_2M(\mu\text{-}Me)_2AlMe_2^+$ may be dependent on the cocatalyst used in the formation of the "cation-like" metallocene. Bochmann used a triphenycarbenium borate salt to form the "cation-like" metallocene while we initially used MAO. Additional studies of the reactions of C_6F_5-substituted metallocenes with weakly coordinating anions such as $[B(C_6F_5)_4]^-$ and Me_3Al could provide a more definitive explanation for our results.

Reactions of $B(C_6F_5)_3$ with MAO

Some industrial reports (patents)[167,168] indicate the use of both $B(C_6F_5)_3$ (activator) and MAO or other alkylaluminums (scavenger) in catalytic systems. However, Park and Chen showed B/Al exchange with $B(C_6F_5)_3$ and Me_3Al. We thought we could investigate what happens when $B(C_6F_5)_3$ is added to MAO, and possibly learn a little more about the interaction between a metallocene and such a mixture.

Park[169] reported the reaction between $B(C_6F_5)_3$ and MAO at 65 °C for 12 h resulted in the exchange of C_6F_5 for methyl groups in MAO. Experimental evidence for these results were provide by broad peaks in the ^{19}F NMR (δ - 49.7, ortho; - 77.7, para; - 86.6, meta) and a sharp signal corresponding to BMe_3 in the ^{11}B NMR (δ 72.3). Klosin and Chen[170] reported the stepwise CH_3/C_6F_5 ligand exchange when $B(C_6F_5)_3$ was treated with an equimolar amount of Me_3Al producing $Al(C_6F_5)_3$, dimeric aluminum species $[Al(C_6F_5)_x(CH_3)_{3-x}]_2$ (x = 1-2), and borane species $B(C_6F_5)_x(CH_3)_{3-x}$ (x = 0-2) (eq 4.10).

$$B(C_6F_5)_3 + 1/2\ Me_6Al_2 \longrightarrow MeB(C_6F_5)_2 + 1/2\ (C_6F_5)_2Al_2Me_4$$
$$\rightleftharpoons \qquad (4.10)$$
$$Me_2B(C_6F_5) + 1/2\ (C_6F_5)_4Al_2Me_2$$
$$\rightleftharpoons$$
$$BMe_3 + Al(C_6F_5)_3$$

Initially a J-Young NMR tube was charged with $B(C_6F_5)_3$ and MAO (B : Al = 1). The solids were dissolved in C_6D_6 and a ^{19}F NMR spectrum was obtained at room temperature. Analysis of the spectrum demonstrated three signals corresponding to

$B(C_6F_5)_3$ along with three signals, shifted upfield representing the coordination of Lewis base present in MAO with $B(C_6F_5)_3$. We assign the new signals according to eq 4.11.

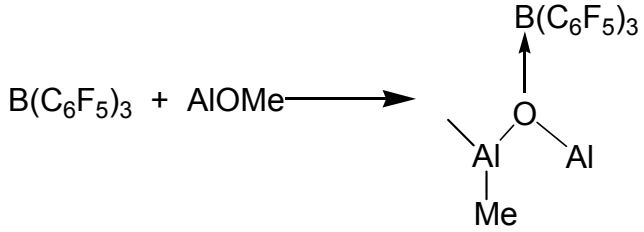

(4.11)

The NMR peaks for both complexes are presented in Table 4.4. A sample of $B(C_6F_5)_3$

Table 4.4. ^{19}F NMR Chemical Shifts of $B(C_6F_5)_3$/MAO Mixtures

Compound	Ortho-F	Para-F	Meta-F
$B(C_6F_5)_3$	- 129.20	- 142.09	- 160.43
$B(C_6F_5)_3$•MAO	- 130.40	- 147.43	- 161.78

and MAO in C_6D_6 was submitted for an EXSY experiment. No exchange between "free" and coordinated $B(C_6F_5)_3$ was observed, so evidently eq 4.11 is not reversible. Upon addition of **62**, there were several changes in the ^{19}F NMR spectrum. The first observation was that the signals corresponding to the free $B(C_6F_5)_3$ disappeared and the peaks corresponding to cationic **66** appeared. Importantly, after all the free $B(C_6F_5)_3$ was consumed, unreacted **62** is still present. While the free, uncoordinated borane activated the metallocene, the $B(C_6F_5)_3$•MAO complex does not react with **62**. After 24 h, another ^{19}F NMR was obtained. The spectrum had changed significantly, however at this time no compounds have been assigned to the new signals. After 24 h at ambient temperatures, the ^1H NMR spectrum demonstrated that a significant amount of BMe_3 (0.72 ppm)[169] had formed indicating that there was exchange between C_6F_5 and methyl groups.

In an attempt to better understand the result from the reaction between $B(C_6F_5)_3$, MAO and **58**, the reaction between $B(C_6F_5)_3$ with MAO was explored further. $B(C_6F_5)_3$ and MAO were reacted in a C_6D_6 solution at 65 °C for 1 h. ^1H NMR analysis

demonstrated three signals. The signal at 0.72 ppm corresponds to BMe_3 (0.73 ppm)[170] and the peak at 0.96 ppm could represent $Me_2B(C_6F_5)$ (1.00 ppm).[170] A broadened peak at -0.22 ppm remains unassigned. The ^{19}F NMR showed several peaks over the range -122 through -163 ppm. Three of these peaks could represent $Al(C_6F_5)_3$ based upon the work done by Park on the preparation of $Al(C_6F_5)_3$,[169] however no signals correspond to the proposed $Me_2B(C_6F_5)_3$.[170]

In a second experiment, the method used by Park was investigated. Two important differences need to be noted. Park and coworkers prepared their own MAO samples while our samples were donated by Albemarle. Also, different internal references were used in the NMR experiments. The mixture of $B(C_6F_5)$ and MAO was heated at 65 °C for 12 h and then analyzed by ^1H and ^{19}F NMR. The ^1H NMR spectrum demonstrated the same signals at 0.72 ppm (BMe_3) and the yet unidentified, broadened signal, centered around - 0.22 ppm. The ^{19}F NMR spectrum demonstrated what appears to be two compounds, in contrast to the complexity observed in the previous experiment. Two large sharp signals (-163.26 and -150.65 ppm) and three smaller signals (- 161.55, -152.5, and - 122.22 ppm) were observed. The three smaller signals may represent the C_6F_5 modified MAO reported by Park (different internal standards).[169] However, the two sharp signals remain unassigned. The observation of additional signals in our spectrum may be the result of the different MAO samples.

A time elapsed ^1H and ^{19}F NMR experiment was performed on a C_6D_6 solution of $B(C_6F_5)_3$ and MAO at 25 °C. The initial spectrum was collected immediately after the two components were combined. ^1H NMR analysis showed the same three peaks as above (-0.23, 0.72, and 0.96 ppm) along with two additional peaks at 1.33 and 2.10

ppm. The peak at 2.10 was assigned to toluene from the commercial MAO sample. Another spectrum was collected after 22 h. The broad peak centered around - 0.20 ppm was still evident along with the peak at 0.720 ppm. The other three peaks were diminished significantly. After ~ 72 h the same two peaks remained. The initial ^{19}F NMR spectrum was representative of $B(C_6F_5)_3$ along with some additional small unassigned signals. After ~ 22 h, the signals for $B(C_6F_5)_3$ were no longer present and three new peaks had emerged. The new peaks (-122.40, 152.20, and –161.33 ppm) were coincidental with the peaks from the earlier experiments that have been tentatively assigned to the C_6F_5-modified MAO. After ~ 72 h the "C_6F_5-modified MAO" signals were still present along with a few additional peaks.

At this time, based on these results in conjunction with those reported by Park and Chen, it can be concluded that $B(C_6F_5)_3$ will exchange C_6F_5 groups for methyl groups with MAO producing a C_6F_5-modified MAO. We now propose that $B(C_6F_5)_3$ coordinates to a specific Lewis-basic site on MAO based on the observation of a single "adduct." The use of well-characterized aluminoxane analogues such as those described by Barron may help us elucidate the structure of that adduct and to identify the Lewis-basic reactive site of MAO. Presumably the same Lewis-basic site is the one involved in contact ion pairing with metallocenes.

Reactions with Additional Alkylaluminum Compounds

We extended our exploratory reactivity studies to alkylaluminum compounds of the general type R_xAlCl_{3-x} (R = Me or Et; X = 1, 2, or 3). These reaction were performed in order to help us determine if ^{19}F NMR is sensitive enough to discriminate among various zirconocene-aluminum interactions, and to understand the reactions of

metallocenes with well-defined alkylaluminum compounds better. Since **58** was only sparingly soluble in C_6D_6, **61** was employed in the reactions with alkylaluminum compounds, Me_xAlCl_{3-x} (X = 1, 2, or 3).

We tried mixing the compounds with Et-Al compounds and Cl-Al-CH_3 compounds because our hope was that we would have relatively clean conversions requiring large excesses of the aluminum reagents to reach equilibrium conditions (MAO as precedent), so our ^{19}F NMR technique seemed like a promising method. Thus we purchased the reagents in hydrocarbon solution because we were not concerned at all about interference in proton NMR. However we found instead that: (1) reactions required only 1 equiv of Al (2) shifts in ^{19}F are not sensitive enough and (3) the whole system is probably better examined by ^{1}H NMR after all. In addition, complications due to the apparent β-H elimination and C-F activation make our system more difficult to understand. However, we made some interesting observations that are worth reporting here, and the remainder of this chapter describes these observations briefly.

Reactions with Methylaluminum Halides

The reaction of **61** with Me_3Al was discussed previously, demonstrating the formation of **84** and the coordination of **61** to the aluminum center. When **61** was treated with Me_2AlCl (Al:Zr = 10) and analyzed by ^{19}F NMR, coordination between the zirconium and aluminum centers was evident. However, there was no chlorine/methyl exchange. ^{19}F NMR analysis of a C_6D_6 solution of **61** with $MeAlCl_2$ (Al:Zr = 10) also demonstrated no chlorine/methyl exchange, but there was coordination of the zirconium center to aluminum (Table 4.5). This demonstrates that even with alkyl aluminum halide

compounds of different Lewis acidities, ^{19}F NMR can detect the effects on $\delta(^{19}F_{para})$ upon coordination.

Table 4.5. $\Delta\delta$ with Alkylaluminum Halides

Metallocene	Alkylaluminum Halide	$\Delta\ \delta(^{19}F_{para})$
$[(C_6F_5)Cp][C_5Me_5]ZrCl_2$ (**61**)	Me_3Al	1.9
$[(C_6F_5)Cp][C_5Me_5]ZrCl_2$ (**61**)	Me_2AlCl	2.2
$[(C_6F_5)Cp][C_5Me_5]ZrCl_2$ (**61**)	$MeAlCl_2$	-0.5

The reaction of **72** with Me_2AlCl (Al:Zr = 1) in C_6D_6 was analyzed by ^{19}F NMR and demonstrated the formation of **58** (62%) as well as unreacted **72** (38%) (eq 4.12). The limited solubility of **58** in C_6D_6 resulted in its precipitation. Thus percentages are based only on soluble material, and a true quantitative analysis of the compound ratio was not possible. Treatment of **72** with $MeAlCl_2$ (Al:Zr = 1) in C_6D_6 resulted in the complete conversion into **58** (eq. 4.13). These results indicate that the exchange of a chlorine atom

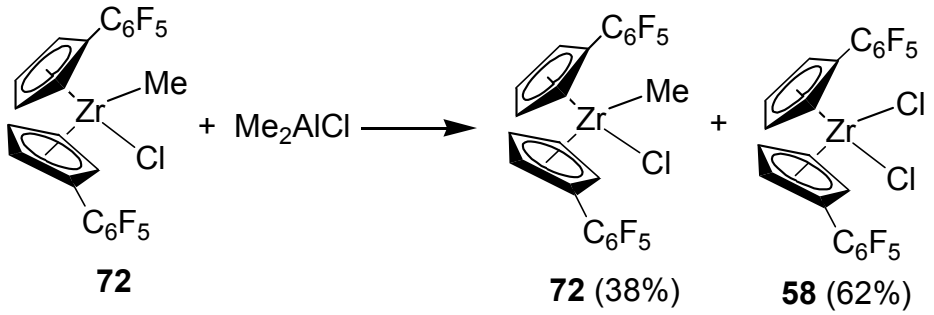

72 **72** (38%) **58** (62%) (4.12)

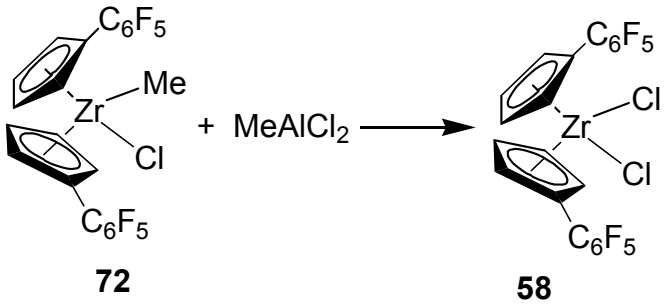

72 **58** (4.13)

from the aluminum center, formation of **58** is favored over the exchange of a methyl and the formation of **62**.

Reactions with Ethylaluminum Halides

In the earliest examples of soluble zirconocene complexes as olefin polymerization catalysts, zirconocene dichloride (**30**) was treated with Et_3Al. Kaminsky[171] investigated the reaction between **30** and Et_3Al to determine the intermediates produced via side reactions. Could these intermediates be observed using ^{19}F NMR?

When a C_6D_6 solution of **58** was treated with Et_3Al (Al:Zr = 1), ^{19}F NMR analysis of the soluble material indicated two compounds were present; unreacted **58** (~ 50%, -155.97 ppm) along with a new compound tentatively assigned as $[(C_6F_5)Cp]_2Zr(Et)Cl$ (**94** (~50 %, -156.49 ppm; eq 4.14). The upfield shift of compound **94** is similar to the shift seen for the formation of **72** from **58** ($\Delta\ \delta(^{19}F_{para})$ = 1.9 for **58** $\rightarrow$ **94** vs $\Delta\ \delta(^{19}F_{para})$ = 1.2 for **58** $\rightarrow$ **72**), indicating an increase in electron density on the metal center as one chlorine atom was exchanged with an ethyl group. In addition to the signals assigned to

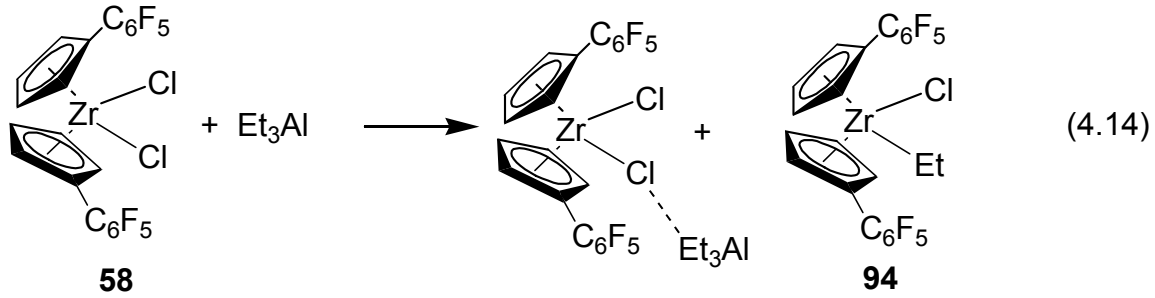

58 **94** (4.14)

58 and **94** there are several small signals in the ^{19}F NMR spectrum. These small signals could represent some of the intermediates assigned by Kaminsky, but definitive assignments could not be made at this time. A second ^{19}F NMR spectrum was obtained

after 3 h. Both the signals for **58** and **94** were still present in the spectrum, however **94** was now the dominant product (~ 85 %).

When **62** was treated with Et_3Al (Al:Zr = 1), analysis by ^{19}F NMR indicated three compounds were present. One set of signals corresponded to **62** (-156.29 ppm), a second set could represent $[(C_6F_5)Cp]_2Zr(Et)Me$ (**95**, -156.69 ppm), and the third set could represent $[(C_6F_5)Cp]_2ZrEt_2$ (**96**, -157.04 ppm). The aromatic region of the ^1H NMR spectrum confirmed that **62** was present and that there were additional compounds present. The ^1H NMR was not useful in attempts to find the ethyl groups of **95** and **96** because the signals for the Et_3Al in hexane occlude them. Attempts to synthesize **96** for independent analysis were unsuccessful. A second ^{19}F NMR spectrum was obtained after 20 h. The original three peaks were replaced by a complex spectrum. The complex nature of the spectrum may be the result of C-F activation. Jones[172,173] has demonstrated that $[Cp_2ZrH_2]_2$ and $Cp^*_2ZrH_2$ can activate the C-F bond of C_6F_6 and aliphatic fluorocarbons, respectively (eq 4.15 and 4.16). If we are actually preparing **95** or **96** then there is the possibility of beta-hydride elimination producing $[(C_6F_5)C_5H_4]_2ZrMeH$ and $H_2C{=}CH_2$. The newly formed Zr-H could potentially activate a C-F bond on the

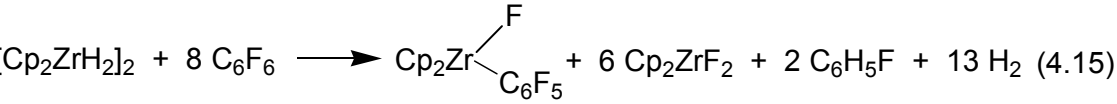

(4.15)

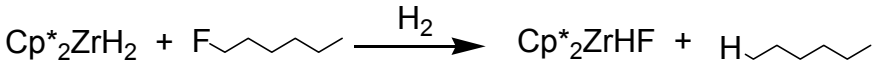

(4.16)

pentafluorophenyl substituted cyclopentadienyl ligand which would result in $[(C_6F_4H)C_5H_4][(C_6F_5)C_5H_4]Zr(F)Me$. This mixture of products would make the ^{19}F NMR very complex (eq 4.17). Interestingly, a singlet is observed in the ^1H NMR at δ 5.28 that may represent $CH_2{=}CH_2$.

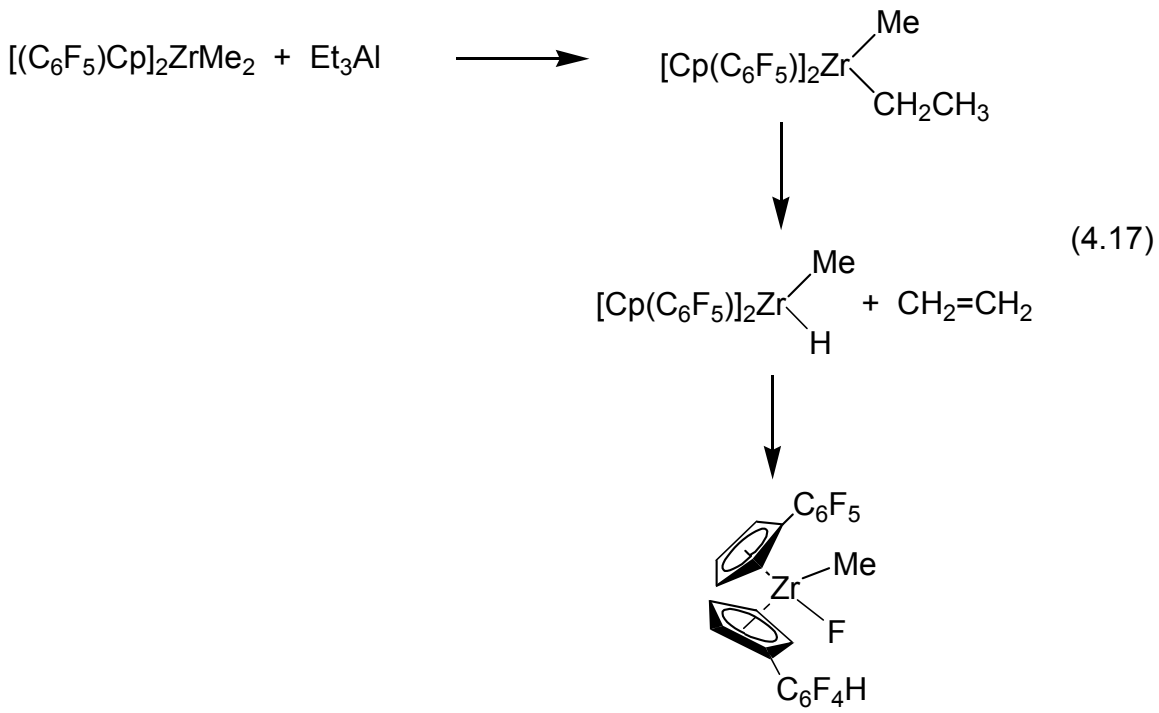

(4.17)

In a separate experiment, we attempted to synthesize $[(C_6F_5)Cp]_2ZrH_2$ (**97**) via the reaction of **62** and H_2. ^{19}F analysis of the reaction mixture demonstrated a very complex spectrum. Two very important signals in the ^{19}F spectrum were δ 68.44 and δ 66.41, which we assign to Zr-F bonds. This course of experimentation was eventually abandoned due to the instability of the Zr-H bond in the C_6F_5 –substituted metallocene system. However, upon comparing the ^{19}F spectra of **62** with H_2 and **62** with Et_3Al, we noted that the two spectra were similar.

^{19}F NMR analysis of a C_6D_6 solution of **62** with Et_2AlCl demonstrated three sets of signals. One small set of signals corresponds to **62**, the dominate set of signals correspond to **72**, and the other small set of signals may be **96**. The combination of **62** with $EtAlCl_2$ results in coordination of aluminum but no exchange of ethyl or chloro groups. Reactions between **72** with Et_2AlCl and $EtAlCl_2$ both produced **59** as a result of a methyl/chlorine exchange. No further reactivity was observed.

Future Work

The NMR analysis with ^{19}F NMR is best suited to reactions that are hard to study with ^{1}H NMR – such as cases where there needs to be a large excess of some reagent (e.g. olefin monomer) is needed. More interesting, are the changes in reactivity that the C_6F_5 groups induce. (1) C_6F_5 groups enhance metal-centered electrophilicity. Can we make a metallocene that is so electrophilic that it doesn't react with MAO or $B(C_6F_5)_3$? (2) It would be interesting to explore the C-F activation which might be intramolecular. (3) C_6F_5 groups should facilitate Zr^{IV} to Zr^{II} reduction. It would be interesting to try some reductive elimination chemistry with our compounds. The photosensitivity of our metallocene dimethyls compared to the unsubstituted parent compoun suggests that possibility

^{19}F NMR has allowed us to observe "cation-like" metallocene species (**67** – **70**) in solution. Previously in our research group, Thornberry[174] demonstrated that **67** was active toward the polymerization of α-olefins. While Gassman[78] (XPS) and Marks[79] (CPMAS ^{13}C NMR) have observed Cp_2Zr-polymeryl ion pairs, the only direct observation in solution has been reported by Tritto[105] (^{13}C NMR). ^{19}F NMR allows us the unique opportunity of identifying intermediates in the polymerization of α-olefins in solution. An initial experiment was conducted between **67** and cyclohexene. ^{19}F NMR analysis of a C_6D_6 solution of 58 with MAO (Al:Zr = 60) indicated the formation of **67**. Upon the addition of cyclohexene, no insertion or coordination of the cyclohexene was evident in the ^{19}F NMR spectrum. Insertion of 1-hexene was observed, but the olefin adduct was not.

A further, ambitious experiment that could be investigated in our lab is a ^{19}F NOESY spectrum of contact-ion-paired species derived from $B(C_6F_5)_3$ or $[Ph_3C^+][B(C_6F_5)_4^-]$. As an example, in **66**, through-space distances between the cation and anion could be estimated, giving a *solution structure* that could be compared with crystallographic data. If successful, we will have an additional method to characterize ion-pairing as a function of catalyst and cocatalyst structure, solvent, and concentration -- all directly in solution.

Conclusions

The utility of ^{19}F NMR as a tool for the identification of C_6F_5-substituted metallocenes within mixtures was shown by establishing a $\delta(^{19}F_{para})$ scale. In the activation of dichlorometallocenes with MAO, the electronic environment of the ligand effects the degree of ion-pair separation and the formation of dimethylmetallocenes. More electron-withdrawing ligands account for a tighter ion pair and the lack of dimethylmetallocene formation. Reactions of $B(C_6F_5)_3$ and MAO resulted in the coordination of $B(C_6F_5)_3$ to Lewis basic sites within the MAO mixture forming ill-defined adducts. Further reaction with C_6F_5-substituted metallocenes did not provide the desired insight into the adduct structure. Reactions of both methyl- and ethylaluminum halides showed that the aluminum center will not exchange a methyl group with the zirconium center of either a dichloro- or methylchlorometallocene. However, they will exchange a chlorine for the methyl of the methylchlorometallocene producing the dichlorometallocene. Reactions of ethylaluminium halides with C_6F_5-substituted

metallocenes resulted in β-hydride elimination and C-F bond activation, making the system extremely difficult to understand.

Experimental Section

General Considerations. All manipulations were carried out using standard nitrogen-atmosphere techniques. Et_3Al, Et_2AlCl, $EtAlCl_2$, Me_3Al, Me_2AlCl, $MeAlCl_2$ were purchased from Aldrich as 2.0 M solutions in toluene (ethyl compounds) and 1.0 M solutions in hexane (methyl compounds). MAO was received from Albemarle as a 10% toluene solution, filtered, and dried under high vacuum (3×10^{-5} torr) for 15 h to remove "free" trimethylaluminum. The same sample of MAO was used for all the experiments described here. $B(C_6F_5)_3$ was obtained as a gift from Albemarle, sublimed (120 °C, 5×10^{-6} torr), recrystallized from hexanes, and found to be 99+% pure according to ^{19}F NMR spectroscopy. NMR spectra were recorded on a Varian U-400 instrument at 22 °C. ^{19}F NMR spectra are referenced to external C_6F_6 in $CDCl_3$ at -163.0 ppm.

NMR Tube Reaction of 59 with Me_3Al. A J-Young NMR tube was charged with $[(C_6F_5)C_5H_4]C_5H_5ZrCl_2$ (10.0 mg, 2.2×10^{-2} mmol), 5 drops of Me_3Al (2.0 M in toluene) and C_6D_6 (1.0 mL). ^1H and ^{19}F NMR analysis indicated a mixture of $[(C_6F_5)C_5H_4]C_5H_5ZrCl_2$ (~ 14 %) and $[(C_6F_5)C_5H_4]C_5H_5Zr(Me)Cl$ (~ 86%).

Preparative Scale Reaction of 59 with Me_3Al. A swivel-frit reaction apparatus, was charged with a mixture of $[(C_6F_5)C_5H_4]C_5H_5ZrCl_2$ (350 mg, 7.64×10^{-1} mmol), Me_3Al (220 mg, 3.0 mmol, 1.5 mL, 2.0 M in Toluene) and toluene (15 mL). The mixture was stirred at ambient temperature for 3 h. The solvent was removed *in vacuo*, residue washed with hexane and the product was collected on a frit. ^1H and ^{19}F NMR analysis

indicated a mixture of $[(C_6F_5)C_5H_4]C_5H_5ZrCl_2$ (50 %) and $[(C_6F_5)C_5H_4]C_5H_5Zr(Me)Cl$ (50 %).

NMR Tube Reaction of 61 with Me_3Al. A J-Young NMR tube was charged with $[C_5Me_5][(C_6F_5)C_5H_4]ZrCl_2$ (15.0 mg, 2.8 x 10^{-2} mmol), Me_3Al (22 mg, 2.8 x 10^{-1} mmol, 710 μL, 0.4 M in C_6D_6) and C_6D_6 (1 mL).

NMR Tube Reaction of 72 with Me_3Al. A J-Young NMR tube was charged with $[(C_6F_5)C_5H_4]_2Zr(Me)Cl$ (22.5 mg, 3.7 x 10^{-1} mmol), Me_3Al (26.0 mg, 3.7 x 10^{-1} mmol, 860 μL, 0.04 M in C_6D_6). ^1H and ^{19}F NMR analysis indicated coordination, but no reaction.

NMR Tube Reaction of 58 with MAO. A J-Young NMR tube was charged with $[C_6F_5)C_5H_4]_2ZrCl_2$ (14 mg, 2.3 x 10^{-2} mmol), MAO (26 mg, 4.5 x 10^{-1} mmol) and C_6D_6 (1 mL). The solution became yellow upon mixing. ^{19}F NMR analysis indicated the formation of $[(C_6F_5C_5H_4)_2ZrMe]^+[MeMAO]^-$ and $[(C_6F_5)C_5H_4]_2Zr(Me)Cl$.

NMR Tube Reaction of 72 with MAO. A J-Young NMR tube was charged with $[(C_6F_5)C_5H_4]_2Zr(Me)Cl$ (12.2 mg, 2.0 x 10^{-2} mmol), MAO (30 mg, 5.1 x 10^{-1} mmol) and C_6D_6 (1.5 mL). The solution became yellow upon mixing. ^{19}F NMR analysis indicated the formation of $[(C_6F_5)C_5H_4]_2Zr(Me)Cl$ (63 %) $[(C_6F_5)C_5H_4]_2ZrMe]^+[MeMAO]^-$ (25 %), and $[(C_6F_5)C_5H_4]_2ZrMe_2$ (12 %). A second ^{19}F spectrum was obtained after 4 h demonstrating $[(C_6F_5)C_5H_4]C_5H_4Zr(Me)Cl$ (65%), $[(C_6F_5)C_5H_4]C_5H_4ZrMe]^+[MeMAO]^-$ (24 %), and $[(C_6F_5)C_5H_4]C_5H_4ZrMe_2$ (11 %).

NMR Tube Reaction of 61 with MAO. A J-Young NMR tube was charged with $[(C_6F_5)C_5H_4][C_5Me_5]ZrCl_2$ (12.0 mg, 2.3 x 10^{-2} mmol), MAO (26 mg, 4.5 x 10^{-1} mmol) and C_6D_6 (1.5 mL). The solution became yellow upon mixing. ^{19}F NMR analysis

indicated the formation of $[(C_6F_5)C_5H_4][C_5Me_5]Zr(Me)Cl$ (22.9 %) $[(C_6F_5)C_5H_4][C_5Me_5]ZrMe]^+[MeMAO]^-$ (14.1 %), and $[(C_6F_5)C_5H_4][C_5Me_5]ZrMe_2$ (63.0 %).

NMR Tube Reaction of 62 with MAO and Me_3Al. A J-Young NMR tube was charged with $[(C_6F_5)C_5H_4]_2ZrMe_2$ (13.2 mg, 2.3 x 10^{-2} mmol), MAO (8.0 mg, 1.38 mmol) and C_6D_6 (1 mL). The solution became yellow upon mixing. ^1H and ^{19}F NMR analysis indicated formation of the "cation-like" metallocene **67**. The J-Young NMR tube was then charged with Me_3Al (340 μL, 0.067 M solution in C_6D_6). ^1H and ^{19}F NMR analysis indicated no change in the "cation-like" spectrum.

NMR Tube Reaction of 62 with $B(_6F_5)_3$ and Me_3Al. A J-Young NMR tube was charged with $[(C_6F_5)C_5H_4]_2ZrMe_2$ (15.9 mg, 2.7 x 10^{-2} mmol), $B(C_6F_5)_3$ (15.3 mg, 3.0 x 10^{-2} mmol) and C_6D_6 (1 mL). The solution became yellow upon addition. ^1H and ^{19}F NMR analysis indicated formation of the "cation-like" metallocene **66**. The J-Young NMR tube was then charged with Me_3Al (400 μL, 0.067 M solution in C_6D_6). ^1H and ^{19}F NMR analysis indicated several new peaks that were not assigned.

NMR Tube Reaction of $B(C_6F_5)_3$, MAO, and 62. A screw-capped vial was charged with $B(C_6F_5)_3$ (120 mg, 0.234 mmol), MAO (13.6 mg, 0.234 mmol) and enough C_6D_6 to dissolve the solids. ~ 1.0 mL of this solution was transferred to a J-Young NMR tube and a ^{19}F NMR spectrum was obtained. Data for $B(C_6F_5)_3$: ^{19}F NMR (C_6D_6) δ - 129.20 (m, 6 F), - 142.09 (m, 3 F), -160.43 (m, 6 F). Data for $B(C_6F_5)_3$•MAO: ^{19}F NMR (C_6D_6) δ - 130.40 (m, 6 F), - 147.43 (m, 3 F), -161.78 (m, 6 F). $[(C_6F_5)C_5H_4]_2ZrMe_2$ (25.8 mg, 4.4 x 10^{-2} mmol) was added to the J-Young NMR tube. Data for $(C_6F_5C_5H_4)_2ZrMe^+$ $MeB(C_6F_5)_3^-$: ^{19}F NMR (C_6D_6) δ -134.54 (m, 6 F), -140.54 (m, 4 F), -151.54 (m, 2 F), -

158.61 (m, 3 F), -160.53 (m, 4 F), -164.32 (m, 6 F). ^{19}F NMR analysis after 24 h indicated a significant change in the spectrum. The signals corresponding to $(C_6F_5C_5H_4)_2ZrMe^+$ $MeB(C_6F_5)_3^-$ disappeared and several new unassigned signals were evident.

NMR Tube Reaction of $B(C_6F_5)_3$ with MAO. (A) A screw-capped vial was charged with $B(C_6F_5)_3$ (17.9 mg, 3.5 x 10^{-2} mmol), MAO (11.1 mg, 1.9 x 10^{-1} mmol) and C_6D_6 (2.0 mL). ~ 1.0 mL of this solution was transferred into a J-Young NMR tube and the tube heated to 65 °C for 1 h. ^{1}H and ^{19}F NMR spectra were obtained. ^{1}H NMR (C_6D_6) δ 0.95 ($Me_2B(C_6F_5)_3$, 0.72 (BMe_3) and an unassigned broad peak (-0.22). The ^{19}F NMR showed several peaks over the range -122 through -163 ppm. Three of these peaks could represent $Al(C_6F_5)_3$ based upon the work done by Park on the preparation of $Al(C_6F_5)_3$,[169] however no signals correspond to the proposed $Me_2B(C_6F_5)_3$.[170]

(B) A J-Young NMR tube was charged with $B(C_6F_5)_3$ (9.0 mg, 1.8 x 10^{-2} mmol), MAO (10 mg, 1.7 x 10^{-1} mmol) and C_6D_6 (1 mL). The mixture was heated at 65 °C for 12 h. ^{1}H and ^{19}F spectra were obtained. ^{1}H NMR spectrum showed a singal at 0.72 ppm (BMe_3) and the unassigned –0.22 ppm signal. The ^{19}F NMR spectrum two possible compounds. Two sharp unassigned peaks (-163.26 and –150.65 ppm) and three signals (-161.55, -152.5, -122.2 ppm) tentatively assigned to C_6F_5-modified MAO.

(C) A J-Young NMR tube was charged with $B(C_6F_5)_3$ (38.0 mg, 7.6 x 10^{-2} mmol), MAO (10 mg, 1.7 x 10^{-1} mmol) and C_6D_6 (1 mL). ^{19}F EXSY spectrum was obtained and no exchange was observed.

(D) A J-Young NMR tube was charged with $B(C_6F_5)_3$ (21 mg, 4.0 x 10^{-2} mmol), MAO (10 mg, 1.7 x 10^{-1} mmol) and C_6D_6 (1 mL). ^{1} H and ^{19}F NMR spectra were collected < 5

min, 22 h and 72 h. The NMR spectra initially looked like the spectrum from experiment (a) and progressed to become similar to the spectrum from experiment (b).

NMR Tube Reaction of 61 with Me_2AlCl. A J-Young NMR tube was charged with $[(C_6F_5)C_5H_4][C_5Me_5]ZrCl_2$ (11.1 mg, 2.1 x 10^{-2} mmol) and Me_2AlCl (19.0 mg, 2.1 10^{-1} mmol, 1.0 mL, 0.2 M in C_6D_6). ^{19}F NMR (C_6D_6) δ -138.98 (m, 4 F); -155.89 (m, 2 F); -163.35 (m, 4 F).

NMR Tube Reaction of 61 with $MeAlCl_2$. A J-Young NMR tube was charged with $[(C_6F_5)C_5H_4][C_5Me_5]ZrCl_2$ (13.2 mg, 2.5 x 10^{-2} mmol) and Me_2AlCl (28.0 mg, 2.5 10^{-1} mmol, 1.5 mL, 0.16 M in C_6D_6). ^{19}F NMR (C_6D_6) δ -138.80 (m, 4 F); -153.31 (m, 2 F); -162.07 (m, 4 F).

NMR Tube Reaction of 58 with Et_3Al. A J-Young NMR tube was charged with $[(C_6F_5)C_5H_4]_2ZrCl_2$ (10.0 mg, 1.6 x 10^{-2} mmol) and Et_3Al (1.8 mg, 1.6 x 10^{-2} mmol, 800 μL, 0.02 M in C_6D_6). Data for $[(C_6F_5)C_5H_4]_2ZrCl_2$: ^{19}F NMR (C_6D_6) δ -140.16 (m, 4 F); -155.97 (t, ^3J = 21 Hz, 2 F); -162.78 (m, 4 F). Data for $[(C_6F_5)C_5H_4]_2Zr(Et)Cl$: ^{19}F NMR (C_6D_6) δ - 140.56 (m, 4 F); -156.494 (t, ^3J = 21 Hz, 2 F); -163.11 (m, 4 F).

NMR Tube Reaction of 62 with Et_3Al. A J-Young NMR tube was charged with $[(C_6F_5)C_5H_4]_2ZrMe_2$ (11.4 mg, 2.0 x 10^{-2} mmol) and Et_3Al (2.2 mg, 2.0 x 10^{-2} mmol, 980 μL, 0.02 M in C_6D_6).

NMR Tube Reaction of 62 with Et_2AlCl. A J-Young NMR tube was charged with $[(C_6F_5)C_5H_4]_2ZrCl_2$ (13.6 mg, 2.3 x 10^{-2} mmol) and Et_2AlCl (2.8 mg, 2.3 x 10^{-2} mmol, 935 μL, 0.025 M in C_6D_6).

NMR Tube Reaction of 62 with $EtAlCl_2$. A J-Young NMR tube was charged with $[(C_6F_5)C_5H_4]_2ZrCl_2$ (10.0 mg, 1.7 x 10^{-2} mmol) and $EtAlCl_2$ (2.2 mg, 1.7 x 10^{-2} mmol, 855 μL, 0.02 M in C_6D_6).

NMR Tube Reaction of 72 with Et_2AlCl. A J-Young NMR tube was charged with $[(C_6F_5)C_5H_4]_2Zr(Me)Cl$ (13.6 mg, 2.3 x 10^{-2} mmol) and Et_3Al (2.7 mg, 2.3 x 10^{-2} mmol, 1.1 mL, 0.02 M in C_6D_6).

Chapter Five: Coordination Chemistry of C_6F_5-Substituted Chromocenes

Introduction

Several groups have investigated the reactivity of coordinatively unsaturated group 6 metallocenes.[175-178] While both molybdocene, $(C_5H_5)_2Mo$ and tungstocene, $(C_5H_5)_2W$ undergo several basic addition and insertion reactions, chromocene, $(C_5H_5)_2Cr$ (**97**) appears to be less reactive. This trend is not especially surprising because within a triad, the heavier metals tend to favor higher oxidation states. Brintzinger demonstrated a reversible coordination of, CO with **97** producing $(C_5H_5)_2Cr(CO)$ (**98**, eq 5.1) through the

$$\underset{\mathbf{97}}{(C_5H_5)_2Cr\ (sol)} + CO(g) \rightleftharpoons \underset{\mathbf{98}}{(C_5H_5)_2Cr(CO)\ (sol)} \qquad (5.1)$$

disappearance and reappearance of **97's** characteristic absorption at 454 nm.[179] At room temperature and P(CO) < 1 atm the formation of **98** is not complete. A variable temperature study provided equilibrium constants for CO binding (Table 5.1).

Table 5.1. Equilibrium Constants for the Coordination of CO to Cp_2Cr[179]

T, °K	$P(CO)_{eq}$, Torr	K (atm^{-1})
280	9.4	41.7
295	47.0	6.53
297	53.0	5.81
303	80.0	3.10
308	118.9	1.61

Given the paramagnetic nature of **97** no ^1H NMR spectrum was obtained. However, ^1H NMR analysis of **98** demonstrated one sharp signal at 6.06 ppm consistent with chemical shifts of comparable diamagnetic Cp complexes. In the IR spectrum, a strong, sharp carbonyl absorption was observed at 1900 cm^{-1}. Other than CO, no other molecules have been successfully coordinated to **97**.

In contrast, when ring-bridged ligands were combined with $CrCl_2$ and either CO or ^{t}BuNC, ansa-chromocene complexes were produced (eq 5.2).[180] Theoretical

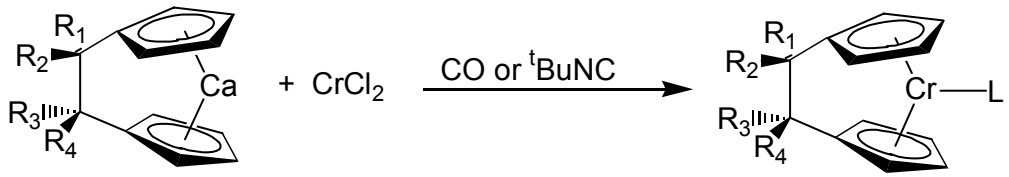

(5.2)

$R_{1\text{-}4}$ = Me, H, or $(MeO)_2C_6H_3$

studies[179,181,182] suggest that the difference in stability of **98** compared to the ansa-chromocene complexes is based upon the spin state of the molecule. The parallel ring geometry of **97** results in a stable triplet state. When CO is coordinated to **97** then the rings are "bent back" resulting in d-electron repulsion associated with the multiplicity change. When the rings are initially "pulled back" by the bridging group, then the chromocene complex cannot relax to the stable triplet state and the coordination of CO becomes more favorable, perhaps even necessary for formation of the ansa-chromocene complex.

In this chapter, pentafluorophenyl-substituted chromocenes were synthesized and their coordination with CO and other compounds isoelectronic to CO were investigated. Compared to chromocene, C_6F_5-substituted chromocenes contain less electron-rich metal centers. When CO is used as the coordinating ligand, we would not expect a large difference in the extent of conversion because CO is a weak σ-donor and an excellent π-acceptor. With **97**, the sigma bond may be weak but the complex is stabilized through back-bonding. The electron-deficient C_6F_5-substituted chromocene compounds could enhance the σ-donation, but lacks the electron density to effectively back-bond. However, when cyanide is used as the coordinating ligand, complex formation should be favored for the C_6F_5-substituted chromocenes. Compared to CO, cyanide is a better σ-donor and weaker π-acceptor. While **97** does not coordinate cyanide compounds, C_6F_5-

substituted chromocenes should stabilize the 18 e^- diamagnetic chromocene compounds. The pentafluorophenyl groups again conveniently allows the use of ^{19}F NMR to examine the coordination reactions quantitatively in solution.

Results and Discussion

Substituted-Chromocene Synthesis

$[(C_6F_5)C_5H_4]_2Cr$ (**99**) was prepared by the reaction of $CrCl_2$ and $Na[(C_6F_5)C_5H_4]$ in THF (eq 5.3) and isolated as a deep purple solid. NaH was added to scavenge

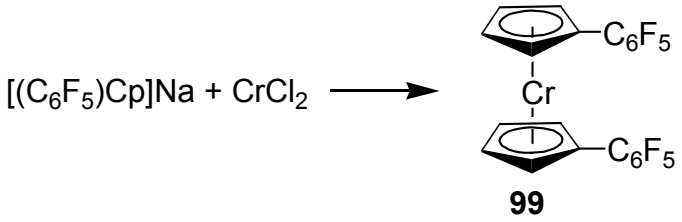

(5.3)

99

adventitious water to improve the yield. Because **99** is a paramagnetic compound, no useful ^1H NMR spectrum could be obtained. However, a diagnostic ^{19}F NMR spectrum was obtained. Both contact shift and dipolar relaxation contain a distance parameter which affects the NMR spectrum of a paramagnetic compound.[183] If we assume that the unpaired electron is localized on the metal, then the NMR signals for the atoms of the ligands will be affected based upon their distance to the metal center. Nuclei closer to the metal exhibit larger shifts and more broadening. In the ^{19}F NMR spectrum the ortho and meta signals are broad and shifted while the para signal remains sharp.

The reaction of $CrCl_2$ and $Na[(C_6F_5)C_5Me_4]$ in THF resulted in the formation of $[(C_6F_5)C_5Me_4]_2Cr$ (**100**, eq 5.4). Two broad signals (δ -0.73 and δ -11.87) are observed

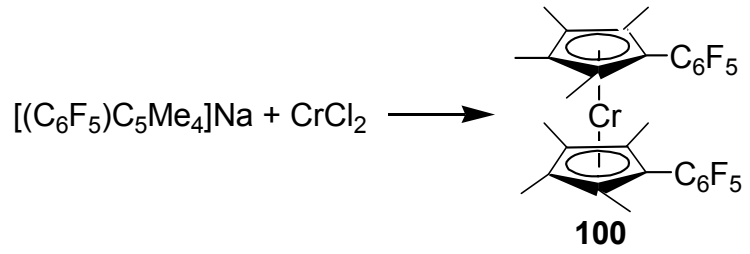

100 (5.4)

in the ^{1}H NMR spectrum corresponding to the methyl substituents. Four equally integrating signals (three sharp and one broad) are observed in the ^{19}F NMR spectrum. The three sharp signals represent the para and meta fluorines while the broad signal corresponds to one of the ortho fluorines. We surmise that the second ortho signal is so broadened and shifted so that it could not be observed.

Attempts to synthesize three other substituted chromocenes met with little success. The reaction of $CrCl_2$ and $Na[(C_6F_5)_2C_5H_3]$ in THF resulted in the formation of $[(C_6F_5)_2C_5H_3]_2Cr$ (**101**) along with the hydrolyzed ligand $(C_6F_5)_2C_5H_3$ (eq 5.5).

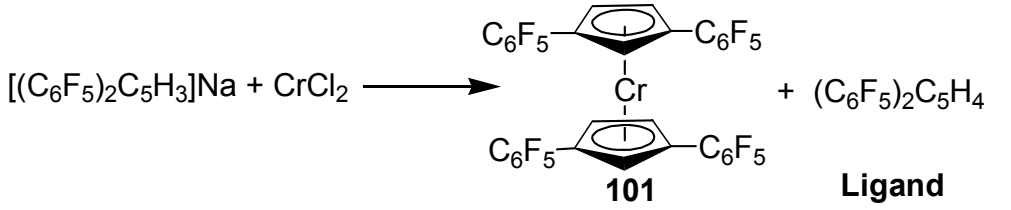

(5.5)

Compound **101** proved to be too unstable to isolate as a pure compound. All attempts to recrystallize **101** resulted in a mixture of product and ligand, while sublimation resulted in the isolation of the ligand on the cold finger. Two additional ligands, $Na[(C_5F_4N)C_5H_4]$ and $Na[(C_6F_5)_2C_5Me_3]$ were also synthesized in our lab. However they proved to be poor ligands for the formation of substituted chromocenes. Coordination studies were performed only on the cleanly isolated compounds **99** and **100**.

Coordination Reactions

The reaction of **99** with CO (eq 5.6) was conducted at 25 °C in a J-Young NMR

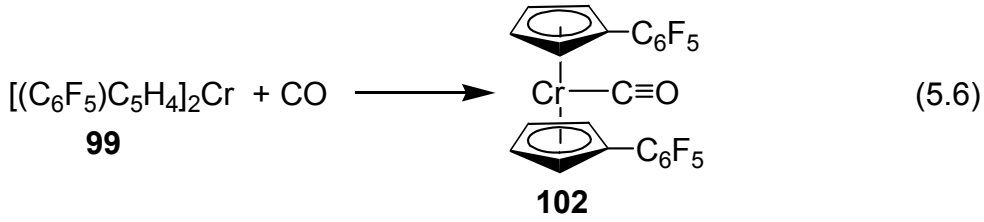

(5.6)

tube and monitored by ^{19}F NMR. Upon the addition of CO, three sharp signals corresponding to $[(C_6F_5)Cp]_2Cr(CO)$ (**102**) appeared in the ^{19}F spectrum along with the three peaks of **99**. Integration of the para region of the spectrum indicated that 10 % of **99** was converted into **102**. While the signals for the otho and meta regions of **99** are broad, the sharp para signal could be integrated along with the para signal of **102** to determine the extent of conversion. A systematic titration study similar to those performed with MAO could not be performed because we had no method for the addition of known concentrations of CO. Brintzinger's method (IR) for accurate delivery and measurment of CO pressures on a small scale would have required the construction of sophisticated, expensive equipment. A variable temperature study over the range of 25 °C through -90 °C was performed in order to determine if more **102** was formed similar to Brintzinger's results. At 25 °C the ^{19}F NMR spectrum demonstrated the six signals for both **99** and **102** (Figure 5.1a, Table 5.2). Cooling the sample to -30 °C resulted in both

Table 5.2. Chemical Shifts of $[(C_6F_5)Cp]_2Cr$ and $[(C_6F_5)Cp]_2Cr(CO)$

Compound	Ortho	Para	Meta
$[(C_6F_5)Cp]_2Cr$	-63.89	-148.43	-213.07
$[(C_6F_5)Cp]_2Cr(CO)$	-136.32	-156.21	-159.25

the broadening and shift of the peaks for **99** (Figure 5.1b). Continued cooling to -90 °C further shifted the para signal of **99** making the determination of the equilibrium constant unreliable (Figure 5.1c). ^{19}F NMR analysis of a mixture of **100** and CO indicated there was no coordination at room temperature or when the temperature was lowered to -90 °C.

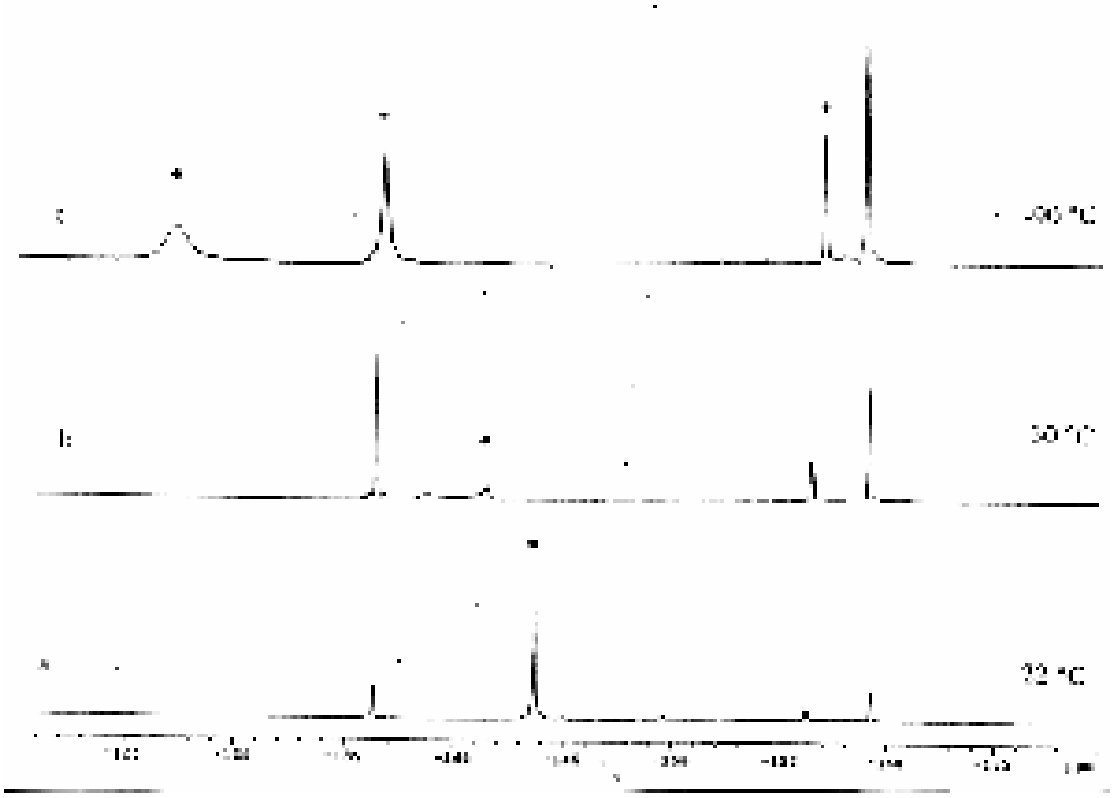

Figure 5.1. VT NMR Spectra of $[(C_6F_5)Cp]_2Cr$ + CO
• $[(C_6F_5)Cp]_2Cr$ * $[(C_6F_5)Cp]_2Cr(CO)$

In addition to CO, several other compounds (^tBuNC, FC_6H_4CN, $[Bu_4N][CN]$, NEt_3, 2,6-$Me_2C_6H_3NC$, PPh_3, and PMe_3) were investigated as potential coordinating reagents with **99**. ^{19}F NMR analysis of each reagent demonstrated that only cyanide coordinated to **99**. Unlike CO, a stock solution of $[Bu_4N][CN]$ in C_6D_6 could be prepared and used to titrate a sample of **99** to determine an equilibrium constant for the reaction (eq 5.7). However, stepwise addition of $[Bu_4N][CN]$ resulted in the formation of

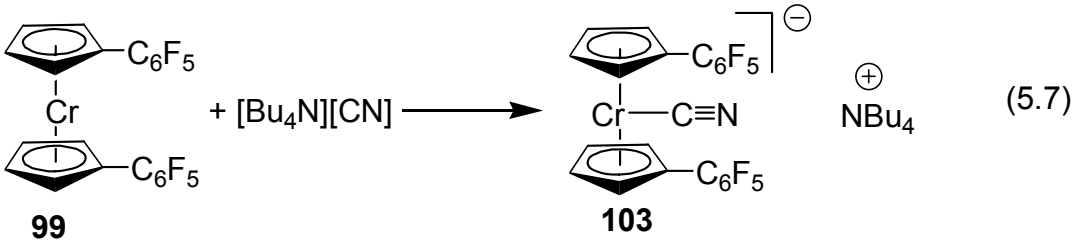

99 **103** (5.7)

a precipitate and an increasingly decolorized supernatant. Apparently the product cyanide complex is not soluble.

Formation of a precipitate (eq 5.8) prevents us from determining the binding constant for coordination (eq 5.9) because we cannot uncouple the associated solubility product constant ($1/K_{eq}$ for eq 5.10).

$$Cp'_2Cr + [CN][NBu_4] \underset{}{\overset{k_{eq}}{\rightleftharpoons}} [Cp'_2CrCN][NBu_4]\ (ppt) \qquad (5.8)$$

$$Cp'_2Cr + [CN][NBu_4] \overset{k_{eq}}{\rightleftharpoons} [Cp'_2CrCN][NBu_4]\ (aq) \qquad (5.9)$$

$$[Cp'_2CrCN][NBu_4]\ (aq) \overset{k_{eq}}{\rightleftharpoons} [Cp'_2CrCN][NBu_4]\ (ppt) \qquad (5.10)$$

A preparative scale reaction was performed and elemental analysis showed that the solid product collected was not $[(C_6F_5Cp)_2CrCN][NBu_4]$. Coordination studies with **100** and the above compounds all proved unsuccessful. Thornberry[174] demonstrated the electron-withdrawing ability of the pentafluorophenyl group by comparing the CO stretching frequencies of mono-, di-, tri-, and tetra-C_6F_5-substituted $CpM(CO)_3$ (M = Mn and Re). He found that the metal center becomes more electron-deficient upon the addition of each C_6F_5 group. However, the tetramethyl(pentafluorophenyl)cyclopentadienyl ligand was not included in the study.

One $C_6F_5 \cong 2\ CH_3$ groups so it should be perhaps somewhat more electron-rich than Cp_2Cr. The lack of coordination of cyanide suggests the tetramethyl(pentafluorophenyl)-cyclopentadiene is less electron-withdrawing than (pentafluorophenyl)cyclopentadiene. Lack of CO coordination, however, suggests that steric effects may preclude ligand coordination.

Conclusions

Two paramagnetic pentafluorophenyl-substituted chromocene compounds were synthesized and characterized. ^{19}F NMR demonstrated that manipulation of the electronic nature of the chromium center facilitated the coordination of both CO and $[Bu_4N][CN]$. Exact concentrations of CO could not be measured to determine an equilibrium constant for the formation of **102**. Precipitation of **103** precluded an estimate of the binding constant for cycanide ion.

Experimental Section

General Considerations. All manipulations were carried out using standard nitrogen-atmosphere techniques. $C_5Me_4H_2$ was purchased from Boulder Chemical Co. $[Bu_4N][CN]$ was purchased from Aldrich Chemical Co. $Na[(C_6F_5)C_5H_4]$[123], $Na[(C_5F_4N)C_5H_4]$[184], $Na[(C_6F_5)_2C_5Me_3]$, $Na[(C_6F_5)C_5Me_4]$ and $Na[(C_6F_5)_2C_5H_3]$[123] were prepared according to our own methods. NMR spectra were recorded on a Varian U-400 instrument at 22 °C except where indicated. ^{19}F NMR spectra are referenced to external C_6F_6 in $CDCl_3$ at –163.0 ppm.

$[(C_6F_5)C_5H_4]_2Cr$ (99). A swivel-frit apparatus was charged with a mixture of $CrCl_2$ (1.0 g, 8.14 mmol), $Na[(C_6F_5)C_5H_4]$ (4.3 g, 17.1 mmol), NaH (39 mg, 1.63 mmol) and THF (50 mL). The mixture was stirred at 25 °C for 18 h. The solution became deep purple

upon stirring. The solution was filtered and the filtrate evaporated. The deep purple residue was washed with pentane (3x, 35 mL) and dried under vacuum to afford 3.3 g (6.46 mmol, 79 %) of a purple solid. ^{19}F NMR (C_6D_6) δ -63.89 (br, 4 F), -148.43 (s, 2 F), -213.07 (br, 4 F). Anal. Calcd for $C_{22}H_8CrF_{10}$ C, 51.38; H, 1.57. Found C, 50.65; H, 1.37. (This was analyzed several times and these are the "best" results.)

$[(C_6F_5)C_5Me_4]_2Cr$ (100). A swivel-frit apparatus was charged with a mixture of $CrCl_2$ (1.0 g, 8.14 mmol), $Na[(C_6F_5)C_5Me_4]$ (4.3 g, 17.1 mmol), NaH (39 mg, 1.63 mmol) and THF (50 mL). The mixture was stirred at 25 °C for 2.5 h. The solution became deep purple upon stirring. The solution was filtered and the filtrate evaporated. The deep purple residue was washed with pentane (3x 50 mL) to afford 407 mg (0.65 mmol, 40 %) of a purple solid. ^{1}H NMR (C_6D_6) δ -0.73 (br, 6 H), -11.87 (br, 6 H). ^{19}F NMR (C_6D_6) δ -165.13 (s, 1 F), -172.98 (s, 1 F), -179.65 (s, 1 F), -192.77, (br, 2 F). Anal. Calcd for $C_{30}H_{24}CrF_{10}$ C, 57.52; H, 3.86. Found C, 57.92; H, 3.59.

$[(C_6F_5)_2C_5H_3]_2Cr$ (101). A swivel-frit apparatus was charged with a mixture of $CrCl_2$ (113 mg, 0.90 mmol), $Na[(C_6F_5)_2C_5H_3]$ (760 mg, 17.1 mmol), and THF (50 mL). The mixture was stirred at 25 °C for 48 h. The solvent was removed *in vacuo* and the residue was transferred into an alumina soxhlet thimble. Purple solids were extracted with toluene. Anal. Calcd for $C_{34}H_6CrF_{20}$ C, 48.25; H, 0.71. Found C, 47.97; H, 0.72.

NMR Tube Reaction of $[(C_6F_5)C_5H_4]_2Cr$ with CO. A J-Young NMR tube was charged with $[(C_6F_5)C_5H_4]_2Cr$ (11.0 mg, 2.1 x 10^{-2} mmol) and attached to the high vacuum line. Toluene-d_8 (1 mL) was vacuum transferred and the tube was then back-filled with CO and sealed. ^{1}H and ^{19}F NMR analysis demonstrated the coordination of CO. ^{1}H NMR (toluene-d_8) δ 4.47 (br, s, 4 H); 3.78 (br, s, 4 H). ^{19}F NMR (toluene-d_8) δ -68.2 (br, 4 F,

Cp_2'Cr), -136.29 (s, 4 F, Cr(CO)) -143.71 (s, 2 F, Cp_2'Cr), -156.21 (s, 2 F, Cr(CO)), -159.23 (s, 4 F, Cr(CO)) -213.8 (br, 4 F Cp_2'Cr). A variable temperature study was performed over the range of - 90 – 22 °C. The chemical shifts for the signals of $[C_6F_5Cp]_2Cr(CO)$ remained constant over the temperature range. The signals for the uncoordinated $[C_6F_5Cp]_2Cr$ were broadened as the temperature decreased with the ortho and meta peaks becoming unobservable.

NMR Tube Reactions of $[(C_6F_5)C_5H_4]_2Cr$ with $[Bu_4N][CN]$. All weighings were carried out using an analytical balance ($\pm$ 0.1 mg resolution) in a nitrogen glove box. A typical experiment was conducted as follows. A solution of $(C_6F_5C_5H_4)_2Cr$ (1.94×10^{-2} M) in C_6D_6 was prepared by dissolving 50 mg of $(C_6F_5C_5H_4)_2$ in 5.0 mL of C_6D_6. A solution of $[Bu_4N][CN]$ (1.81×10^{-2} M) in C_6D_6 was prepared by dissolving 20 mg of $[Bu_4N][CN]$ in 3.0 mL of C_6D_6. To each of five J-Young NMR tubes was added 380 mg of the C_6D_6 solution of $(C_6F_5C_5H_4)_2Cr$. Assuming that $(C_6F_5C_5H_4)_2Cr$ forms and ideal solution in C_6D_6 ($\rho = 0.95$ g mL^{-1}), the density of the C_6D_6 solution of $(C_6F_5C_5H_4)_2Cr$ was 0.96. A 380 mg aliquot of this solution corresponds to 0.400 mL; therefore, 0.0078 mmol of $(C_6F_5C_5H_4)_2Cr$ was added. To each of the five NMR tubes, a different amount (e.g. 104, 222, 350, 436, 575 mg) of the $[Bu_4N][CN]$ solution was added. Assuming the $[Bu_4N][CN]$ forms an ideal solution in C_6D_6, the density of the C_6D_6 ($\rho = 0.95$ g mL^{-1}) solution of $[Bu_4N][CN]$ was 0.96. The added weights of this solution correspond to 0.10, 0.21, 0.33, 0.42, and 0.55 mL, or 0.002, 0.004, 0.006, 0.008, and 0.0l mmol of $[Bu_4N][CN]$, respectively. Then, sufficient C_6D_6 was added by weight to each tube to bring the total calculated volume to 1.0 mL. The samples were shaken vigorously,

allowed to equilibrate for 5 min, and then subjected to ^{19}F NMR analysis. ^{19}F NMR (C_6D_6) δ -146.88 (s, 4 F), -167.45 (s, 2 F), -176.29 (s, 4 F).

$[(C_6F_5)C_5H_4]_2Cr(CN)$ (103). A swivel-frit apparatus was charged with a mixture of $[(C_6F_5)C_5H_4]_2Cr$ (250 mg, 0.49 mmol), $[Bu_4N][CN]$ (215 mg, 0.80 mmol), and benzene (35 mL). The mixture was stirred at room temperature for 18 h. The solid product was collected on a filter and dried under vacuum to afford 254 mg (0.32 mmol, 67 %) of a black solid.

Bibliography

(1) Montagna, A. A.; Burkhart, R. M.; Dekmezian, A. H. *CHEMTECH* **1997**, *27*, 26.

(2) Boor, J. J. *Ziegler-Natta Catalysts and Polymerizations*; Academic Press: New York, 1979.

(3) Goodall, B. L. *J Chem Ed* **1986**, *63*, 191.

(4) Sinn, H.; Kaminsky, W. *Ziegler-Natta Catalysis*; Academic Press: New York, 1980; Vol. 18.

(5) Johnson, J. C. *Metallocene Technology*; Noyes Data Corporation: Park Ridge, N.J., 1973.

(6) Kealy, T. J.; Pauson, P. L. *Nature* **1951**, *168*, 1039.

(7) Wilkinson, G.; Pauson, P. L.; Birmingham, J. M.; Cotton, F. A. *J. Am. Chem. Soc.* **1953**, *75*, 1011.

(8) Natta, G.; Pino, P.; Mazzanti, G.; Giannini, U. *J. Am. Chem. Soc.* **1957**, *79*, 2975.

(9) Breslow, D. S.; Newburg, N. R. *J. Am. Chem. Soc.* **1957**, *79*, 5072.

(10) Bochmann, M. *J. Chem. Soc. Dalton. Trans.* **1996**, 255.

(11) Kaminsky, W.; Arndt, M. *Adv. Polym. Sci.* **1997**, *127*, 143.

(12) Reichert, K. H.; Meyer, K. R. *Makromol. Chem.* **1973**, *169*, 163.

(13) Long, W. P.; Breslow, K. R. *Justus Liebigs Annalen der Chemie* **1975**, 463.

(14) Cihlar, J.; Mejlik, J.; Hamrik, O.; Hudea, P.; Majer, J. *Makromol. Chem.* **1980**, *181*, 2549.

(15) Cihlar, J.; Mejlik, J.; Hamrik, O. *Makromol. Chem.* **1978**, *179*, 2553.

(16) Sinn, H.; Kaminsky, W.; Vollmer, H.-J.; Woldt, R. *Angew. Chem. Int. Ed.* **1980**, *19*, 390.

(17) Chen, E. Y. X.; Marks, T. J. *Chem. Rev.* **2000**, *100*, 1391.

(18) Kaminsky, W. *Macromol. Chem. Phys.* **1996**, *197*, 3907.

(19) Alt, H. G.; Koppl, A. *Chem. Rev.* **2000**, *100*, 1205.

(20) Brintzinger, H. H.; Fischer, D.; Mulhaupt, R.; Rieger, B.; Waymouth, R. M. *Angew. Chem. Int. Edit.* **1995**, *34*, 1143.

(21) Pedeutour, J. N.; Radhakrishnan, K.; Cramail, H.; Deffieux, A. *Macromol. Rapid Comm.* **2001**, *22*, 1095.

(22) Pasynkiewicz, S. *Polyhedron* **1990**, *9*, 429.

(23) Saegusa, T.; Fuji, Y.; Fuji, H.; Furukawa, J. *Makromol. Chem.* **1962**, *55*, 232.

(24) Longiave, C.; Castelli, R. *J. Polym. Sci.* **1963**, *C-4*, 387.

(25) Sakharovskaya, G.; Korneev, N. N.; Popov, A. F.; Larikov, E. J.; Zhigach, A. F. *Zh. Obshch. Khim* **1964**, *34*, 3435.

(26) Storr, A.; K, J.; Laubengayer, A. W. *J. Am. Chem. Soc.* **1968**, *90*, 3173.

(27) Razuvaev, G. A.; Sangalov, Y. A.; Nel'kenbaum, Y. Y.; Minsker, K. S. *Izv. Akad. Nauk SSSR, Ser. Khim* **1975**, 2547.

(28) Reddy, S. S.; Sivaram, S. *Prog. Polym. Sci.* **1995**, *20*, 309.

(29) Zakharkin, L. J.; Khorlina, I. M. *Izv. Akad. Nauk SSSR, Ser. Khim* **1959**, 2146.

(30) Harney, D. W.; Meisters, A.; Mole, T. *Aust. J. Chem.* **1974**, *27*, 1639.

(31) Kosinska, W.; Kunicki, A.; Boleslawski, M.; Pasynkiewicz, S. *J. Organomet. Chem.* **1978**, *161*, 289.

(32) Boleslawski, M.; Pasynkiewicz, S. *J. Organomet. Chem.* **1972**, *43*, 81.

(33) Giannetti, E.; Nicoletti, G. M.; Mazzocchi, R. *J. Polym. Sci. Polym. Chem.* **1985**, *23*, 2117.

(34) Imhoff, D. W.; Simeral, L. S.; Blevins, D. R.; Beard, W. R. *Olefin Polymerization* **2000**, *749*, 177.

(35) Sinn, H. *Macromol. Symp.* **1995**, *97*, 27.

(36) Tritto, I.; Mealares, C.; Sacchi, M. C.; Locatelli, P. *Macromol. Chem. Phys.* **1997**, *198*, 3963.

(37) Vonlacroix, K.; Heitmann, B.; Sinn, H. *Macromol. Symp.* **1995**, *97*, 137.

(38) Yamamoto, O.; Hayamiza, J.; Yamagisawa, M. *J. Organomet. Chem.* **1974**, *73*, 17.

(39) Cocco, L.; Eyman, D. P. *J. Organomet. Chem.* **1979**, *179*, 1.

(40) Sugano, T.; Matsubara, K.; Fujita, T.; Takahashi, T. *J. Mol. Catal.* **1993**, *82*, 93.

(41) Benn, R.; Rukinska, A. *Angew. Chem. Int. Edit.* **1986**, *25*, 861.

(42) Bryant, P. L.; Harwell, C. R.; Mrse, A. A.; Emery, E. F.; Gan, Z. H.; Caldwell, T.; Reyes, A. P.; Kuhns, P.; Hoyt, D. W.; Simeral, L. S.; Hall, R. W.; Butler, L. G. *J. Am. Chem. Soc.* **2001**, *123*, 12009.

(43) Cam, D.; Albizzati, E.; Cinquina, P. *Makromol. Chem.* **1990**, *191*, 1641.

(44) Sinn, H.; Bliemeister, J.; Clausnitzer, D.; Tikwe, L.; Winter, H.; Zamke, O. *Transition Metals and Organometallics as Catalysts for Olefin Polymerization*; Springer Verlag: Berlin, 1988.

(45) Bliemeister, J.; Hagendorf, W.; Clausnitzer, D.; Harder, A.; Heitmann, B.; Schimmel, I.; Schmedt, E.; Schnuchel, W.; Sinn, H.; Tikwe, L.; von Thienen, N.; Urlass, K.; Winter, H.; Zarnke, O. *Ziegler Catalysts*; Springer: Berling, 1995.

(46) Wolinska, A. *J. Organomet. Chem.* **1982**, *234*, 1.

(47) Atwood, J. L.; Hrncir, D. C.; Priester, R. D.; Rogers, R. D. *Organometallics* **1983**, *2*, 985.

(48) Atwood, J. L.; Zaworotko, M. J. *J. Chem. Soc. Chem. Commun.* **1983**, 302.

(49) Mason, M. R.; Smith, J. M.; Bott, S. G.; Barron, A. R. *J. Am. Chem. Soc.* **1993**, *115*, 4971.

(50) Ystenes, M.; Eilertsen, J. L.; Liu, J. K.; Ott, M.; Rytter, E.; Stovneng, J. A. *J. Polym. Sci. Pol. Chem.* **2000**, *38*, 3106.

(51) Harlan, C. J.; Bott, S. G.; Barron, A. R. *J. Am. Chem. Soc.* **1995**, *117*, 6465.

(52) Koide, Y.; Bott, S. G.; Barron, A. R. *Organometallics* **1996**, *15*, 5514.

(53) Breslow, D. S.; Newburg, N. R. *J. Am. Chem. Soc.* **1959**, *81*, 81.

(54) Dyachkovskii, F. S.; Shilova, A. K.; Shilov, A. E. *J. Polym. Sci. C. Polym. Symp.* **1967**, *16*, 2333.

(55) Zefirova, A. K.; Shilov, A. E. *Dok. Ak. Nauk. SSSR.* **1961**, *136*, 599.

(56) Long, W. P.; Breslow, D. S. *J. Am. Chem. Soc.* **1960**, *82*, 1953.

(57) Cossee, P. *J. Catal.* **1964**, *3*, 80.

(58) Arlman, E. J.; Cossee, P. *J. Catal.* **1964**, *3*, 99.

(59) Thompson, M. E.; Bercaw, J. E. *Pure. Appl. Chem.* **1984**, *56*, 1.

(60) Jeske, G.; Lauke, H.; Mauermann, H.; Sweptson, P. N.; Schumann, H.; Marks, T. J. *J. Am. Chem. Soc.* **1985**, *107*, 8091.

(61) Watson, P. L.; Parshall, G. W. *Acc. Chem. Res.* **1985**, *18*, 51.

(62) Watson, P. L. *J. Am. Chem. Soc.* **1982**, *104*, 337.

(63) Watson, B. T.; Roe, D. C. *J. Am. Chem. Soc.* **1982**, *104*, 6471.

(64) Eisch, J. J.; Piotrowski, A. M.; Brownstein, S. K.; Gabe, E. J.; Lee, F. L. *J. Am. Chem. Soc.* **1985**, *107*, 7219.

(65) Eisch, J. J.; Caldwell, K. R.; Werner, S.; Kruger, C. *Organometallics* **1991**, *10*, 3417.

(66) Noth, H.; Rurlander, R.; Wolfgardt, P. Z. *Naturforsch* **1982**, *37B*, 29.

(67) Jordan, R. F.; Bajgur, C. S.; Willett, R.; Scott, B. *J. Am. Chem. Soc.* **1986**, *108*, 7410.

(68) Jordan, R. F.; Lapointe, R. E.; Bradley, P. K.; Baenziger, N. *Organometallics* **1989**, *8*, 2892.

(69) Hlatky, G. G.; Turner, H. W.; Eckman, R. R. *J. Am. Chem. Soc.* **1989**, *111*, 2728.

(70) Taube, R.; Krukowka, L. *J. Am. Chem. Soc.* **1988**, *347*, C9.

(71) Bochmann, M.; Jaggar, A. J.; Nicholls, J. C. *Angew. Chem. Int. Edit.* **1990**, *29*, 780.

(72) Canich, J. M.; Hlatky, G. G.; Turner, H. W. In *US Patent*: United States, 1992.

(73) Bochmann, M.; Lancaster, S. J. *Organometallics* **1993**, *12*, 633.

(74) Massey, A. G.; Park, A. J. *J. Organomet. Chem.* **1964**, *2*, 245.

(75) Yang, X. M.; Stern, C. L.; Marks, T. J. *J. Am. Chem. Soc.* **1991**, *113*, 3623.

(76) Jordan, R. F. *Adv. Organomet. Chem.* **1991**, *32*, 325.

(77) Erker, G.; Albrecht, M.; Werner, S.; Kruger, C. *Zeitschrift Fur Naturforschung Section B-a Journal of Chemical Sciences* **1990**, *45*, 1205.

(78) Gassman, P. G.; Callstrom, M. R. *J. Am. Chem. Soc.* **1987**, *109*, 7875.

(79) Sishta, C.; Hathorn, R. M.; Marks, T. J. *J. Am. Chem. Soc.* **1992**, *114*, 1112.

(80) Vander Hart, D. L.; Perez, E. *Macromolecules* **1986**, *19*, 1902.

(81) Tritto, I.; Li, S. X.; Sacchi, M. C.; Zannoni, G. *Macromolecules* **1993**, *26*, 7111.

(82) Tritto, I.; Sacchi, M. C.; Li, S. X. *Macromol. Rapid. Comm.* **1994**, *15*, 217.

(83) Tritto, I.; Li, S. X.; Sacchi, M. C.; Locatelli, P.; Zannoni, G. *Macromolecules* **1995**, *28*, 5358.

(84) Tritto, I.; Donetti, R.; Sacchi, M. C.; Locatelli, P.; Zannoni, G. *Macromolecules* **1997**, *30*, 1247.

(85) Beck, S.; Prosenc, M. H.; Brintzinger, H. H.; Goretzki, R.; Herfert, N.; Fink, G. *J. Mol. Catal. a-Chem.* **1996**, *111*, 67.

(86) Siedle, A. R.; Lamanna, W. M.; Newmark, R. A.; Schroepfer, J. N. *J. Mol. Catal. a-Chem.* **1998**, *128*, 257.

(87) Kaminsky, W.; Steiger, R. *Polyhedron* **1988**, *7*, 2375.

(88) Pedeutour, J. N.; Cramail, H.; Deffieux, A. *J. Mol. Catal. a-Chem.* **2001**, *174*, 81.

(89) Pedeutour, J. N.; Coevoet, D.; Cramail, H.; Deffieux, A. *Macromol. Chem. Phys.* **1999**, *200*, 1215.

(90) Coevoet, D.; Cramail, H.; Deffieux, A. *Macromol. Chem. Phys.* **1999**, *200*, 1208.

(91) Coevoet, D.; Cramail, H.; Deffieux, A. *Macromol. Chem. Phys.* **1998**, *199*, 1459.

(92) Coevoet, D.; Cramail, H.; Deffieux, A. *Macromol. Chem. Phys.* **1998**, *199*, 1451.

(93) Pieters, P. J. J.; Vanbeek, J. A. M.; Vantol, M. F. H. *Macromol. Rapid. Comm.* **1995**, *16*, 463.

(94) Makela, N. I.; Knuuttila, H. R.; Linnolahti, M.; Pakkanen, T. A.; Leskela, M. A. *Macromolecules* **2002**, *35*, 3395.

(95) Woo, T. K.; Margl, P. M.; Ziegler, T.; Blochl, P. E. *Organometallics* **1997**, *16*, 3454.

(96) Woo, T. K.; Margl, P. M.; Lohrenz, J. C. W.; Blochl, P. E.; Ziegler, T. *J. Am. Chem. Soc.* **1996**, *118*, 13021.

(97) Fan, L. Y.; Harrison, D.; Woo, T. K.; Ziegler, T. *Organometallics* **1995**, *14*, 2018.

(98) Margl, P.; Lohrenz, J. C. W.; Ziegler, T.; Blochl, P. E. *J. Am. Chem. Soc.* **1996**, *118*, 4434.

(99) Bierwagen, E. P.; Bercaw, J. E.; Goddard, W. A. *J. Am. Chem. Soc.* **1994**, *116*, 1481.

(100) Yang, X. M.; Stern, C. L.; Marks, T. J. *J. Am. Chem. Soc.* **1994**, *116*, 10015.

(101) Deck, P. A.; Marks, T. J. *J. Am. Chem. Soc.* **1995**, *117*, 6128.

(102) Li, L. T.; Marks, T. J. *Organometallics* **1998**, *17*, 3996.

(103) Jia, L.; Yang, X. M.; Stern, C. L.; Marks, T. J. *Organometallics* **1997**, *16*, 842.

(104) Bochmann, M.; Lancaster, S. J. *Angew. Chem. Int. Edit.* **1994**, *33*, 1634.

(105) Tritto, I.; Donetti, R.; Sacchi, M. C.; Locatelli, P.; Zannoni, G. *Macromolecules* **1999**, *32*, 264.

(106) Rappe, A. T.; Skiff, W. M.; Casewit, C. J. *Chem. Rev.* **2000**, *100*, 1435.

(107) Lanza, G.; Fragala, I. L.; Marks, T. J. *J. Am. Chem. Soc.* **1998**, *120*, 8257.

(108) Chan, M. S. W.; Ziegler, T. *Organometallics* **2000**, *19*, 5182.

(109) Lanza, G.; Fragala, I. L. *Top. Catal.* **1999**, *7*, 45.

(110) Xu, Z. T.; Vanka, K.; Firman, T.; Michalak, A.; Zurek, E.; Zhu, C. B.; Ziegler, T. *Organometallics* **2002**, *21*, 2444.

(111) Reddy, S. S.; Shashidhar, G.; Sivaram, S. *Macromolecules* **1993**, *26*, 1180.

(112) Kaminsky, W.; Bark, A.; Steiger, R. *J. Mol. Catal.* **1992**, *74*, 109.

(113) Chien, J. C. W.; Wang, B. P. *J. Polym. Sci. Polym. Chem.* **1988**, *26*, 3089.

(114) Forlini, F.; Fan, Z. Q.; Tritto, I.; Locatelli, P.; Sacchi, M. C. *Macromol. Chem. Phys.* **1997**, *198*, 2397.

(115) Coevoet, D.; Cramail, H.; Deffieux, A. *Macromol. Chem. Phys.* **1996**, *197*, 855.

(116) Herfert, N.; Fink, G. *Makromol. Chem.* **1992**, *193*, 773.

(117) Carpentier, J. F.; Wu, Z.; Lee, C. W.; Stromberg, S.; Christopher, J. N.; Jordan, R. F. *J. Am. Chem. Soc.* **2000**, *122*, 7750.

(118) Deck, P. A.; Beswick, C. L.; Marks, T. J. *J. Am. Chem. Soc.* **1998**, *120*, 1772.

(119) Nekhaeva, L. A.; Bondarenko, G. N.; Rykov, S. V.; Nekhaev, A. I.; Krentsel, B. A.; Marin, V. P.; Vyshinskaya, L. I.; Khrapova, I. M.; Polonskii, A. V.; Korneev, N. N. *J. Organomet. Chem.* **1991**, *406*, 139.

(120) Zhang, Z. Y.; Duan, X. F.; Zheng, Y.; Wang, J. Z.; Tu, G. Z.; Hong, S. L. *J. Appl. Polym. Sci.* **2000**, *77*, 890.

(121) Babushkin, D. E.; Semikolenova, N. V.; Zakharov, V. A.; Talsi, E. P. *Macromol. Chem. Phys.* **2000**, *201*, 558.

(122) Babushkin, D. E.; Brintzinger, H. H. *J. Am. Chem. Soc.* **2002**, *124*, 12869.

(123) Deck, P. A.; Jackson, W. F.; Fronczek, F. R. *Organometallics* **1996**, *15*, 5287.

(124) Siedle, A. R.; Newmark, R. A. *J. Organomet. Chem.* **1995**, *497*, 119.

(125) Dahmen, K. H.; Hedden, D.; Burwell, R. L.; Marks, T. J. *Langmuir* **1988**, *4*, 1212.

(126) Haselwander, T.; Beck, S.; Brintzinger, H. H. *Ziegler Catalysts*; Springer: Berlin, 1995.

(127) Imhoff, D. W.; Simeral, L. S.; Sangokoya, S. A.; Peel, J. H. *Organometallics* **1998**, *17*, 1941.

(128) Perrin, C. L.; Dwyer, T. J. *Chem. Rev.* **1990**, *90*, 935.

(129) Deck, P. A.; Fronczek, F. R. *Organometallics* **2000**, *19*, 327.

(130) Thornberry, M. P.; Slebodnick, C.; Deck, P. A.; Fronczek, F. R. *Organometallics* **2001**, *20*, 920.

(131) Maldanis, R. J.; Chien, J. C. W.; Rausch, M. D. *J. Organomet. Chem.* **2000**, *599*, 107.

(132) Chien, J. C. W.; Song, W.; Rausch, M. D. *Macromolecules* **1993**, *26*, 3239.

(133) Vizzini, J. C.; Chien, J. C. W.; Babu, G. N.; Newmark, R. A. *J. Polym. Sci. Pol. Chem.* **1994**, *32*, 2049.

(134) Fink, G.; Steinmetz, B.; Zechlin, J.; Przybyla, C.; Tesche, B. *Chem. Rev.* **2000**, *100*, 1377.

(135) Jezequel, M.; Dufaud, V.; Ruiz-Garcia, M. J.; Carrillo-Hermosilla, F.; Neugebauer, U.; Niccolai, G. P.; Lefebvre, F.; Bayard, F.; Corker, J.; Fiddy, S.; Evans, J.; Broyer, J. P.; Malinge, J.; Basset, J. M. *J. Am. Chem. Soc.* **2001**, *123*, 3520.

(136) Talsi, E. P.; Semikolenova, N. V.; Panchenko, V. N.; Sobolev, A. P.; Babushkin, D. E.; Shubin, A. A.; Zakharov, V. A. *J. Mol. Catal. a-Chem.* **1999**, *139*, 131.

(137) Lund, E. C.; Livinghouse, T. *Organometallics* **1990**, *9*, 2426.

(138) Surtees, J. R. *J. Chem. Soc. Chem. Commun.* **1965**, 567.

(139) Reid, A. F.; Shannon, J. S.; Swan, J. M.; Wailes, P. C. *Aust. J. Chem.* **1965**, *18*, 173.

(140) Reddy, K. P.; Petersen, J. L. *Organometallics* **1989**, *8*, 2107.

(141) Hunter, W. E.; Hrncir, D. C.; Vann Bynum, R.; Pentilla, R. A.; Atwood, J. L. *Organometallics* **1983**, *2*, 750.

(142) Fronczek, F. R.; Baker, E. C.; Sharp, P. R.; Raymond, K. N.; Alt, H. G.; Rausch, M. D. *Inorg. Chem.* **1976**, *15*, 2284.

(143) Hillhouse, G. L.; Bercaw, J. E. *J. Am. Chem. Soc.* **1984**, *106*, 5472.

(144) Moore, E. J.; Strauss, D. A.; Armantrout, J.; Santarsiero, B. D.; Grubbs, R. H.; Bercaw, J. E. *J. Am. Chem. Soc.* **1983**, *105*, 2068.

(145) Jordan, R. F. *J. Organomet. Chem.* **1985**, *294*, 321.

(146) Lisowsky, R. In *US Patent*; GmbH, W.: United States, 1996.

(147) Wailes, P. C.; Weigold, H.; Bell, A. P. *J. Organomet. Chem.* **1972**, *34*, 155.

(148) Wendt, O. F.; Bercaw, J. E. *Organometallics* **2001**, *20*, 3891.

(149) Sweeney, Z. K.; Salsman, J. L.; Andersen, R. A.; Bergman, R. G. *Angew. Chem. Int. Edit.* **2000**, *39*, 2339.

(150) Obrey, S. J.; Bott, S. G.; Barron, A. R. *Organometallics* **2001**, *20*, 5162.

(151) Pouchert, C. J.; Behnke, J. *The Aldrich Library of ^{13}C and ^{1}H FT NMR Spectra*; First ed.; Aldrich Chemical Company: Milwaukee, 1993; Vol. 2.

(152) Colle, T. H.; Glaspie, P. S.; Lewis, E. S. *J. Org. Chem.* **1978**, *43*, 2722.

(153) Hawrelak, E. J.; Deck, P. A.; Liable-Sands, L. M.; Rheingold, A. J. *Submitted for publication* **2002**.

(154) Lappert, M. F. P., C. J.; Riley, P. I.; Yarrow, P. I. W. *Journal of the Chemical Society Dalton Transactions* **1981**, *3*, 805.

(155) Winter, C. H.; Zhou, X. X.; Heeg, M. J. *Organometallics* **1991**, *10*, 3799.

(156) Setton, R. S., E. *Journal of Organometallic Chemistry* **1965**, *4*, 156.

(157) Nakazawa, O.; Sano, A.; Matsuura, K. In *Eur. Patent*: Japan, 1997, p 28.

(158) Gray, D. R.; Brubaker, C. H. J. *Inorg. Chem.* **1971**, *10*, 2143.

(159) Wade, S. R.; Willey, G. R. *Inorg. Chem.* **1981**, *10*, 2143.

(160) Antinolo, A.; Lappert, M. F.; Singh, A.; Winterborn, D. J. W.; Engelhardt, L. M.; Raston, C. L.; White, A. H.; Carty, A. J.; Taylor, N. J. *J. Chem. Soc. Dalton. Trans.* **1987**, 1463.

(161) Henrici-Olive, G.; Olive, S. *Angew. Chem.* **1967**, *79*, 764.

(162) Fink, G.; Rottler, R.; Schnell, D.; Zoller, W. *J. Appl. Chem.* **1976**, *20*, 2779.

(163) Eisch, J. J.; Pombrik, S. I.; Zheng, G. X. *Organometallics* **1993**, *12*, 3856.

(164) Cam, D.; Giannini, U. *Makromol. Chem.* **1992**, *193*, 1049.

(165) Resconi, L.; Bossi, S.; Abis, L. *Macromolecules* **1990**, *23*, 4489.

(166) Barron, A. R. *Organometallics* **1995**, *14*, 3581.

(167) Biagini, P.; Lugli, G.; Abis, L.; Andreussi, P. In *US Patent*: United States, 1997.

(168) Carnahan, E. M.; Chen, E. Y. X.; Jacobsen, G. B.; Stevens, J. C. In *PCT Int. Appl.*, 1999.

(169) Lee, C. H.; Lee, S. J.; Park, J. W.; Kim, K. H.; Lee, B. Y.; Oh, J. S. *J. Mol. Catal. a-Chem.* **1998**, *132*, 231.

(170) Klosin, J.; Roof, G. R.; Chen, E. Y. X.; Abboud, K. A. *Organometallics* **2000**, *19*, 4684.

(171) Kaminsky, K.; Vollmer, H. J.; Heins, E.; Sinn, H. *Makromol. Chem.* **1974**, *175*, 443.

(172) Kraft, B. M.; Lachicotte, R. J.; Jones, W. D. *J. Am. Chem. Soc.* **2000**, *122*, 8559.

(173) Edelbach, B. L.; Rahman, A. K. F.; Lachicotte, R. J.; Jones, W. D. *Organometallics* **1999**, *18*, 3170.

(174) Thornberry, M. P. In *Chemistry*; Virginia Polytechnic Institute and State University: Blacksburg, 2001, p 146.

(175) Wong, K. L. T.; Thomas, J. L.; Brintzinger, H. H. *J. Am. Chem. Soc.* **1974**, *96*, 3694.

(176) Gianotti, C.; Green, M. L. H. *J. Chem. Soc. Chem. Comm.* **1972**, 1114.

(177) Green, M. L. H.; Knowles, P. J. *J. Chem. Soc. A.* **1971**, 1508.

(178) Thomas, J. L.; Brintzinger, H. H. *J. Am. Chem. Soc.* **1972**, *94*, 1386.

(179) Wong, K. L. T.; Brintzinger, H. H. *J. Am. Chem. Soc.* **1975**, *97*, 5143.

(180) Matare, C. J.; Foo, D. M.; Kane, K. M.; Zehnder, R.; Wagener, M.; Shapiro, P. J.; Concolino, T.; Rheingold, A. L. *Organometallics* **2000**, *19*, 1534.

(181) Simpson, K. M.; Rettig, M. F.; Wing, R. M. *Organometallics* **1992**, *11*, 4363.

(182) Green, J. C.; Jardine, C. N. *J. Chem. Soc. Dalton. Trans.* **1999**, 3767.

(183) Drago, R. S. *Physical Methods for Chemists*; 2nd Edition ed.; Saunders College Publishing: New York, 1992.

(184) Warren, A. D. In *Chemistry*; Virginia Polytechnic Institute and State University: Blacksburg, 2001, p 49.

Vita

Eric J. Hawrelak was born on May 16, 1973 in Auburn, New York. He earned a Bachelor of Arts degree in chemistry from Hamilton College (1991-1995) in Clinton, New York. While there, he participated in undergraduate research under the guidance of Dr. Karen S. Brewer. He earned a Masters of Science in Chemistry from the University of Kentucky (1995-1998) in Lexington, Kentucky under the guidance of Dr. Folami Ladipo. He began graduate school at Virginia Polytechnic Institute and State University in the fall of 1998 with Dr. Paul Deck as his research advisor. Upon completion of his Ph.D. in chemistry, he will begin post-doctoral research at Cornell University with Dr. Paul Chirik.